

Wilfrid Laurier University

Scholars Commons @ Laurier

Theses and Dissertations (Comprehensive)

2022

Utilization of the Yamamoto Cyclotrimerization Reaction Towards the Synthesis of Polycyclic Aromatic Compounds

Josh LeDrew
ledr1250@mylaurier.ca

Follow this and additional works at: <https://scholars.wlu.ca/etd>

 Part of the [Organic Chemistry Commons](#)

Recommended Citation

LeDrew, Josh, "Utilization of the Yamamoto Cyclotrimerization Reaction Towards the Synthesis of Polycyclic Aromatic Compounds" (2022). *Theses and Dissertations (Comprehensive)*. 2433.
<https://scholars.wlu.ca/etd/2433>

This Thesis is brought to you for free and open access by Scholars Commons @ Laurier. It has been accepted for inclusion in Theses and Dissertations (Comprehensive) by an authorized administrator of Scholars Commons @ Laurier. For more information, please contact scholarscommons@wlu.ca.

**UTILIZATION OF THE YAMAMOTO CYCLOTRIMERIZATION
REACTION TOWARDS THE SYNTHESIS OF POLYCYCLIC
AROMATIC COMPOUNDS**

by

Josh LeDrew

Honours Bachelor of Science in Chemistry, Wilfrid Laurier University, 2019

THESIS

Submitted to the Department of Chemistry and Biochemistry

Faculty of science

in partial fulfilment of the requirements for

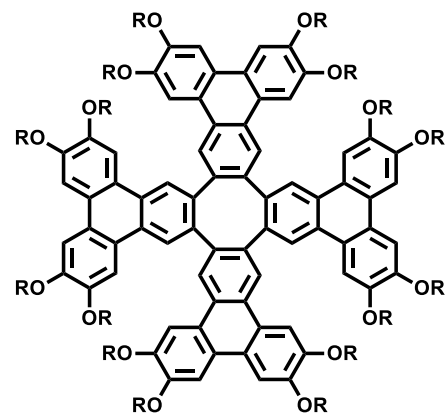
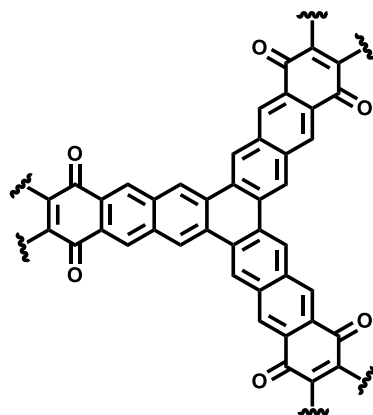
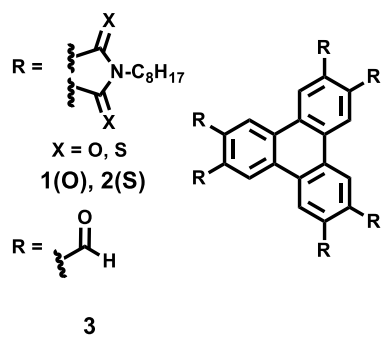
Master of Science in Chemistry

Wilfrid Laurier University

2021

ABSTRACT

The overall theme of this research was to synthesize and study the structure-property relationships of novel polycyclic aromatic compounds capable of self-assembling to form liquid crystalline, and microporous structures, as well as molecules capable of molecular recognition. The unifying theme that connects this research is the utilization of the Yamamoto coupling reaction to access the desired polycyclic aromatic hydrocarbon targets. More specifically, the scope of the Yamamoto coupling reaction was explored for the synthesis of electron-deficient triphenylene derivatives that are otherwise difficult to prepare. The molecules prepared via the Yamamoto coupling reaction are expected to be further utilized as intermediates for the synthesis of novel target materials. This thesis had three main goals. The first goal was the synthesis of electron-deficient triphenylene **1** via the Yamamoto coupling reaction followed by the study of the influences of thionation on the liquid crystalline and electron properties through the synthesis of **2**. In the second goal, we sought to prepare electron-deficient triphenylene **3** via the Yamamoto coupling reaction and use as a building block towards the preparation of a covalent organic framework **4**. Finally, we investigated a novel route to access an extended tetraphenylene derivative **5**. Thus far, targets **1** and **2** have been prepared in 65% and 60% yield, respectively and the affects of thionation on the mesomorphic and electronic properties of **1** were investigated. Moreover, progress towards the synthesis of triphenylene **3** has been made, however, purification of **3** has proven to be difficult under the current conditions. Finally, important intermediates have been accessed in good yields towards compound **5**, and its construction remains in progress.



ACKNOWLEDGMENTS

Firstly, I would like to thank Dr. Ken Maly for taking me on as an undergraduate researcher in 2018, as a 4th year thesis student, and as a master's student. I also want to thank Dr. Maly for being an excellent mentor, for always being available to give advice and feedback throughout my time in the lab, and for providing all the resources necessary for my research.

I want to thank Lana Hiscock for her mentorship, and guidance throughout my entire time in Dr. Maly's lab. Lana has always been there whenever I needed advice and I am very grateful and lucky to have her as a lab colleague. I would also want to thank other past and present lab colleagues whom I worked with in the Maly lab and those who have contributed to my project, specifically Zachary Schroeder, and Katie Psutka. It was a pleasure getting to know and work with all of you.

I would also like to acknowledge Dr. Dmitri Goussev at Wilfrid Laurier University for glove box training, and for allowing us to use the glove box for reactions that were important to the success and progress of this research.

Finally, I would like to acknowledge all the organizations that have contributed funding for this research; Government of Ontario graduate scholarship (OGS, 2019-2020), Natural Sciences and Engineering Research Council of Canada (NSERC, 2020-2021) and Wilfrid Laurier University.

TABLE OF CONTENTS

CHAPTER 1: INTRODUCTION.....	1
1.1 Organic Electronics.....	1
1.2 Polycyclic Aromatic Hydrocarbons.....	2
1.3 Liquid Crystals: Disc-Shaped Aromatic Compounds	6
1.4 Covalent Organic Frameworks.....	16
1.5 Supramolecular Chemistry and Nonplanar Polycyclic Aromatic Hydrocarbons	20
1.6 The Yamamoto Coupling Reaction	23
1.7 Research Objectives	29
<i>1.7.1 Synthesis of Tris(dicarboxyimide)triphenylene 1 and Exploring the Effects of Thionation on the Liquid Crystalline Properties</i>	<i>31</i>
<i>1.7.2 Preparing a Novel Covalent Organic Framework from an Electron-Deficient Triphenylene Building Block</i>	<i>33</i>
<i>1.7.3 Synthesis of a Novel Extended Tetraphenylene for Molecular Recognition</i>	<i>35</i>
CHAPTER 2: NOVEL SYNTHESIS OF A CARBOXIMIDE-SUBSTITUTED TRIPHENYLENE AND A STUDY OF THE EFFECTS OF THIONATION	38
2.1 Introduction	38
2.2 Results and Discussion	46
<i>2.2.1 Synthesis and Properties of Tris(dicarboxyimide)-Substituted Triphenylene 1</i>	<i>46</i>
<i>2.2.2 Synthesis of Dicarboxythioimide-Substituted Triphenylene and the Investigation of the Influences of Thionation on Mesomorphic and Electronic Properties</i>	<i>49</i>

2.3 Conclusions and Future Work	59
CHAPTER 3: EXPLORATION OF ALTERNATIVE NICKEL-MEDIATED	
CYCLOTRIMERIZATION REACTION CONDITIONS	61
3.1 Introduction	61
3.1.1 Reductive Polymerization via Nickel(0)-Catalyzed Coupling of Aryl Halides	65
3.1.2 Nickel-catalyzed [2+2+2] Cycloaddition Reactions	68
3.1.3 Air-Stable Binary Nickel(0)-Olefin Precatalysts	72
3.2 Results and Discussion	73
3.2.1 Yamamoto coupling reaction using Ni(0) precatalyst Ni(COD)(DQ)	76
3.2.2 Nickel-catalyzed [2+2+2] cycloaddition reactions	76
3.3 Summary and Future Work	80
CHAPTER 4: TOWARDS THE SYNTHESIS OF A NOVEL COVALENT ORGANIC	
FRAMEWORK.....	83
4.1 Introduction	83
4.2 Results and Discussion	86
4.3 Summary and Future Work	95
CHAPTER 5: TOWARDS THE SYNTHESIS OF NOVEL TETRAPHENYLENES	
5.1 Introduction	98
5.2 Results and Discussion	100
5.3 Summary and Future Work	105

CHAPTER 6: CONCLUSIONS AND FUTURE WORK	107
CHAPTER 7: METHODOLOGY AND EXPERIMENTAL PROCEDURES.....	111
7.1 Materials and Methods of Characterization.....	111
<i>7.1.1 NMR Spectroscopy.....</i>	<i>111</i>
<i>7.1.2 High Resolution Mass Spectrometry.....</i>	<i>111</i>
<i>7.1.3 Melting Points</i>	<i>111</i>
<i>7.1.4 Mesophase Characterization Techniques</i>	<i>111</i>
<i>7.1.5 Thermogravimetric Analysis</i>	<i>111</i>
<i>7.1.6 Ultraviolet-visible (UV-Vis) Spectroscopy</i>	<i>112</i>
<i>7.1.7 Chemicals and Solvents</i>	<i>112</i>
7.2 Experimental Procedures	113
REFERENCES.....	134
APPENDIX A: ¹H AND ¹³C NUCLEAR MAGNETIC RESONANCE (NMR) SPECTRA	
.....	146

LIST OF FIGURES

Figure 1. Simplest example of a polycyclic aromatic hydrocarbon, naphthalene (6).....	2
Figure 2. Clar structures of linear PAHs: anthracene (7), tetracene (8) and pentacene (9).	3
Figure 3. Depiction of Clar sextet rings in PAH examples; triphenylene (10) and tetracene (8). ¹⁰	3
Figure 4. Structure of 6,13-bis(triisopropylsilyl)ethynylpentacene (11) as reported by Anthony <i>et al.</i> ¹⁶	5
Figure 5. Structures of an acene (pentacene) with diene conjugation (9) and an acene-analogue with quinoidal conjugation as a result of the introduction of heteroatoms (12).	6
Figure 6. Representation of a common stacking-type arrangement discotic liquid crystals like, hexaalkoxytriphenylenes (13).	8
Figure 7. Series of disk-shaped compounds; dibenzo[<i>f,h</i>]quinoxaline (14), dibenzo[<i>a,c</i>]phenazine (15) and tribenzo[<i>a,c,i</i>]phenazine (16) with increasing core size prepared by Williams <i>et al.</i> ²⁶	9
Figure 8. Dibenzo[<i>a,c</i>]phenazine (15a-k) series prepared by Williams <i>et al.</i> ²⁶	10
Figure 9. Dibenzo[<i>a,c</i>]anthracenedicarboximide (17a-f) series prepared by Maly <i>et al.</i> ²⁷	11
Figure 10. Dibenzo[<i>a,c</i>]anthracenedicarboxy-imide and -thioimide series (17b,d , 18a,b and 19a,b) prepared by Maly and coworkers. ²⁹	12
Figure 11. Triphenylenedicarboxy-imide and -thioimide series (20-22) prepared by Maly <i>et al.</i> ³⁰	14
Figure 12. Chemical and X-ray crystallographic structures of tetraphenylene (25). ³⁹	21
Figure 13. Novel substituted tetraphenylene precursor prepared by Wong <i>et al.</i> ³⁷	22

Figure 14. Tetracyclic (32) and tricyclic (10) materials prepared by Yamamoto <i>et al.</i> via the Yamamoto coupling. ⁴²	25
Figure 15. Suite of electron-deficient triphenylenes (37-39) and trinaphthylene (40) derivatives previously prepared in the Maly lab.	28
Figure 16. PDI (44) prepared by Seferos <i>et al.</i> , and NDI (45) prepared by Zhang <i>et al.</i> ^{47,48}	39
Figure 17. Structures of target compounds 1 and 2	39
Figure 18. Dicarboxyimide- and dicarboxythioimide-substituted trinaphthylenes and triphenylenes previously prepared by the Maly group to explore the effects of thionation on the mesomorphic properties. ^{29,30}	44
Figure 19. Polarized optical micrographs of Left) 1 at 200 °C, Right) 1 at 217 °C. All micrographs were near the isotropic-columnar phase transition on cooling and were taken at. ..	48
Figure 20. Chemical structure of Lawesson's reagent (54).....	50
Figure 21. Polarized optical micrographs of A) 2 at room temperature before heating, B) 2 at 45 °C, C) 2 cooling from second heating cycle at 230 °C, D) 2 cooling from third heating cycle at 200 °C. All micrographs were taken upon cooling from the isotropic-columnar phase transition.. ..	54
Figure 22. Differential scanning calorimetry plot for triphenylene 2 with a constant scan rate of 5 °C/min on heating.	55
Figure 23. Thermogravimetric analysis plot for triphenylene 2	56
Figure 24. UV-Vis spectra of 2x10 ⁻⁶ M solutions of triphenylenes 1 and 2 in CH ₂ Cl ₂	58
Figure 25. Structures of poly(paraphenylene) derivatives prepared by Yang <i>et al.</i> for blue light-emitting diodes. ⁵⁸	66
Figure 26. Structures of <i>o</i> -dibromoarene substrates tested.	73

LIST OF SCHEMES

Scheme 1. Synthesis of PPy-COF (24) via self-condensation of PDPA (23) as reported by Jiang <i>et al.</i> ³⁵	19
Scheme 2. Yamamoto coupling of <i>o</i> -dibromoarene mediated by the zerovalent nickel complex Ni(COD)(bpy) proposed by Yamamoto <i>et al.</i> ⁴³	24
Scheme 3. Preparation of a series of novel trinaphthylenes (34a-f) via Yamamoto coupling of <i>o</i> -dibromonaphthalene precursors, reported by Bunz and coworkers. ⁴⁴	26
Scheme 4. Synthesis of a nanographene helicene propeller molecule 36 using a Yamamoto-type cyclotrimerization reaction as reported by Gingras and coworkers. ⁴⁵	27
Scheme 5. Nickel-mediated cyclotrimerization of <i>o</i> -dibromoarenes via the Yamamoto coupling reaction.....	30
Scheme 6. Proposed synthesis of tris(dicarboxyimide)triphenylene 1 via Yamamoto coupling of <i>o</i> -dibromoarene 41	31
Scheme 7. Thionation of tris(dicarboxyimide)-substituted triphenylene 1 with Lawesson's Reagent.	32
Scheme 8. Synthesis of hexa(aldehyde)triphenylene 3 via Yamamoto coupling of <i>o</i> -dibromoarene 42	33
Scheme 9. Preparation of novel covalent organic framework 4 via aldol condensation of hexaaldehyde 3 and 1,4-cyclohexanedione.....	34
Scheme 10. Preparation of tetrathiophene via the Yamamoto coupling reaction of 3,4-dibromothiophene, towards the preparation of tetraphenylene 5	35
Scheme 11. Synthesis of extended tetraphenylene 5 from tetrathiophene 32 , via oxidation, [4+2] cycloaddition and oxidative ring closing.	36

Scheme 12. Previously reported synthetic approach to access compound 1 by Wu and coworkers. ⁴⁶	40
Scheme 13. In situ generation of [6]-radialene (48), followed by [4+2] Diels-Alder with N-octylmaleimide (47) and subsequent aromatization.	41
Scheme 14. Retrosynthetic approach to carboximide-substituted triphenylene (1).	43
Scheme 15. Retrosynthetic approach to thioimide-substituted triphenylene 2 from triphenylene 1	45
Scheme 16. Retrosynthetic approach to 2 via thionation of the imide-substituted <i>o</i> -dibromoarene 41 and subsequent Yamamoto cyclotrimerization.	45
Scheme 17. Synthetic route to 1 via Yamamoto coupling of 41	47
Scheme 18. Unsuccessful synthesis of 2 through Yamamoto coupling of thioimide 55	51
Scheme 19. Successful 6-fold thionation of 1 using Lawesson's reagent.	52
Scheme 20. The Yamamoto cyclotrimerization reaction.	62
Scheme 21. Preparation of a series of novel trinaphthylenes (34a-f) via Yamamoto coupling of <i>o</i> -dibromonaphthalene precursors, reported by Bunz <i>et al.</i> ⁴⁴	63
Scheme 22. Synthesis of DO-PPP 61 via Ni(0)-catalyzed coupling of 64 as reported by Yang <i>et al.</i> ⁵⁸	67
Scheme 23. Synthesis of poly(4'-methyl-2,5-benzophenone) macromonomers via Ni(0)-catalyzed coupling as reported by Bloom and coworkers. ⁵⁹	67
Scheme 24. Nickel-catalyzed cycloaddition of <i>o</i> -diiodoarenes with disubstituted alkynes as reported by Cheng and coworkers. ⁶⁰	69
Scheme 25. Synthesis of phenanthridine derivatives in the presence of Ni(dppe)Br ₂ and zinc without additional dppe. ⁶⁰	70

Scheme 26. Synthesis of triphenylenes using NiBr ₂ (PPh ₃) in tetrahydrofuran. ⁶⁰	70
Scheme 27. Proposed nickel(0)-catalyzed mechanism for the [2+2+2] homo-cycloaddition of Ni(0)-assisted generation of benzyne to form triphenylene. ⁶⁰	71
Scheme 28. Proposed retrosynthetic approach to hexaaldehyde-substituted triphenylene 3	85
Scheme 29. Retrosynthetic approach to COF 4 from aldehyde 3	86
Scheme 30. Initial synthetic route attempted to prepare hexa(aldehyde)triphenylene 3	87
Scheme 31. Attempted synthesis of hexa(formyl)triphenylene 3 via protection of aldehyde 42	88
Scheme 32. Synthesis of hexa(methanol)triphenylene 80 from hexa(methyl ester)triphenylene 37	90
Scheme 33. Proposed synthetic approach to novel covalent organic framework (4) via the aldol condensation of hexa(formyl)-substituted triphenylene 3 and cyclohexanedione.....	97
Scheme 34. Retrosynthetic approach to tetraphenylene 5 starting from 3,4-dibromothiophene 43	99
Scheme 35. Synthesis of tetrathiophene 32	100
Scheme 36. Attempted synthesis of oxidized tetrathiophene 83 via Yamamoto coupling of 3,4-dibromothiophene-1,1-oxide 86	103
Scheme 37. Synthesis of dienophile 82 , towards the preparation of an extended tetraphenylene.	104
Scheme 38. Synthesis of dienophile acenaphthylene as a building block towards a novel tetraphenylene by treatment of acenaphthene with DDQ.	105
Scheme 39. Future work, synthesis of extended tetraphenylene derivatives via [4+2] cycloaddition reaction.	106

LIST OF TABLES

Table 1. Summary of Yamamoto coupling results with <i>o</i> -dibromoarenes as reported by Maly and coworkers. ⁵⁵	64
Table 2. Summary of alternative Ni-catalyzed cyclotrimerization reactions vs Yamamoto coupling.....	75
Table 3. Summary of oxidation trials of hexa(methanol)triphenylene 83	91

LIST OF ABBREVIATIONS

Ac ₂ O	acetic anhydride
acac	acetylacetone
APCI	atmospheric-pressure chemical ionization
bpy	2,2'-bipyridine
Ni(COD) ₂	bis(1,5-cyclooctadiene) nickel(0)
dppe	1,2-bis(diphenylphosphino)ethane
BH ₃ -THF	borane-tetrahydrofuran complex
¹³ C NMR	carbon-13 nuclear magnetic resonance
<i>J</i>	coupling constant
COF	covalent organic framework
COD	1,5-cyclooctadiene
OSC	organic semiconductor
OTFT	organic thin film transistor
DMP	Dess-Martin periodinane
DMSO- <i>d</i> ₆	deuterated dimethyl sulfoxide
DSC	differential scanning calorimetry
DMF	dimethylformamide

DMSO	dimethyl sulfoxide
<i>d</i>	doublet
ESI	electrostatic spray ionization
EtOAc	ethyl acetate
eq.	equivalents
Hz	hertz
HOMO	highest occupied molecular orbital
HRMS	high resolution mass spectrometry
LUMO	lowest unoccupied molecular orbital
MHz	megahertz
MOF	metal organic framework
MeOH	methanol
Me	methyl (CH ₃)
<i>m</i>	multipet
Ni(OAc) ₂	nickel(II) acetate
OLED	organic light emitting-diode
<i>p</i> -TsOH	<i>para</i> -toluenesulfonic acid
PAH(s)	polycyclic aromatic hydrocarbon(s)

^1H NMR	proton nuclear magnetic resonance
PCC	pyridinium chlorochromate
<i>q</i>	quartet
rt	room temperature
<i>s</i>	singlet
THF	tetrahydrofuran
PhMe	toluene
NEt ₃	triethylamine
UV-vis	ultraviolet-visible spectroscopy
δ	chemical shift in parts per million (ppm)

CHAPTER 1: INTRODUCTION

1.1 Organic Electronics

For more than 50 years,¹ mainstream electronics have been dominated by thin film transistors based on inorganic semiconductors like silicon.² The fabrication of inorganic-based thin film transistors requires high temperatures and expensive techniques, resulting in high production costs and restriction from being utilized in large-area electronics such as printable, flexible and organic electronics.¹ Recently there has been a wide interest in organic semiconducting (OSC) materials being used in organic thin film transistors (OTFTs) for electronic applications. OSC materials is an emerging field in chemistry and materials science. Research in organic semiconducting materials is allowing electronic and photonic devices to reach new heights and obtain new capabilities.³ Organic semiconducting materials offer an attractive alternative to inorganic materials because of their potentially lower cost, ease of synthesis, ease of processability, lower production temperatures and reduced environmental impact.^{1,4} Significant recent developments have been made in organic semiconducting materials research making them promising candidates for use in next generation electronic devices. Organic semiconducting materials have a wide array of potential applications in the electronics industry. These OSCs are drawing attention for applications such as organic light emitting diodes (OLEDs),¹ organic thin film transistors (OTFTs)^{1,5,6} and organic photovoltaics.^{1,3,7,8} However, current OSCs are facing limitations for their development in potential electronic applications due to limited stability, difficulty in controlling molecular packing and unoptimized charge mobility.

1.2 Polycyclic Aromatic Hydrocarbons

Organic semiconductors based on extended polycyclic aromatic hydrocarbon systems are the focus of intensive research efforts due to their potential applications as components in next generation electronic devices. Polycyclic aromatic hydrocarbons (PAHs) are characterized as two or more fused, π -conjugated rings consisting of purely hydrogen and carbon atoms with the simplest example being naphthalene **6** (Figure 1).

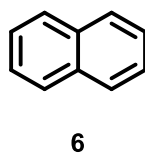


*Figure 1. Simplest example of a polycyclic aromatic hydrocarbon, naphthalene (**6**).*

Polycyclic aromatic compounds are sought after targets for research and development in the fields of organic electronics and related applications due to their extended π -conjugated systems, giving rise to interesting electronic and optical properties.⁹ Furthermore, PAHs are of interest because they are excellent targets for understanding fundamental structure-property relationships.¹⁰ Although polycyclic aromatic compounds offer great promise as components of next generation electronic materials, their inherent instability to photooxidation and photodimerization with increasing size has limited their applications.^{9,11,12} Poor stability of PAHs, especially linear acenes, can be explained by Clar's Sextet rule.¹³ According to Clar's theory, a linear acene regardless of length, contains one aromatic sextet, represented by the circle within the ring (Figure 2).¹³ Hence, only one aromatic sextet is shared among the many rings, in which, increasing size results in a decrease the overall benzenoid character and increase the diene

character.⁹ Adhering to Clar's rule, Figure 2 depicts three linear acenes in an order of decreasing stability; anthracene (**7**), tetracene (**8**) and pentacene (**9**), respectively.

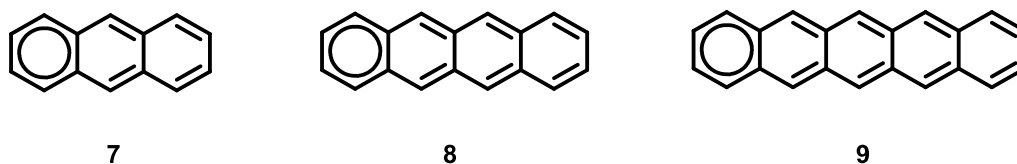


Figure 2. Clar structures of linear PAHs: anthracene (**7**), tetracene (**8**) and pentacene (**9**).

To further explain the stability of PAHs using Clar's theory, Figure 3 displays triphenylene (**10**), a colourless compound possessing low reactivity and tetracene (**8**), an orange compound with high reactivity yet, both compounds contain an identical molecular formula ($C_{18}H_{12}$).¹⁰ This difference in reactivity between these two compounds is attributed to triphenylene containing three full aromatic sextet rings compared to that of tetracene's one aromatic sextet.

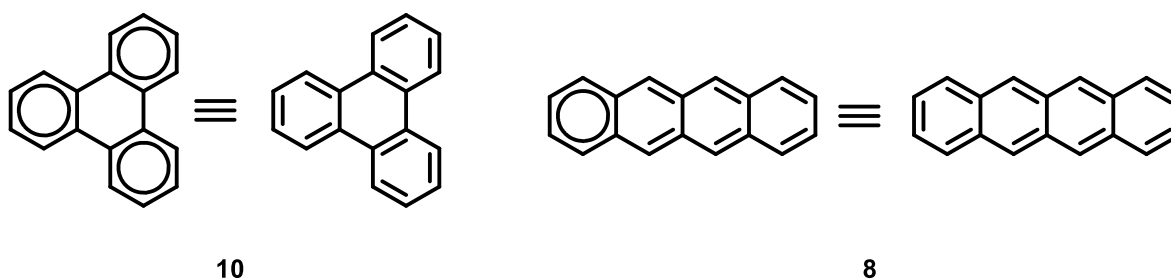


Figure 3. Depiction of Clar sextet rings in PAH examples; triphenylene (**10**) and tetracene (**8**).¹⁰

Polycyclic aromatic compounds which readily undergo photooxidation and photodimerization under any conditions are not suitable for mainstream electronic device applications. To alleviate this phenomenon, researchers have employed different strategies including the installation of electron-deficient substituents and the introduction of various heteroatoms into the PAH framework.^{9,14}

For example, within the class of fused acenes, pentacene (**9**) and its derivatives are the most promising of these materials. Pentacene is at the forefront of semiconductor device performance development studies due to strong absorption in the visible part of the solar spectrum and high charge-carrier mobility in thin film transistors.^{4,14} However, the performance of pentacene-based electronics has been limited due to the stability of pentacene regarding photooxidation and photodimerization.^{11,12,15} In attempts to alleviate the instability as well as improving upon the charge transporting properties of pentacene, Anthony and coworkers described the synthesis of 6,13-(triisopropylsilyl)ethynyl pentacene **11** (Figure 4) in 2001.¹⁶ Not only do the triisopropylsilyl-ethynyl groups allow for improved physical characteristics including, solid-state packing, solubility and orbital overlap, but the chemical stability and resistance to that of photooxidation and photodimerization in comparison to pentacene is also greatly enhanced.

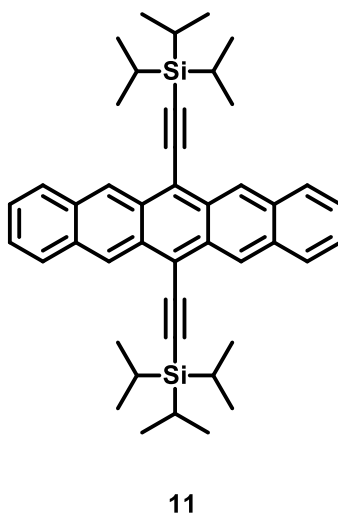


Figure 4. Structure of 6,13-bis(triisopropylsilyl)ethynylpentacene (**11**) as reported by Anthony *et al.*¹⁶

Another strategy to increase the stability of acenes and polycyclic aromatic hydrocarbon is through the introduction of heteroatoms such as nitrogen, sulfur and oxygen into the framework.⁹ More recently, it was found that introduction of two heteroatoms (S, O, N-R) into an acene framework such as pentacene, at the *para*-positions of the central benzenoid ring will produce quinoidal acene-like structures (Figure 5).⁹ The introduction of heteroatoms at these positions within pentacene ultimately decreased the overall diene-character, thus increasing the stability against photooxidation and photodimerization. Although compound **12** is no longer considered an acene, but an acene-analogue, the introduction of heteroatoms into the acene framework is an efficient method to improve the stability of acene-based materials as the quinoidal conjugation allows for one more additional aromatic sextet ring in comparison to normal acene, such as pentacene (**9**).⁹

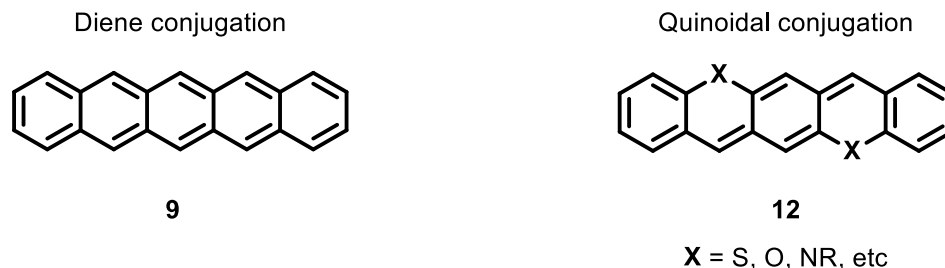


Figure 5. Structures of an acene (pentacene) with diene conjugation (**9**) and an acene-analogue with quinoidal conjugation as a result of the introduction of heteroatoms (**12**).

Unquestionably, further effort is required to develop suitable polycyclic aromatic compounds that combine stability, efficiency, low cost, and a clean and scalable synthetic process. In addition, researchers will need to facilitate deeper analyses of structure-property relationships through the synthesis of novel PAHs to investigate and provide insight on how the structure of PAHs can be used to predict subsequent properties.

1.3 Liquid Crystals: Disc-Shaped Aromatic Compounds

Liquid crystals are alluring materials with noteworthy electronic and optoelectronic capabilities.^{17,18} The liquid crystalline state is considered to be the fourth state of matter, an intermediate phase between solid and liquid, sharing both the properties of isotropic liquids and crystalline solids, referred to as a mesophase.¹⁷ Liquid crystalline architectures are a highly diverse group of materials ranging from DNA in biological systems to small organic molecules found in electronic displays. The numerous applications of liquid crystals are ever-present, to be specific, they are most well-known for their use in optoelectronic devices functioning as displays in watches, calculators, cell phones, computers and televisions.^{17,18} Two categories of liquid crystals

exist, thermotropic and lyotropic. The thermotropic class is defined as a material that displays a liquid crystalline phase dependent on temperature in the absence of a solvent.^{17,18} In contrast, the lyotropic class of liquid crystals contains materials that exclusively form a liquid crystalline phase in the presence of an appropriate solvent.^{17,18} Thermotropic liquid crystals can be further classed into two sub-categories based on molecular shape. Calamitic liquid crystals are characterized by their rod-like shape on the other hand, discotic liquid crystals possess disk-like architectures.

Discotic liquid crystals are a unique and well-studied class of PAHs due to their charge transport and self-annealing properties,¹⁸ thus making them potential candidates as materials in organic electronics as next generation light emitting diodes,^{14,17–19} photovoltaic devices^{17,18} and field effect transistors^{17–19}. A discotic liquid crystal consists of a rigid disc-shaped polycyclic aromatic core bearing three to eight peripheral flexible side chains.^{17,20} As a result of their unique structure, discotic mesogens will self-assemble into extended π -stacked columns.¹⁸ Consequently, the extensive π -overlap within the columnar liquid crystal phase (mesophase) allows charge transport to occur along the columns.¹⁸ It is this feature that makes discotic liquid crystals promising candidates as semiconducting materials in organic electronics. To this date, the number of discotic liquid crystals derived from more than 50 unique aromatic cores is approximately 3000.¹⁷

Substituted triphenylenes are a well-known class of discotic mesogens containing a rigid aromatic core and generally three to eight flexible side chains (Figure 6, left). The characteristic shape of triphenylenes is represented by a flat disk (Figure 6, right). These disk-like molecules self-assemble on top of one another to form π -stacked columns (Figure 6, right). Hexaalkoxytriphenylenes (**13**) are notably one of the most widely studied triphenylene-based discotic mesogens, displaying a mesogenic columnar phase over a broad temperature range.^{21,22}

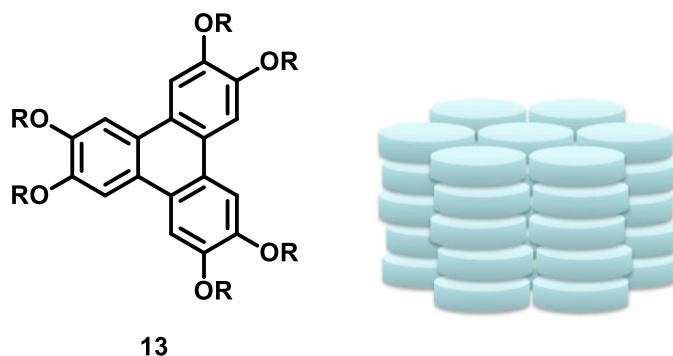
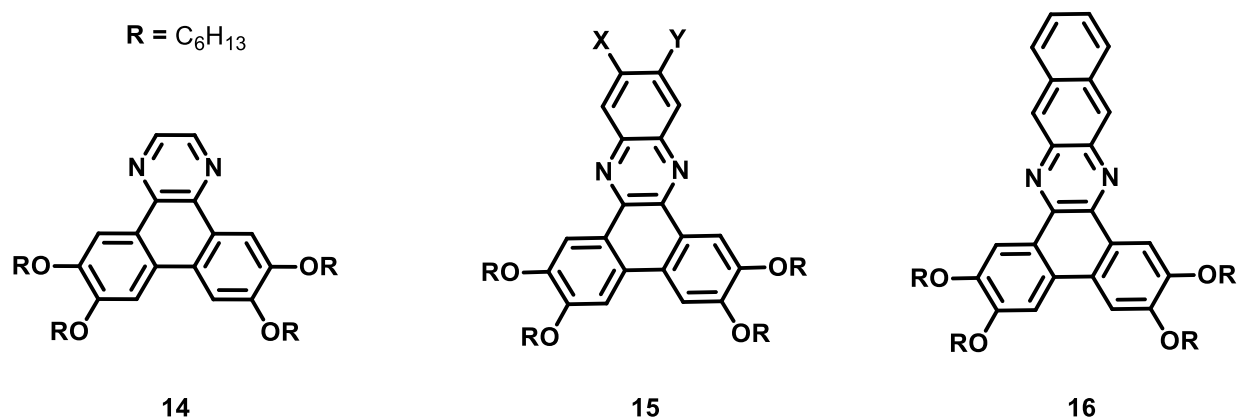


Figure 6. Representation of a common stacking-type arrangement discotic liquid crystals like, *hexaalkoxytriphenylenes (13)*.

Moreover, there is an incredibly high interest in determining how the molecular composition (core structure and substituents) of discotic mesogens affects the liquid crystalline properties to build ideal structurally stable liquid crystalline materials with broad columnar phases. Recently, several research papers have described the installation of electron-withdrawing substituents and the subsequent promotion of broad columnar phases of discotic mesogens.^{23–26}

Extended triphenylene-type compounds have also been shown to display columnar liquid crystalline phases. In a 2006 paper,²⁶ Williams and coworkers prepared a series of novel disk-shaped molecules with increasing core size and varying substituent attachments. The objective of this study was to investigate the structure-property relationships between core size and substituent type on self-assembly of columnar liquid crystalline phases. Firstly, the effects of core size on columnar mesophase formation were assessed. Williams and coworkers determined that both compounds **14** and **15** (Figure 7), where X and Y are hydrogen substituents, are non-mesogenic.²⁶ In contrast, compound **16** is liquid crystalline over a broad temperature range.²⁶ Thus, these

findings imply that molecules with increased core size have a greater tendency to form columnar liquid crystalline phases.²⁶



*Figure 7. Series of disk-shaped compounds; dibenzo[f,h]quinoxaline (**14**), dibenzo[a,c]phenazine (**15**) and tribenzo[a,c,i]phenazine (**16**) with increasing core size prepared by Williams et al.²⁶*

Furthermore, the effects of substituents on columnar mesophase formation was examined via the synthesis of a series of a dibenzo[a,c]phenazines (Figure 8).²⁶ Compound **15** containing electron-withdrawing (**15a-f**) substituents was directly compared to its electron-donating derivatives (**15g-k**). Interestingly, it was found that compound **15** formed columnar mesophases when electron-withdrawing substituents (**15a-f**) were incorporated.²⁶ Conversely, compound **15** bearing electron-donating groups (**15g-k**) was found to be nonmesogenic.²⁶ In addition to this, the clearing temperatures of the columnar mesophases of **15** increased with an increase in the electron-withdrawing nature of the substituents where **15e** bearing the nitro substituent displayed the highest clearing point of the series. The structure-property study performed by Williams is an

excellent example of how core size and type of substituent can influence the liquid crystalline properties exhibited by disk-shaped molecules.

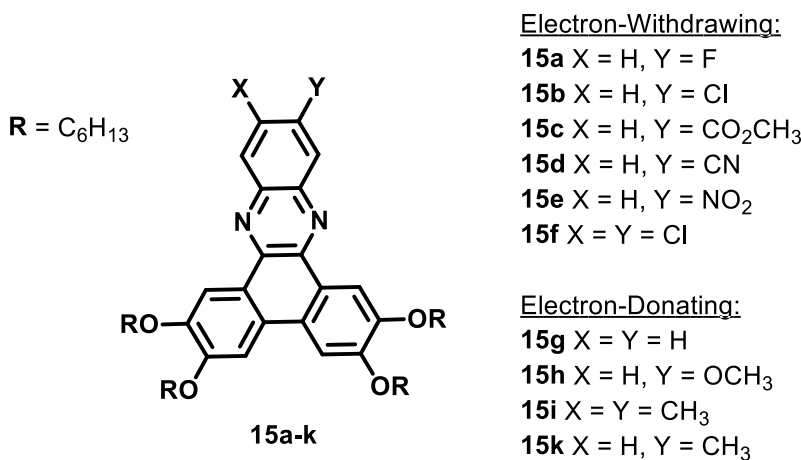


Figure 8. Dibenzo[*a,c*]phenazine (**15a-k**) series prepared by Williams *et al.*²⁶

Based on the previous research above, Maly and coworkers published a 2014 paper describing the synthesis of a dibenzo[*a,c*]anthracene series bearing electron-withdrawing imide-groups.²⁷ The hypothesis was that the dibenzanthracene derivatives could be designed to exhibit broad columnar mesophases with a lower melting transition and high clearing point through the installation of an electron-withdrawing imide-group bearing a flexible alkyl chain. This theory stemmed from previous examples of imide-containing compounds (e.g. perylene bisimides) being used in electronic applications as electron-accepting materials due to their inherent photochemical stability and high transport properties.²⁸ In addition to the favourable electron-withdrawing nature of imide-groups that stabilize the columnar phase and increase the clearing point, *N*-substitution allows flexible alkyl side chains to be introduced into the compound without compromising the electron-withdrawing effect of the imide group. These *N*-alkyl substituents may be strategically

exploited to disrupt the stability of the crystalline phase and lower the melting transition temperature of solid-to-mesophase.

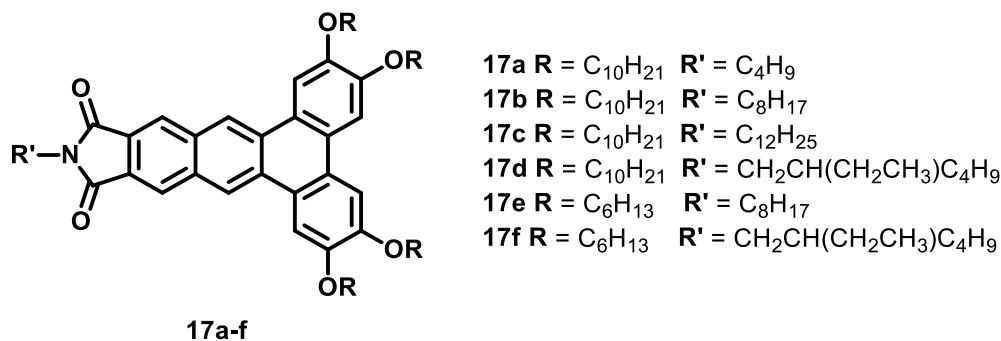


Figure 9. Dibenz[*a,c*]anthracenedicarboximide (**17a-f**) series prepared by Maly et al.²⁷

Moreover, Maly and coworkers determined that as the *N*-alkyl chain length increased, the columnar mesophase of **17a-c** was broadened primarily due to the lowering of the melting transition temperature.²⁷ Interestingly, **17d** containing the branched *N*-alkyl substituent did not show any destabilization of the columnar mesophase and conversely showed a decrease in the melting transition point. As a consequence of this, **17d** showed the broadest columnar mesophase of the series suggesting that branched chain substitutions can favourably broaden the mesophase by disrupting the crystalline phase all while playing no effect in destabilizing the mesophase.²⁷ Furthermore, a similar trend was noticed with compounds **17e** and **17f**. The trends observed in the dibenz[*a,c*]anthracenedicarboximide series by Maly and coworkers demonstrated that the introduction of an imide group bearing flexible alkyl chains to the aromatic core produced stable discotic materials with broad columnar temperature ranges.²⁷

In a subsequent 2016 study,²⁹ Maly *et al.* investigated the influence thionation has on self-assembling properties of a novel discotic dibenz[*a,c*]anthracenecarboximide series **17b** and **17d** (Figure 10). It was anticipated that the replacement of one or both carbonyl functionalities of the dibenz[*a,c*]anthracenecarboximides with thiocarbonyl groups would allow subsequent tunability of the mesophase as well as the lowering of the lowest unoccupied molecular orbital (LUMO) energy levels, both of which are attractive features for materials in potential electronic device applications.²⁹ In this series, compounds **17b**, **17d** and **18a** through **19b** exhibit a columnar mesophase over a broad temperature range however, there is a slight increase in the melting transition point with increasing thionation.²⁹ This finding suggests that increasing thionation stabilizes the crystalline phase due to improved intermolecular interactions involving the sulfur atom. In addition to sulfur effects on the columnar phase, the alkyl chain substituent was also considered, leading to the realization that in fact, thionation only displayed a subtle influence on mesophase stability.

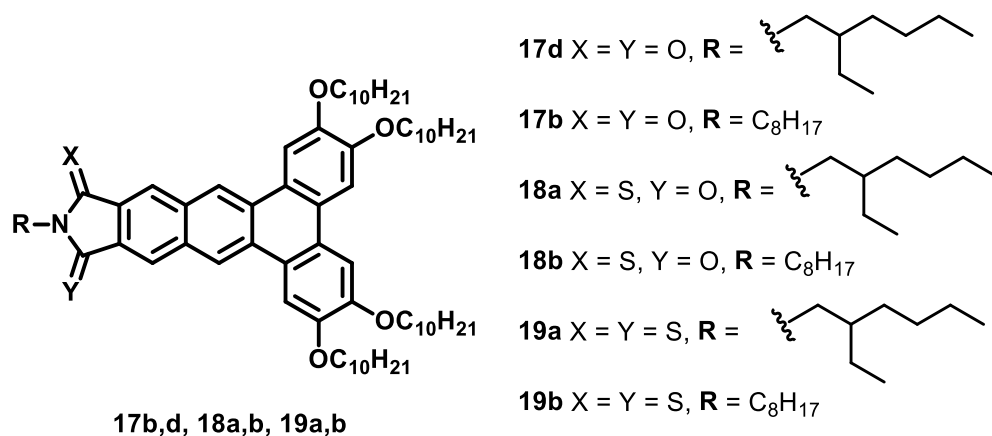


Figure 10. Dibenz[*a,c*]anthracenedicarboxy-imide and -thioimide series (**17b,d**, **18a,b** and **19a,b**) prepared by Maly and coworkers.²⁹

Furthermore, the self-assembly of the dibenzanthracenecarboximides and thionated derivatives in solution was also investigated via proton NMR concentration studies. The results obtained present a general trend of increasing self-assembly in solution with increasing thionation thus, implying that thionation may be a method to impart improved self-assembly on imide-bearing cores.²⁹ In addition to this, the spectroscopic properties of branched derivatives **17d**, **18a** and **19a** were studied. Ultraviolet-Visible (UV-Vis) spectra of the branched derivatives showed a red shift with increasing thionation suggesting that increasing sulfur content reduces the highest occupied molecular orbital (HOMO)-LUMO gap.²⁹ To further investigate the effects of thionation on the dibenzanthracenedicarboxyimide series, cyclic voltammetry and density functional theory calculations were utilized to experimentally and theoretically calculate the HOMO and LUMO energies and thus the HOMO-LUMO gap. The results collected by Maly and coworkers are consistent with the findings of Seferos and others, where increasing thionation consequently leads to a decrease in the HOMO-LUMO gap of compounds **20-22** mainly due to the lowering of the LUMO energy, an attractive quality for materials in device applications.²⁹ Overall, Maly showed that thionation can be utilized to tune the electronic properties of imide-containing columnar liquid crystalline materials without detrimentally affecting the liquid crystalline properties, and that thionation may be a promising new method to designing novel electron-deficient discotic liquid crystals.

Subsequently, Maly and coworkers extended this study on the effects of thionation on the self-assembling properties of a series of triphenylenedicarboxyimides (**20a, b**) (Figure 11).³⁰ Maly and coworkers proposed that the replacement of one or both of the imide carbonyl functionalities with thiocarbonyl groups, would allow access to tuning of the self-assembly and mesomorphic

properties as well as lowering the LUMO energy and the HOMO-LUMO band gap. The results obtained in this work were directly compared to the data collected on the dibenzanthracene series prepared in 2016. All of the triphenylenedicarboxy-imide and -thioimide derivatives displayed broad columnar liquid crystalline phases, however, the temperature range of the mesophase was slightly narrower compared to that of the dibenzanthracene series.³⁰ This finding was likely due to the larger core size of the dibenzanthracenes promoting the formation of a stable mesophase in a more effective way, in comparison to the smaller triphenylene core.²⁶

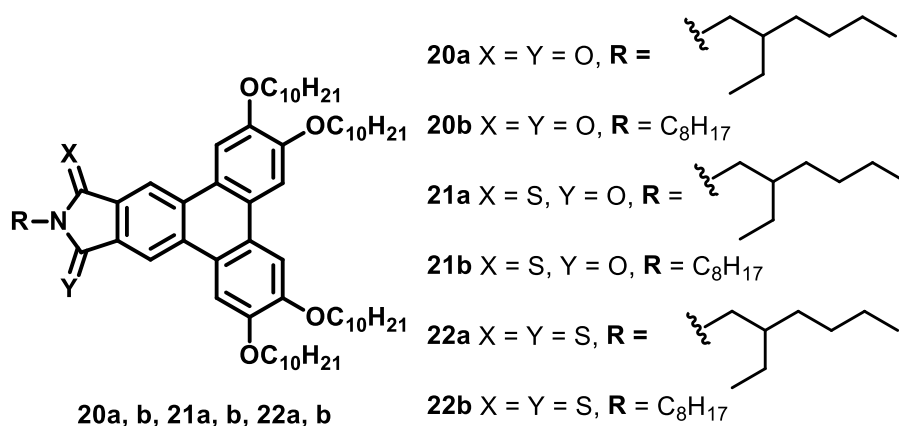


Figure 11. Triphenylenedicarboxy-imide and -thioimide series (20-22) prepared by Maly et al.³⁰

Moreover, when comparing the melting transition point from crystalline solid to the liquid crystalline phase the data showed a similar trend to that seen with the dibenzanthracene series. The trend revealed that the thionated derivatives exhibited higher melting transition points with increasing thionation, implying that the sulfur atoms are contributing to the stabilization of the crystalline phase. In contrast, the clearing transition temperatures from liquid crystalline to isotropic liquid were compared. It was found that with the linear chain triphenylene derivatives

that an increase in the clearing point temperature was observed between the parent imide (**20b**) and the monothionated derivative (**21b**) however, the dithionated derivative (**22b**) did not experience any further increase in the clearing point temperature.³⁰ Furthermore, the branched chain triphenylene derivatives (**21a** and **22a**) showed an increase in clearing point with increasing thionation compared to the parent imide derivative, results that are consistent with the previously studied dibenzanthracene series.³⁰ The self-assembly of the triphenylene derivatives was investigated using variable concentration proton NMR studies where a slight trend of increasing self-assembly in solution was observed with an increase in thionation.³⁰ The spectroscopic properties of these materials were probed. The UV-Vis absorbance spectra for **20a**, **21a** and **22a** were compared and distinctly showed a bathochromic shift in the absorbance spectra with increasing thionation, analogous to the results obtained with the dibenzanthracene series.³⁰ Finally, the electrochemical properties of the triphenylene derivatives bearing the branched alkyl chains were investigated via cyclic voltammetry and computational studies which showed that increasing thionation lowers the LUMO energy and narrows the HOMO-LUMO band gap.³⁰ Ultimately, Maly and coworkers showed that triphenylenes bearing an electron-withdrawing imide and thioimide functionality displayed broad columnar phases where the clearing point temperatures were affected by both the degree of thionation and structural composition of the *N*-alkyl substituent. Furthermore, a slight increase in self-assembly in solution was observed with increasing thionation as well as a decrease in the LUMO and HOMO-LUMO energies when compared to the parent imide derivative. These results, with regards to the data obtained with the dibenzanthracene series, show that thionation may be a viable way to tune and design novel electron-withdrawing discotic liquid crystalline materials containing an imide-group without negatively effecting the mesophase.

The sheer number of discotic liquid crystals derived from more than 50 unique aromatic cores equates to approximately 3000 derivatives.¹⁷ Although discotic liquid crystalline materials are a well known and well studied group of compounds, they still remain in a somewhat immature phase of preparation as commercial device applications have yet to be realized. Importantly, much work is still required to form a better understanding of the structure-property relationships these discotic architectures display. Understanding and having the ability to predict functions and properties of discotic liquid crystals based on structure is the key to designing ideal discotic mesogens for organic electronic applications. Currently, research is a long way away from being able to predict structure-property relationships of discotic mesogens. However, if research continues on the path of discovering novel discotic liquid crystals and investigating the effects substituents and core size have on liquid crystalline properties, device applications do not seem so farfetched and may be realized in the near future.

1.4 Covalent Organic Frameworks

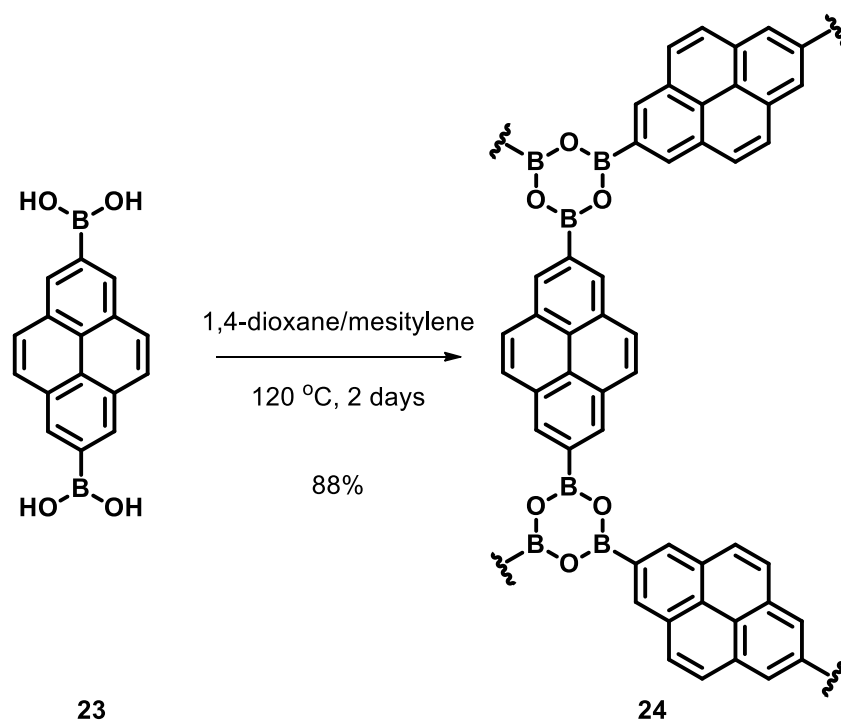
Macromolecular structures containing pores such as cavities, channels or interstices are classified as porous materials.³¹ The applications of porous materials are dependent on their individually varying properties such as size, arrangement and shape of pores as well as the overall composition of the material itself.³¹ Intense efforts are being made in the field of materials science to better understand the structure-property relationships of these porous materials with the ultimate goal of being able to manipulate the structures of porous materials in order to illicit desired functions for specific applications. The development of porous materials has come a long way over recent years, primarily due to the advancement of modular construction of these nanostructures. This has lead to the progress of a suite of porous materials including, metal-organic frameworks

(MOFs),^{32,33} which metal atoms and organic ligands are held together by coordination bonds, and covalent organic frameworks (COFs), which are constructed of carbon and other light elements in a covalently linked framework.³¹ In particular, covalent organic frameworks have garnered much interest as functional nanostructures due to their potential design opportunities and various applications. Moreover, covalent organic frameworks combine high crystallinity, tunable pore sizes, large surface area and unique architectures thus, allowing them to be used in a wide range of applications such as gas storage and separations, catalysis, environmental remediation, sensing, enzyme and drug uptake and materials science.^{31,34}

Covalent organic frameworks are primarily constructed using a bottom-up approach, meaning, that smaller subunits are designed and then linked together through reversible covalent bond formations. Slightly reversible condensation reactions of organic linkers are utilized to build COFs.^{31,34} As a consequence, the covalent bonds formed establish a thermally stable framework. However, the reversible nature of the coupling reactions allow for the formation of a crystalline structure as the reversible nature permits for error correction and rearrangement of the network.³⁴ COF synthesis has been successful in expanding an ever growing assortment of COF materials linked by a variety of organic linking groups primarily containing B-O, C-N, and C-C bonds.^{31,34} The types of linkages commonly seen in COFs include, boroxines, boronic esters, imines, hydrazones, azines, and ketoenamines, all of which affect the properties displayed by COF materials and their subsequent applications.³⁴

Covalent organic frameworks containing polycyclic aromatic hydrocarbon units, with well-defined crystalline structures are of particular interest for use as semiconductors due to their potential of forming conduction pathways that transports charge across the framework. For example, Jiang and coworkers reported the synthesis of the first photoconductive covalent organic

framework **24** via the self-condensation of 2,7-pyrenediboronic acid (PDPA) under solvothermal conditions (Scheme 1).³⁵ Characterization of PPy-COF showed that **24** was a super-microporous crystalline macromolecule with a perfectly eclipsed arrangement of polypyrene sheets in 2D that favours exciton migration and carrier transport.³⁵ The photoconductivity of PPy-COF was investigated via preparation of devices containing **24** deposited between Al and Au electrodes. The COF device was highly responsive to light irradiation and is capable of repetitive on-off photocurrent switching with large on-off ratios.³⁵ Jiang's unique design of **24** led to the formation of the first reported photoconductive COF that displayed unprecedented properties at the time. The novel work completed by Jiang and coworkers was ultimately a step in the right direction towards the use of COFs in optoelectronic and photovoltaic applications.



Scheme 1. Synthesis of PPy-COF (**24**) via self-condensation of PDPA (**23**) as reported by Jiang *et al.*³⁵

With the diverse range of synthetic chemistry methodologies available, a suite of different functionalities, and numerous possible designs and applications, the scope of COF synthesis is seemingly endless. Furthermore, the geometry, size, and the framework structure of COFs can be specifically tuned using appropriately functionalized organic linkers and post synthetic transformations.³¹ With this in mind, COFs are specifically designed to have low density through the incorporation of light elements, high stability via strong covalent bonds, high crystallinity, porosity, and modularity, which allows for the adjustment of the structure and properties of COFs.³¹ The boundless design and functionality potential of COFs make them attractive targets for studying structure-property relationships and an array of applications such as gas storage and

separations, catalysis, environmental remediation, sensing, enzyme and drug uptake and materials science.^{31,34}

1.5 Supramolecular Chemistry and Nonplanar Polycyclic Aromatic Hydrocarbons

The development of novel macrocyclic host molecules is an important research area in the advancement of host-guest supramolecular chemistry. Various classes of macrocyclic hosts have been prepared in previous years including, crown ethers, cyclodextrins, calixarenes, cyclophanes, triptycene- and tetraphenylene-based macrocycles to name a few.^{36,37} The unique conformational and cavity structures and molecular recognition properties of these host molecules allows for a wide range of potential applications in molecular machines, supramolecular chemistry, materials science and biological chemistry.^{36,38} Moreover, further exploration of efficacious syntheses of novel, functional host molecules is required to realize the potential applications of these materials in biological and supramolecular chemistry.

Tetraphenylene (**25**) is a rigid, nonplanar polycyclic aromatic compound possessing a saddle-shape conformation due to the formal antiaromaticity of the central 8-membered ring (Figure 12).³⁹ The unique structure of tetraphenylene makes it an interesting target for supramolecular chemistry applications as a binding-host of curved structures like, fullerenes and other organic compounds.

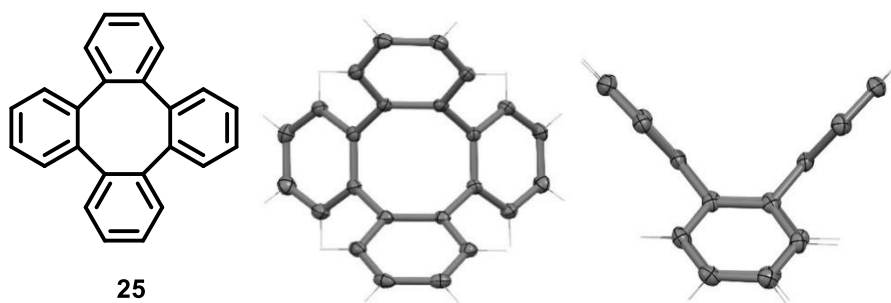


Figure 12. Chemical and X-ray crystallographic structures of tetraphenylene (**25**).³⁹

Tetraphenylene-derivatives have been prepared and utilized as building blocks in larger macrocycles for a variety of supramolecular chemistry applications including molecular devices, asymmetric catalysis, molecular recognition and materials science.³⁷ However, tetraphenylene's supramolecular properties have not been extensively explored.

In a 1987 review paper published by Wong *et al.*,⁴⁰ discusses the first syntheses accessing tetraphenylene and related substituted and extended derivatives as well as the subsequent abilities of these derivatives to bind a variety of guest molecules. Wong *et al.* tested tetraphenylene's ability to bind a suite of guest molecules including but not limited to, chloroform, carbon tetrachloride, benzene, and cyclohexane. It was determined via X-ray crystallographic studies that the cavity size of tetraphenylene was able to adapt to accommodate the steric requirements of various guest molecules tested.⁴⁰ Furthermore, Wong *et al.* reviewed the synthesis of a variety of tetraphenylene derivatives such as substituted tetraphenylenes, tetraphenylenes fused with carbocycles and heterocycles, heterocyclic tetraphenylenes and finally tetraphenylene endoxide.⁴⁰ Subsequent X-ray crystallographic studies of the numerous tetraphenylenes prepared have showed that they are a promising class of compounds for host-guest applications.

More recently, a 2015 paper published by Wong *et al.*³⁷ communicated the preparation of novel substituted tetraphenylenes and the ensuing preparation of novel tetraphenylene-based macrocycles. Substituted tetraphenylenes are difficult to access and are reported to be challenging to prepare and usually obtained in low yields.^{37,40} Direct aromatic substitution reactions can be performed on tetraphenylenes however, it is difficult to predict the substitution patterns. Consequently, substituted tetraphenylenes are typically accessed via precursors containing the desired substituents thus leading to tetraphenylenes with substituents at the desired positions.⁴⁰ The latter method was exploited by Wong *et al.* to access substituted tetraphenylene **26** (Figure 13). However, the synthesis was cumbersome and met with limited success as **26** was obtained in a 3% overall yield starting from the appropriately substituted precursors.

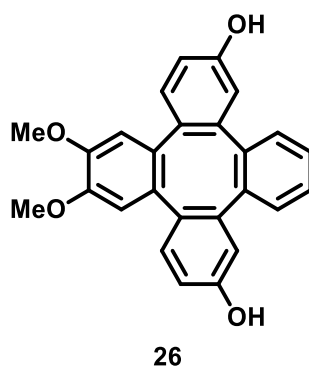


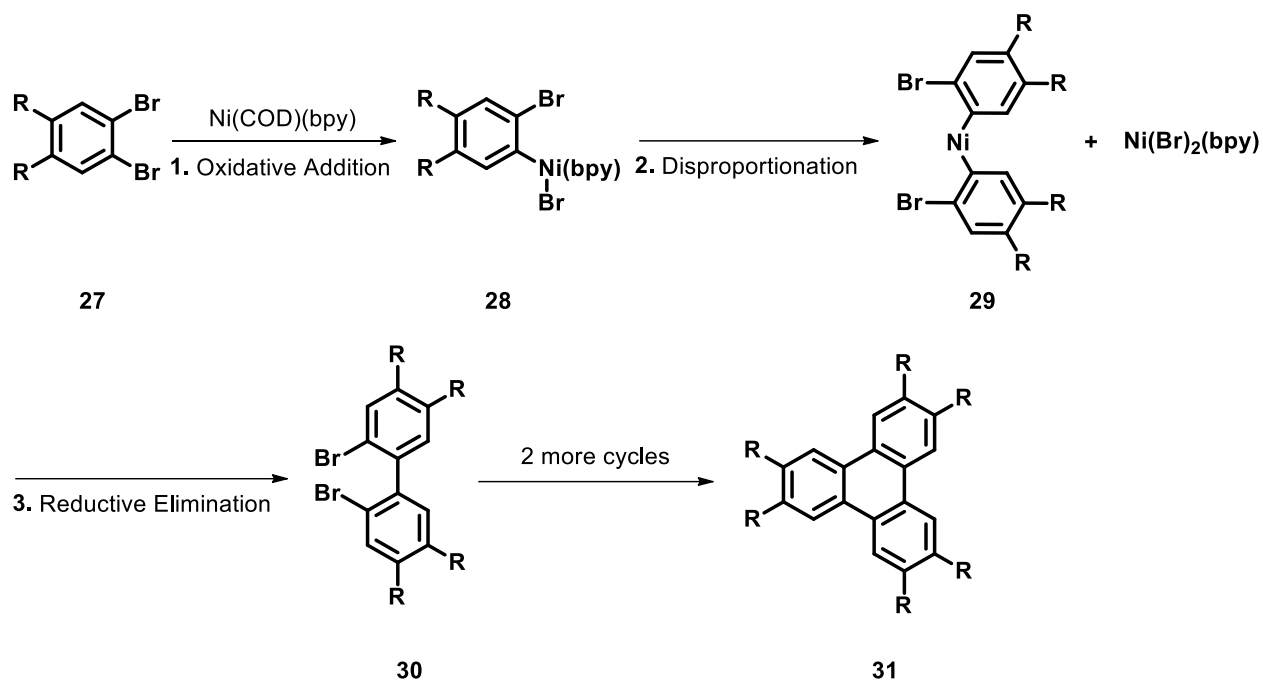
Figure 13. Novel substituted tetraphenylene precursor prepared by Wong *et al.*³⁷

Moreover, the desired macrocycles prepared using **26** as the primary building block were accessed in low yields. Subsequent structural studies via X-ray crystallography and molecular modelling showed that the tetraphenylene macrocycles have well-defined structures with suitable cavities that were able to bind fullerenes C₆₀ and C₇₀.³⁷ Overall, the results obtained in this study

will promote more research based on tetraphenylene derivatives in host-guest chemistry applications.

1.6 The Yamamoto Coupling Reaction

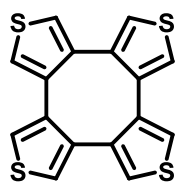
Transition-metal promoted couplings of organic halides has played an important role in synthetic organic chemistry (e.g., Suzuki-Miyaura and Heck reaction) for the formation of carbon-carbon bonds.⁴¹ Moreover, zerovalent nickel complexes are known to react with aryl halides to afford dehalogenative carbon-carbon coupling products.⁴² The Yamamoto coupling is a dehalogenative carbon-carbon coupling reaction of *o*-dibromoarenes and other *o*-dihaloarene compounds. The Yamamoto coupling utilizes zerovalent nickel complexes consisting of a mixture of bis(1,5-cyclooctadiene)nickel(0) [Ni(COD)₂], 1,5-cyclooctadiene (COD), and the neutral ligand 2,2'-bipyridine (bpy) in an appropriate solvent such as dimethylformamide (DMF) or tetrahydrofuran (THF).^{42,43} The Yamamoto coupling proceeds through a catalytic cycle (Scheme 2), involving the oxidative addition of an *o*-dibromoarene **27** to Ni(COD)(bpy) to give (**28**).⁴³ Subsequently, disproportionation occurs to give Ni(Br)₂(bpy) and Ni(Ar)₂(bpy) **29**.⁴³ Finally, **29** undergoes reductive elimination, the rate-limiting step of this reaction, to yield biaryl **30**.⁴³ In addition to this, the dibromobiaryl compound **30** may undergo two more subsequent Yamamoto coupling cycles to form triphenylene **31**, as seen in Scheme 2 or in some cases, the tetramer, which is not shown.



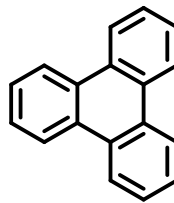
Scheme 2. Yamamoto coupling of *o*-dibromoarene mediated by the zerovalent nickel complex

Ni(COD)(bpy) proposed by Yamamoto *et al.*⁴³

The Yamamoto coupling has been reported to form both tetracyclic and tricyclic materials. For example, Yamamoto *et al.* reported the formation of cyclotetrathiophene (**32**) and triphenylene (**10**) via the Yamamoto coupling of the respective *o*-dibromoaromatic precursors in higher yields than originally described (Figure 14).⁴²



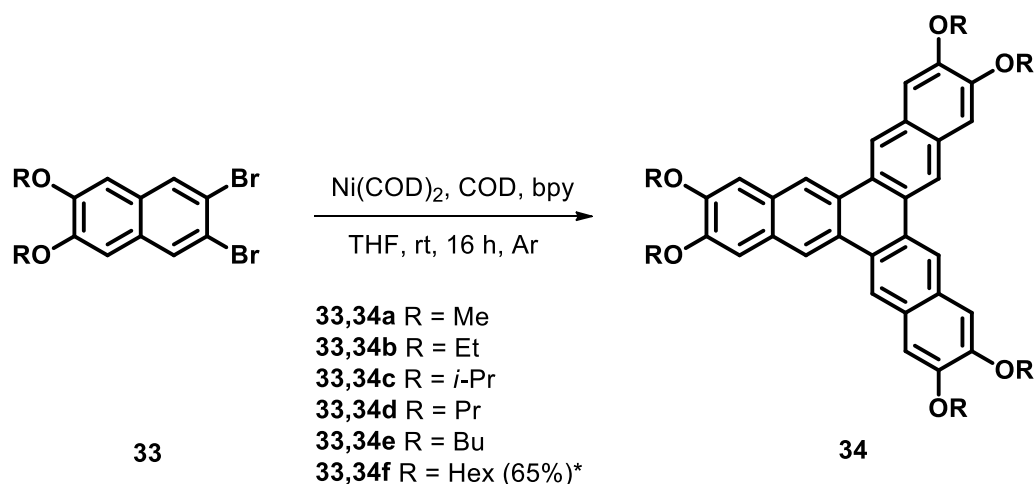
32



10

Figure 14. Tetracyclic (**32**) and tricyclic (**10**) materials prepared by Yamamoto *et al.* via the Yamamoto coupling.⁴²

Furthermore, Bunz and coworkers reported the successful synthesis of a series of novel hexakis(alkoxy)trinaphthylenes via the Yamamoto coupling.⁴⁴ By using the nickel-mediated Yamamoto coupling, Bunz and coworkers dramatically shortened the synthesis of hexakis(alkoxy)trinaphthylenes (**34a-f**). The original synthesis of trinaphthylene **34f**, described by Maly *et al.* is a cumbersome 4-step sequence starting from dibromonaphthalene **33f** with a total overall yield of 23%.²⁵ Scheme 3 shows the synthetic conditions Bunz developed for the efficient 1-step process from **33a-f** to afford trinaphthylenes **34a-f** in 38-65% yields.⁴⁴

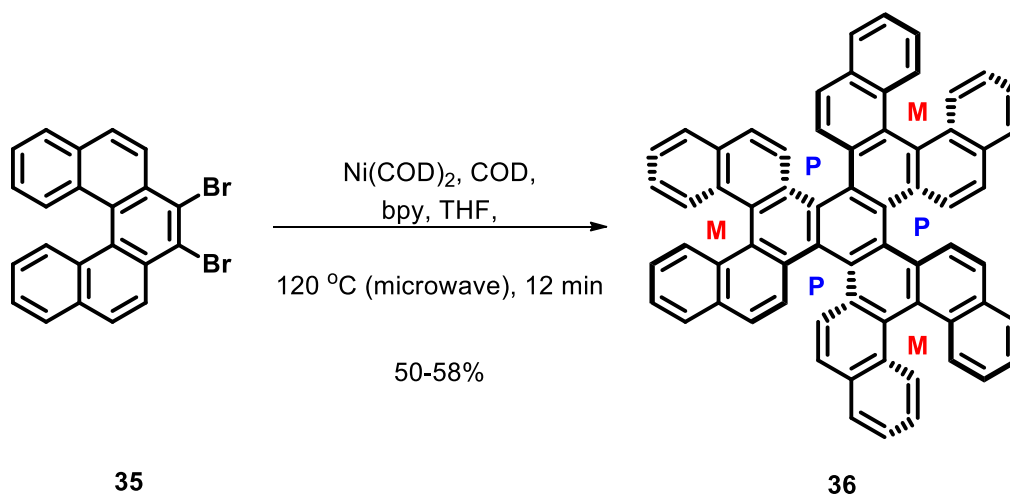


Scheme 3. Preparation of a series of novel trinaphthylenes (34a-f) via Yamamoto coupling of o-dibromonaphthalene precursors, reported by Bunz and coworkers.⁴⁴

Bunz and coworkers showed that by using the Yamamoto coupling protocol hexa(substituted)-trinaphthylenes could be easily accessed in an efficient, short, and high yielding process. Moreover, this discovery shows the synthetic utility of the Yamamoto coupling reaction as a viable approach to access extended triphenylene type systems, in this case, trinaphthylenes.

Another excellent example displaying the synthetic capabilities of the Yamamoto coupling reaction was demonstrated by Gingras *et al.* in a 2017 publication.⁴⁵ Gingras and coworkers reported the synthesis of a chiral propeller-shaped D_3 -symmetric polycyclic aromatic hydrocarbon **36** containing [5]helicene units bent in and out of the plane of the molecule. The synthesis of propeller **36** is shown in Scheme 4.⁴⁵ 7,8-dibromo[5]helicene **35** is reacted under modified Yamamoto cyclotrimerization conditions in the presence of Ni(COD)_2 , 1,5-cyclooctadiene, and 2,2'-bipyridine in tetrahydrofuran at 120 °C under microwave irradiation to form **36** in fair yields ranging from 50-58%.⁴⁵ Notably, this modified Yamamoto coupling is completed after 12 minutes of reaction time at 120 °C using a microwave reactor, as compared to the originally reported

Yamamoto coupling conditions at room temperature and requiring a reaction time of approximately 24 hours to prepare cyclotrimer derivatives.⁴²



Scheme 4. Synthesis of a nanographene helicene propeller molecule **36** using a Yamamoto-type cyclotrimerization reaction as reported by Gingras and coworkers.⁴⁵

The synthetic utility of the Yamamoto coupling was further displayed in the synthesis of a series of electron-deficient triphenylenes **37-39** and trinaphthylene **40** (Figure 15) by our group where we explored the scope of the Yamamoto coupling reaction with a focus on the synthesis of electron-deficient triphenylenes and related analogs which are otherwise difficult to prepare.

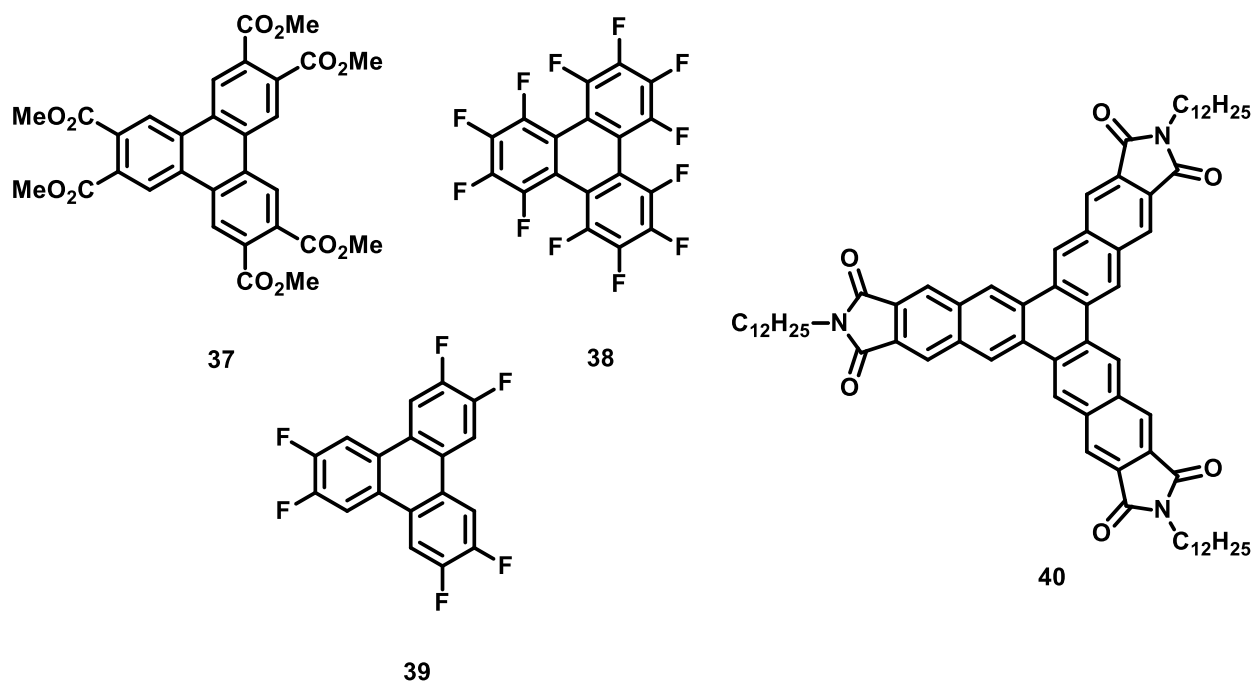


Figure 15. Suite of electron-deficient triphenylenes (**37-39**) and trinaphthylene (**40**) derivatives previously prepared in the Maly lab.

Triphenylene derivative **37** was prepared in 74% yield, while fluorinated triphenylenes **38** and **39** were prepared in 20% and 44%, respectively. The lower yields of **38** and **39** is most likely due to the low tolerance of the fluoro-functional groups under the Yamamoto coupling conditions. In contrast, trinaphthylenedicarboxyimide **40**, was prepared in an efficient 70% yield. Thus far, no clear trends were observed with respect to the electron-withdrawing group functionality on the substrate being tested. Moreover, further assessment of the tolerance of electron-withdrawing groups under the Yamamoto coupling reaction conditions is required to broaden the scope of the reaction and understand the limitations.

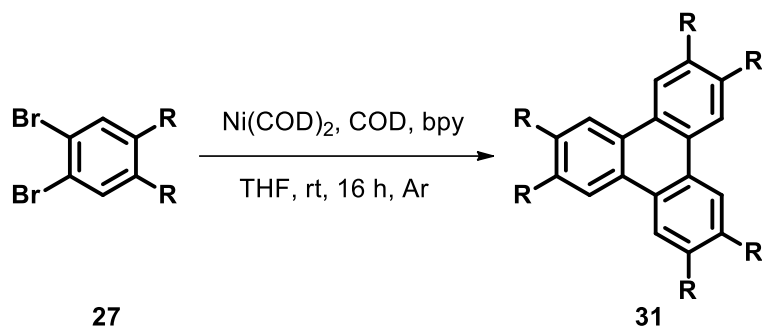
1.7 Research Objectives

The overall goal of the proposed research is to synthesize and study the structure-property relationships of novel polycyclic aromatic compounds capable of self-assembling to form liquid crystalline, and microporous structures, as well as molecules capable of molecular recognition. Ultimately, this research project hopes to provide further insight into how aromatic systems self-assemble and assist in guiding the design of novel materials with favourable properties, as well as contributing to the field of organic chemistry through the synthesis of novel polycyclic aromatic compounds.

The development of new conjugated organic molecules for organic electronic and supramolecular chemistry applications has garnered much attention over the past several years. Polycyclic aromatic hydrocarbons are attractive targets for organic electronic and supramolecular chemistry applications due to their self-assembling properties via π -stacking interactions, allowing these materials to act as semiconductors or as host-molecules, depending on their structure. Due to the favourable properties exhibited by polycyclic aromatic hydrocarbons, they have the potential to become components of next generation organic electronic devices such as displays and solar cells, and in next generation supramolecular chemistry applications in sensing and catalysis. Although significant progress has been made in the development of functional organic compounds for large scale material science applications, current limitations in stability, solubility, controlling molecular packing, and unoptimized properties have thus far restricted their integration into mainstream devices and applications.

The unifying theme that connects this research is the utilization of the Yamamoto coupling reaction (Scheme 5) to access the desired polycyclic aromatic hydrocarbon targets. More specifically, the scope of the Yamamoto coupling reaction will be further explored for the synthesis

of electron-deficient triphenylene derivatives that are otherwise difficult to prepare. The molecules prepared via the Yamamoto coupling reaction will then be further utilized as intermediates or as building blocks for the synthesis of novel target materials.

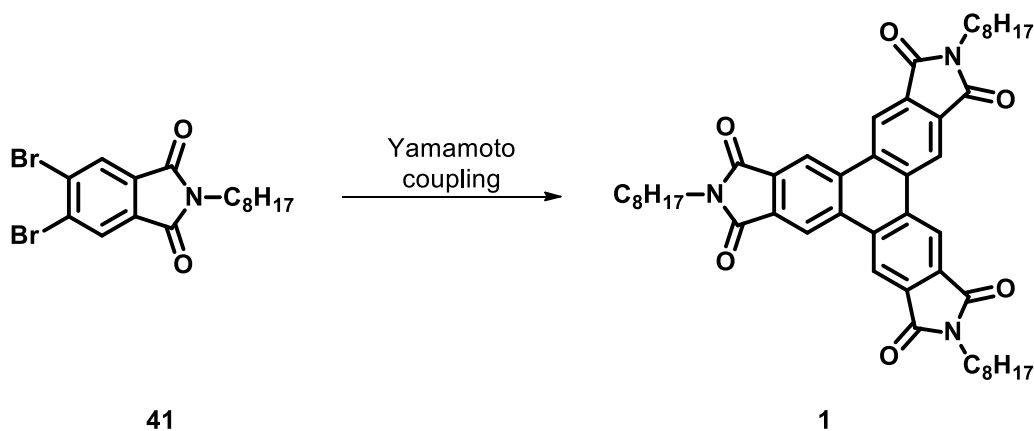


Scheme 5. Nickel-mediated cyclotrimerization of *o*-dibromoarenes via the Yamamoto coupling reaction.

Overall, this research may lead to the development of novel synthetic methodologies that will allow facile access to extended polycyclic aromatic compounds and provide insight into how aromatic systems self-assemble in the liquid crystalline state, as microporous materials and in host-guest interactions. Additionally, the research performed was anticipated to produce novel and tuneable polycyclic aromatic materials with potential applications in sensing, solar cell technologies, catalysis, and other related organic electronic and supramolecular chemistry applications.

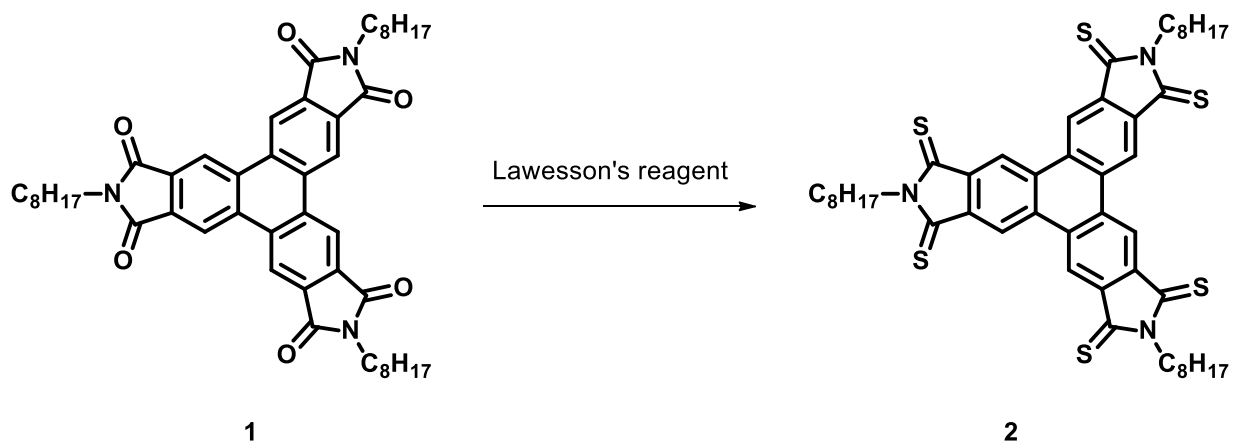
1.7.1 Synthesis of Tris(dicarboxyimide)triphenylene **1** and Exploring the Effects of Thionation on the Liquid Crystalline Properties

Syntheses of electron-deficient triphenylenes are not commonly reported in the literature and those that are, reported in low yields over several challenging synthetic transformations. For example, the synthesis of electron-deficient triphenylene **1** has been reported in 14% yield by Wu and coworkers.⁴⁶ The first major objective of this research was to prepare carboximide-substituted triphenylene **1** via the nickel-mediated Yamamoto coupling reaction (Scheme 6). This work builds upon the previous research conducted by our group, as we have previously studied the scope of the Yamamoto cyclotrimerization reaction by means of preparing a suite of electron-poor triphenylenes and trinaphthylenes. The successful preparation of electron-deficient triphenylene **1** will further demonstrate the potential of the Yamamoto cyclotrimerization to be utilized as a novel and efficient reaction for the preparation of electron-deficient triphenylenes and related extended polycyclic aromatic compounds.



Scheme 6. Proposed synthesis of tris(dicarboxyimide)triphenylene **1** via Yamamoto coupling of *o*-dibromoarene **41**.

Furthermore, the first major research objective explores how subsequent thionation of tris(dicarboxyimide)triphenylene **1** (Scheme 7) to prepare **2** will affect the liquid crystalline phase, and self-assembling properties. Imide-bearing materials (e.g. perylene bisimides) have been used as electron-accepting materials due to their high photochemical stability and charge transport properties.²⁸ Moreover, our lab has demonstrated that the thionation of imide-containing dibenzanthracenedicarboxyimides and triphenylenedicarboxyimides lowered their lowest unoccupied molecular orbital (LUMO) energies and narrowed the highest occupied molecular orbital (HOMO)-LUMO band gap, all while maintaining broad columnar phases and favourable self-assembly.^{29,30} It is predicted based on previous research that thionation of tris(dicarboxyimide)triphenylene **1**, will lower the LUMO energy level, narrow the HOMO-LUMO band gap, and have a subtle impact on the columnar liquid crystalline phase.^{29,30}

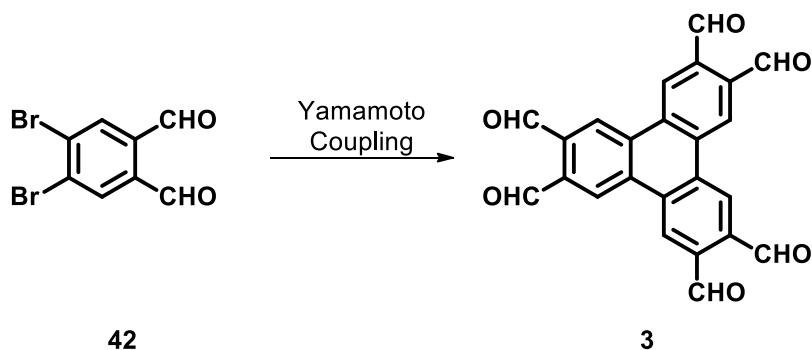


Scheme 7. Thionation of tris(dicarboxyimide)-substituted triphenylene **1** with Lawesson's Reagent.

1.7.2 Preparing a Novel Covalent Organic Framework from an Electron-Deficient

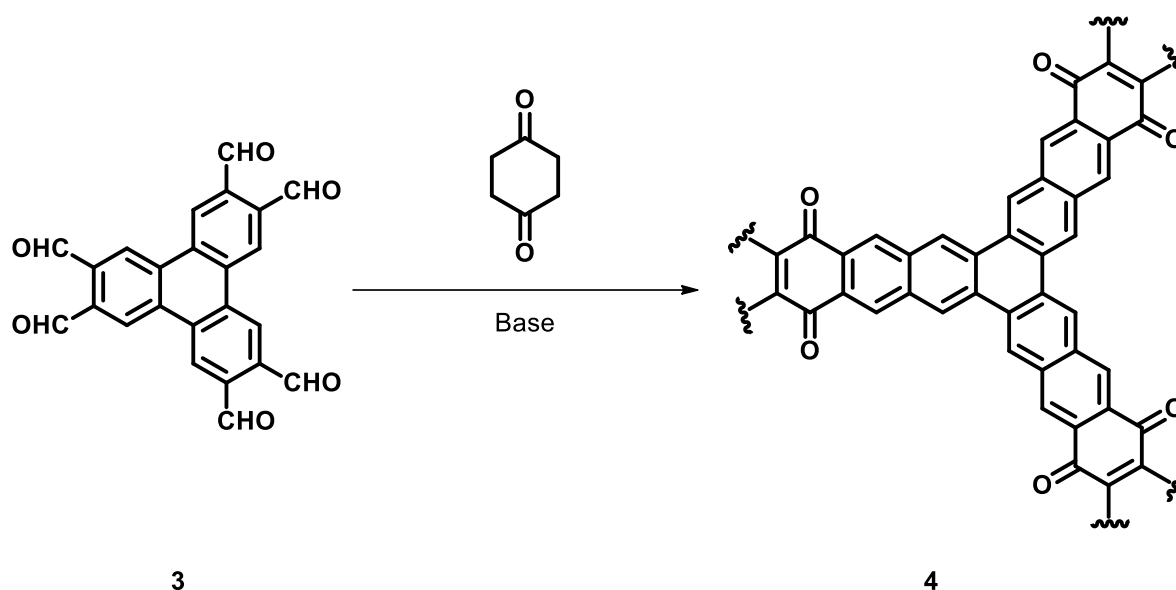
Triphenylene Building Block

Another main objective of this research is to further explore the scope of the Yamamoto coupling reaction for the synthesis of electron-deficient triphenylene derivatives via the preparation of hexa(formyl)-substituted triphenylene **3** (Scheme 8).



Scheme 8. Synthesis of hexa(aldehyde)triphenylene **3** via Yamamoto coupling of *o*-dibromoarene **42**.

Compound **3**, prepared via the Yamamoto coupling reaction, is expected to be utilized as the principal building block for the construction of a novel covalent organic framework **4** (Scheme 9). In theory, condensation of hexa(formyl)triphenylene **3** with 1,4-cyclohexadione under basic conditions will produce a 2-dimensional microporous organic framework (**4**).



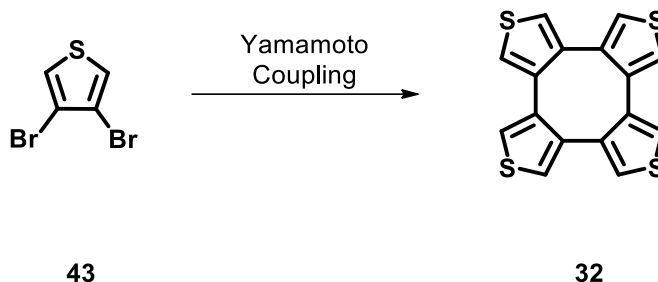
Scheme 9. Preparation of novel covalent organic framework **4** via aldol condensation of hexa(aldehyde) **3** and 1,4-cyclohexanedione.

The investigation of covalent organic frameworks is an important and intriguing area of research due to their potential applications in gas storage, catalysis and sensing.³¹ Several linking groups such as boronates and imines have been utilized for the formation of covalent organic frameworks.³⁴ However, these linking groups are prone to hydrolysis, and under aqueous conditions, the structure of the framework may be compromised. Moreover, single bond linkages between larger units may introduce unwanted flexibility and bond rotation, leading to distorted 2-dimensional networks. In this approach, aldol condensation of hexa(formyl)triphenylene and 1,4-cyclohexadione is expected to produce a covalent organic framework linked by rigid rings consisting of carbon-carbon bonds. Lastly, functionalization of the quinone units within the framework of COF **4** may potentially be explored.

1.7.3 Synthesis of a Novel Extended Tetraphenylene for Molecular Recognition

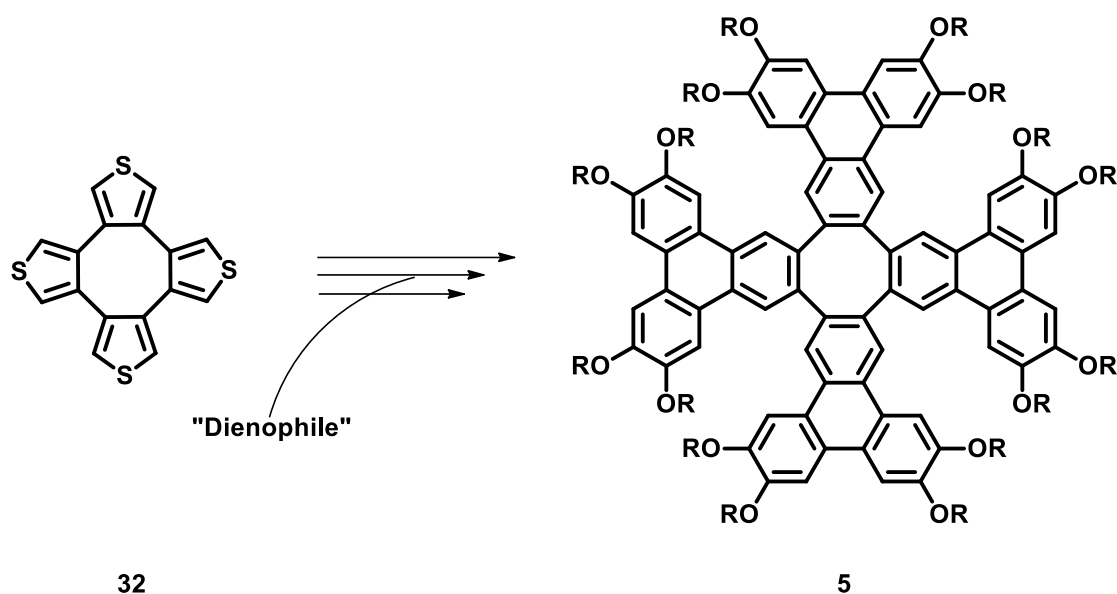
The third and final major objective of this research is to employ a novel synthetic approach to construct extended tetraphenylene **5** (Scheme 11). Tetraphenylenes are characteristically non-planar aromatic structures, allowing them to adopt a saddle-shape configuration and interact with smaller curved guest molecules.^{37,40} Tetraphenylene's adoption of a saddle-shape conformation makes it an interesting target as a host-molecule for applications in supramolecular chemistry.

In this novel approach, 3,4-dibromothiophene **43** is subjected to Yamamoto coupling conditions to produce the tetrathiophene **32** as reported by Yamamoto *et al.* (Scheme 10).⁴²



Scheme 10. Preparation of tetrathiophene via the Yamamoto coupling reaction of 3,4-dibromothiophene, towards the preparation of tetraphenylene **5**.

Oxidation of tetrathiophene **32** will produce a tetrasulfone, and subsequent [4+2] Diels-Alder cycloaddition with the appropriate dienophile will yield a cycloadduct that can undergo oxidative ring closing to hypothetically afford novel extended tetraphenylene **5** (Scheme 11).



Scheme 11. Synthesis of extended tetraphenylene **5** from tetrathiophene **32**, via oxidation, [4+2] cycloaddition and oxidative ring closing.

It is anticipated that by replacing the benzene units of tetraphenylene with extended triphenylene units, a larger π -surface will be formed and thus, increase the capability of binding larger guest molecules like fullerenes and other electron-deficient materials. These potential interactions of extended tetraphenylene derivative **5** make it an interesting target for supramolecular chemistry applications, such as molecular recognition.

The overall theme of this research was to synthesize and study the structure-property relationships of novel polycyclic aromatic compounds capable of self-assembling to form liquid crystalline, and microporous structures, as well as molecules capable of molecular recognition. This thesis had three main goals. The first goal was the synthesis of electron-deficient triphenylene **1** via the Yamamoto coupling reaction followed by the study of the influences of thionation on the liquid crystalline and electron properties through the synthesis of **2**. In the second goal, we sought

to prepare electron-deficient triphenylene **3** via the Yamamoto coupling reaction and use as a building block towards the preparation of a covalent organic framework **4**.

CHAPTER 2: NOVEL SYNTHESIS OF A CARBOXIMIDE-SUBSTITUTED TRIPHENYLENE AND A STUDY OF THE EFFECTS OF THIONATION

2.1 Introduction

Organic semiconductors have been extensively studied for their potential applications in light emitting diodes,¹ organic thin film transistors,^{1,5,6} and organic photovoltaics.^{1,3,7,8} Several syntheses of hole-transporting (p-type) organic semiconductors such as acenes¹² and oligothiophenes⁶ have been reported in the literature. However, electron-transporting (n-type) organic semiconductors are less frequently reported in the literature, but are equally as important as p-type organic semiconductors as they are required for p-n junction diodes, bipolar transistors, and complementary integrated circuits.⁶ For these reasons, the study and preparation of n-type organic semiconductors has recently been receiving attention. P-type organic semiconductors are designed based on electron-rich systems or, through the addition of electron-donating groups. In contrast, n-type organic semiconductors can be prepared through preparation of electron-poor systems by including electron-withdrawing functional groups. For example, disc-like molecules exhibiting n-type character, such as perylene tetracarboxylic diimide (PDI) and naphthalene tetracarboxylic diimide (NDI), containing electron-withdrawing diimide groups have been prepared and successfully used in n-channel OFETs (Figure 16).^{47,48}

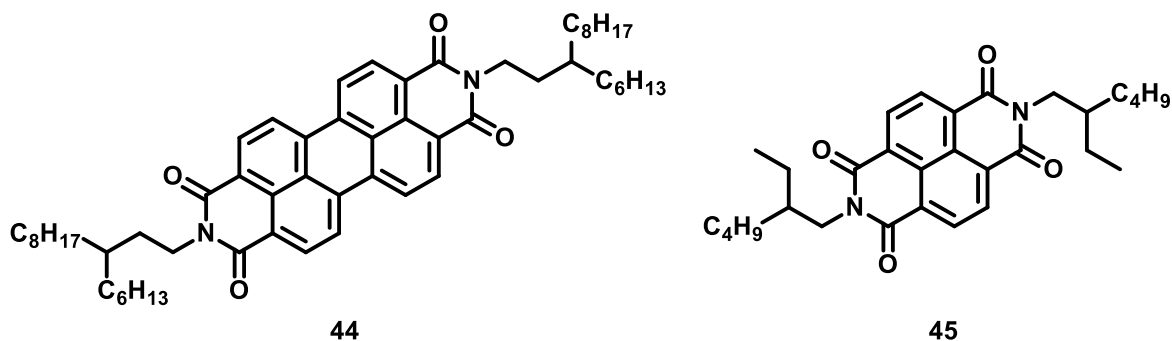


Figure 16. PDI (**44**) prepared by Seferos et al, and NDI (**45**) prepared by Zhang et al.^{47,48}

The first objective of this research is to prepare carboximide-substituted triphenylene **1** via the nickel-mediated Yamamoto coupling reaction and investigate how subsequent thionation influences the self-assembly, mesomorphic and electronic properties of compound **2**. In the literature, syntheses of electron-rich (p-type) triphenylenes containing electron-donating groups (e.g. -OR, -SR) are commonly reported, while only a few reports of electron-deficient (n-type) triphenylenes exist due to synthetic difficulty.

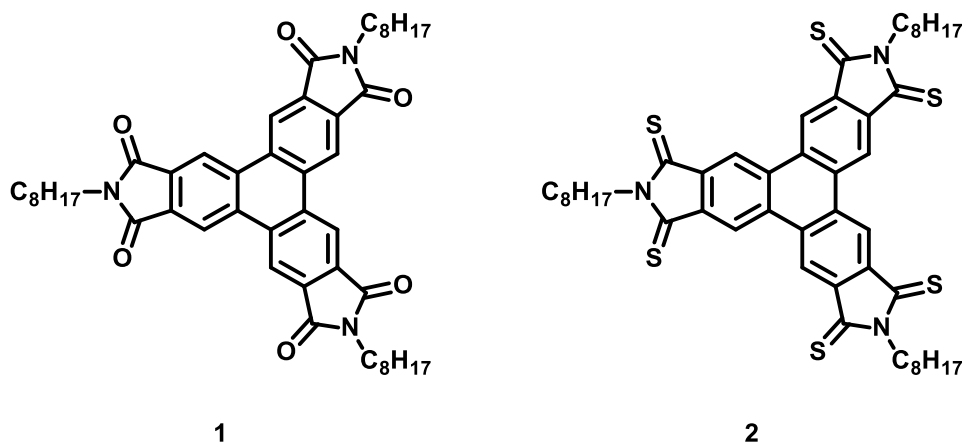
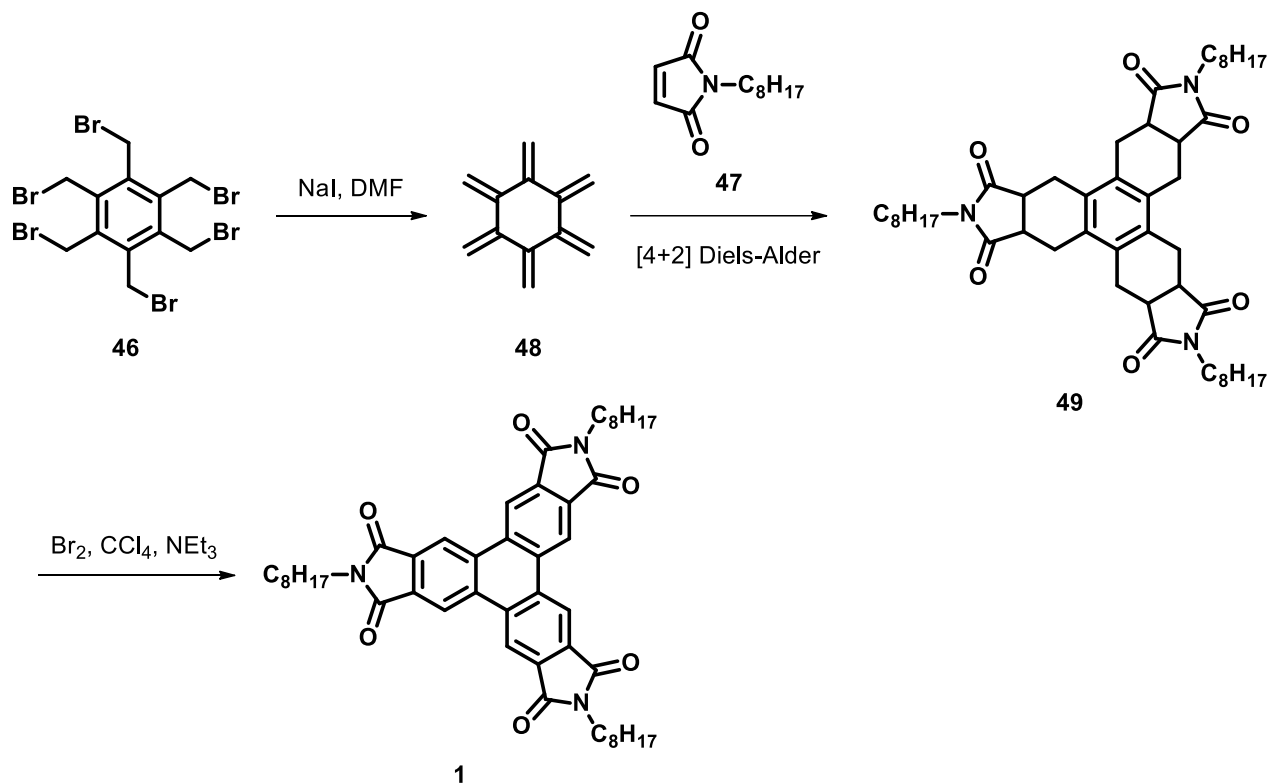


Figure 17. Structures of target compounds **1** and **2**.

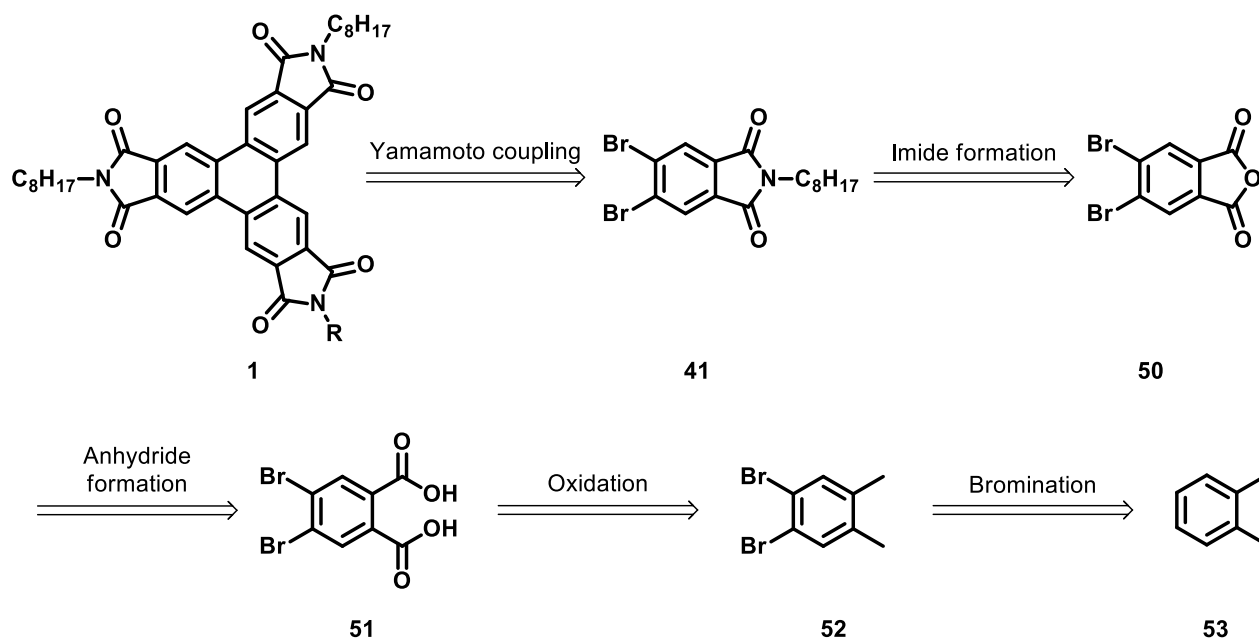
two steps. Although the yield reported was low, it was among the first practical syntheses of dicarboxylic imide-substituted triphenylenes and trinaphthylenes communicated at the time.



Scheme 13. *In situ* generation of [6]-radialene (**48**), followed by [4+2] Diels-Alder with *N*-octylmaleimide (**47**) and subsequent aromatization.

Additionally, compound **1** was reported by Wu and coworkers to exhibit a columnar liquid crystalline phase between 158 and 228 °C with fan-shaped texture. This makes triphenylene **1** an interesting target as the affects of thionation can potentially be explored and further complement work previously published from the Maly group on the influences of thionation on a series of triphenylenes containing one carboximide-functional group.

Previous work within the Maly group has shown that the Yamamoto coupling reaction is an efficient approach for the preparation of a variety of electron-rich and electron-deficient triphenylene and trinaphthylene derivatives. Thus, our group sought to demonstrate that the Yamamoto coupling reaction could be utilized to prepare electron-deficient and liquid crystalline triphenylene derivative **1** previously prepared by Wu and coworkers with the goal of improving the regioselectivity of the reaction, the yield of **1**, and constructing a more concise synthetic route using *o*-xylene as a cheap and readily available starting material. In the retrosynthetic Scheme below (Scheme 14), synthesis of compound **1** may be achieved via the Yamamoto cyclotrimerization of *o*-dibromoimide **41**. Compound **41** can be obtained through a nickel-catalyzed imide formation with the appropriate amine from anhydride **50** adapting from a procedure reported by Branda *et al.*⁴⁹ Anhydride **50** may be prepared via the condensation reaction of *o*-dibromophthalic acid **51** adapting from a previously published procedure reported by Patil *et al.*⁵⁰ Phthalic acid **51** can be prepared from the two-fold bromination of *o*-xylene **55** followed by the subsequent oxidation of 1,2-dibromo-4,5-dimethylbenzene **52** as reported by Zhang *et al.*⁵¹



Scheme 14. Retrosynthetic approach to carboximide-substituted triphenylene (**1**).

Additionally, previous studies of dicarboximide-substituted materials have shown that thionation can be used as a method to tune and improve the electron-accepting ability of dicarboximides ultimately by lowering the LUMO-energy level, producing materials with narrower HOMO-LUMO energy level band gaps.^{29,30,47,48} For example, thionation of materials like NDI and PDI prepared by Seferos *et al.*⁴⁷ and Zhang *et al.*,⁴⁸ respectively using Lawesson's reagent has resulted in a lowering of the LUMO energy levels and an increase in electron-accepting abilities, while additionally altering the surface roughness of these materials, suggesting that thionation may also influence physical properties as well. Moreover, our lab has recently investigated the affects of thionation on a series of dibenzanthracenes and triphenylenes and discovered that thionation has a subtle influence on the mesomorphic properties of these liquid crystalline materials but does have a greater influence on the electronic properties (Figure 18).^{29,30}

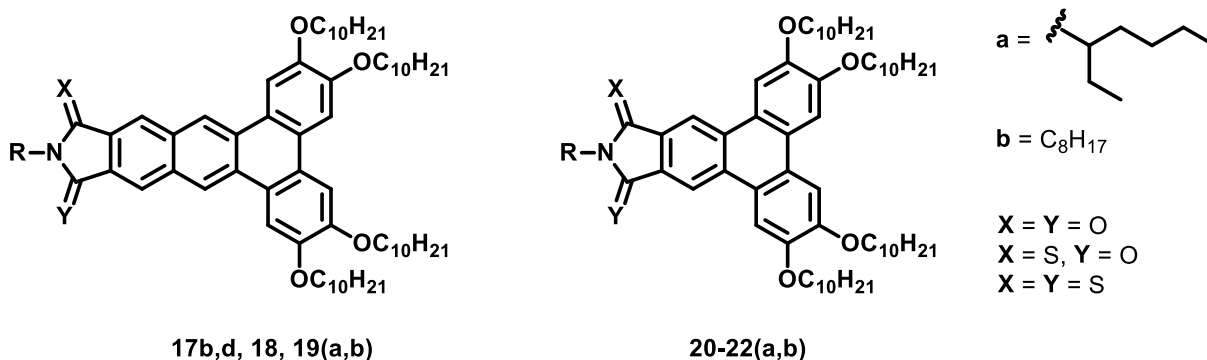
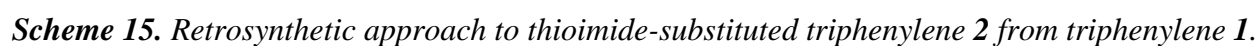


Figure 18. Dicarboxyimide- and dicarboxythioimide-substituted trinaphthylenes and triphenylenes previously prepared by the Maly group to explore the effects of thionation on the mesomorphic properties.^{29,30}

In addition to the attempts to prepare triphenylene **1** via Yamamoto coupling reaction, we sought to also explore the affects of thionation on the liquid crystalline and electronic properties of compound **1** via polarized optical microscopy, differential scanning calorimetry, and UV-Vis spectroscopy. In the retrosynthetic Scheme below (Scheme 15), dicarboxythioimide-substituted triphenylene **2** may be potentially accessed through the thionation of dicarboxyimide-substituted triphenylene **1** using Lawesson's reagent for a 6-fold thionation via a procedure adapted from Tilley and co-workers.⁴⁷



Chemical reaction scheme showing the synthesis of compound 41 from compound 2:

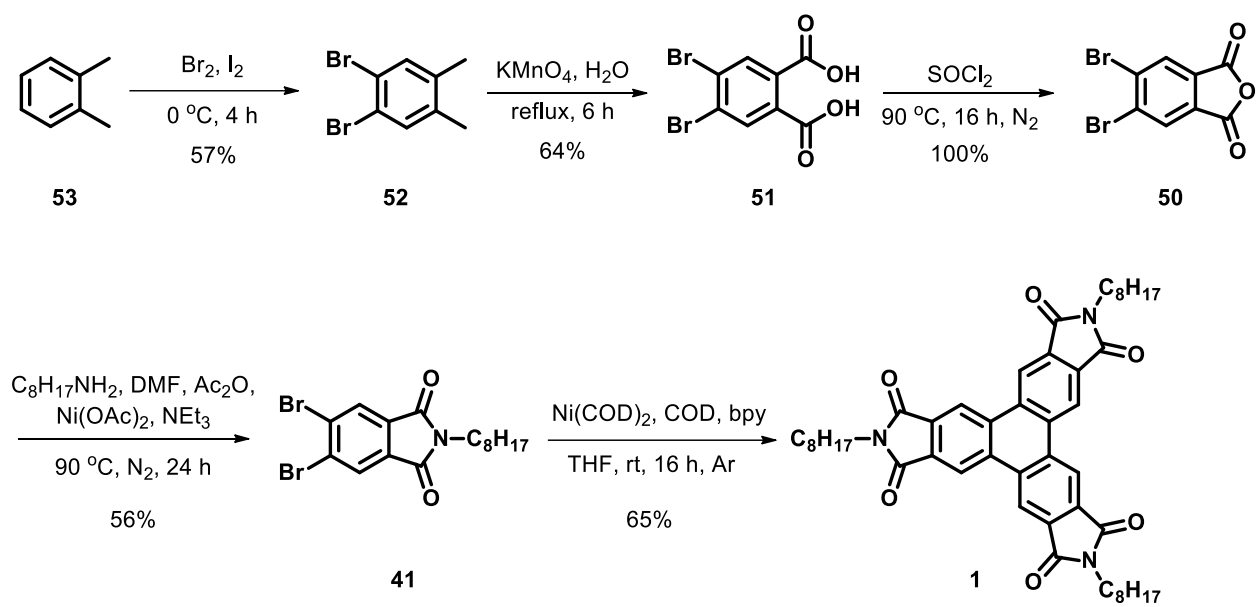
Compound 2 (a tetracyclic thienopyrrole derivative) reacts with 1. Thionation and 2. Yamamoto coupling to yield compound 41 (a brominated thienopyrrole derivative).

Scheme 16. Retrosynthetic approach to **2** via thionation of the imide-substituted *o*-dibromoarene **41** and subsequent Yamamoto cyclotrimerization.

2.2 Results and Discussion

2.2.1 Synthesis and Properties of Tris(dicarboxyimide)-Substituted Triphenylene **1**

The synthesis of triphenylenedicarboxyimide derivative **1** is presented in Scheme 17. Compound **52** was prepared in 57% yield following a two-fold bromination of *o*-xylene (**53**) with molecular bromine and catalytic iodine.⁵¹ Subsequent benzylic oxidation of **52** refluxing in an aqueous solution of potassium permanganate afforded 4,5-dibromophthalic acid (**51**) in a 64% yield following a procedure as reported by Zhang *et al.*⁵¹ Preparation of anhydride **50** was successfully completed by refluxing phthalic acid **51** in thionyl chloride yielding anhydride **50** as a white powder in quantitative yields, following a procedure reported by Patil *et al.*⁵⁰ Adapting from a procedure reported by Branda *et al.*,⁴⁹ anhydride **50** was then subjected to a nickel-catalyzed imide formation reaction in the presence of nickel(II) acetate, acetic anhydride and octylamine, which successfully furnished the desired imide-substituted *o*-dibromoarene precursor as a crystalline white solid, **41** in a 56% yield. Finally, compound **41** was subjected to Yamamoto coupling conditions previously developed in the Maly group, using Ni(COD)₂, COD, and 2,2'-bipyridine in tetrahydrofuran at room temperature to obtain dicarboxyimide-substituted triphenylene **1** as a white solid after recrystallization from dichloromethane and methanol in an efficient 65% yield.



Scheme 17. Synthetic route to **1** via Yamamoto coupling of **41**.

The investigation of the liquid crystalline properties of compound **1** via polarized optical microscopy and differential scanning calorimetry showed that compound **1** exhibits an ordered columnar mesophase (Figure 19). The observed liquid crystalline properties of compound **1** are consistent with the previously reported results by Wu and coworkers.⁴⁶ Polarized optical micrographs at 200x magnification were taken of compound **1** upon cooling from the isotropic liquid phase at 200 and 217 °C (Figure 19). In both polarized optical micrographs, compound **1** exhibited fan-shaped textures, indicating that the mesophase may be hexagonal. Moreover, a clearing point at about 228 °C was qualitatively observed under the polarized optical microscope, which is consistent with the data collected from differential scanning calorimetry experiments and is consistent with reported experimental data.⁴⁶

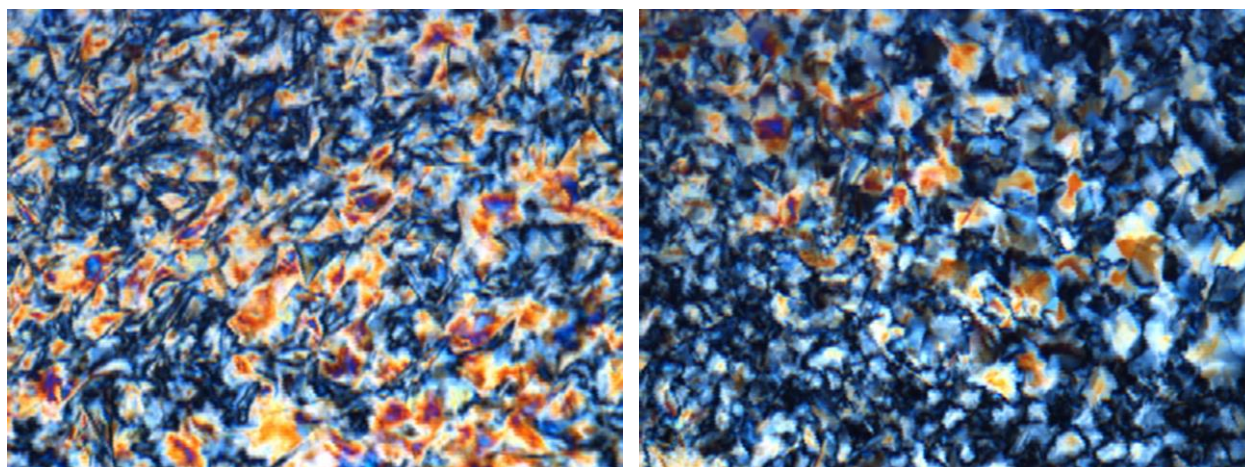


Figure 19. Polarized optical micrographs of Left) **1** at 200 °C, Right) **1** at 217 °C. All micrographs were taken near the isotropic-columnar phase transition on cooling.

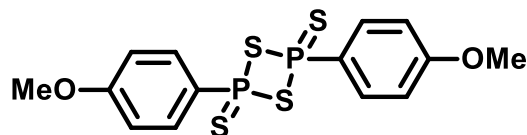
To reiterate, carboximide-substituted triphenylene **1** is a known compound and has been previously prepared by Wu *et al.* as reported in a 2009 publication.⁴⁶ However, Wu's synthetic approach to electron-deficient triphenylene **1**, although a concise 1-pot synthesis required a time consuming purification, via column chromatography. In addition, it suffered from low yields only affording **1** in 14% yield due to regioselectivity issues, as the bis-addition product is favoured over the tris-addition product, as well as time-consuming purification via column chromatography.⁴⁶ Finally, the starting material in Wu's synthetic route, hexamethylbenzene, is far more expensive than our starting material *o*-xylene. Without a doubt, employing the Yamamoto coupling reaction to access compound **1** from *o*-dibromoarene **41** is a superior method in direct comparison to the synthetic route reported by Wu and coworkers. Although our route is a longer 5-step synthesis to **1** with an overall yield of 13%, our synthesis starts with *o*-xylene, which is a cheap and readily available starting material, the synthetic steps performed are not overly complex and require simple purification, and the imide-formation reaction can be amenable to several types of primary

amines which may allow for the preparation of a variety of *N*-substituted triphenylenedicarboximides containing various lengths of alkyl chains or branched alkyl chains. Furthermore, using the Yamamoto coupling allows for the preparation of compound **1** in an improved yield of 65%. The final step of our synthesis also avoids purification via column chromatography, as compound **1** can be simply purified via recrystallization from a mixture of dichloromethane and methanol.

2.2.2 Synthesis of Dicarboxythioimide-Substituted Triphenylene and the Investigation of the Influences of Thionation on Mesomorphic and Electronic Properties

Towards this objective, we looked to explore the effects of thionation of compound **1** as a follow-up to previously reported data and results from our group.^{29,30} We hypothesized that thionation may have a greater influence on the mesomorphic properties of **1** since it contains three dicarboxyimide functional groups, as well as a strong influence on the electronic and optoelectronic properties in comparison to the previously studied dicarboxythioimide-substituted triphenylene series from the Maly group.

Initially, we sought to first synthesize compound **2** via thionation of **41** followed by Yamamoto coupling or via six-fold thionation of **1** using a thionating agent called Lawesson's reagent **54** (Figure 20).

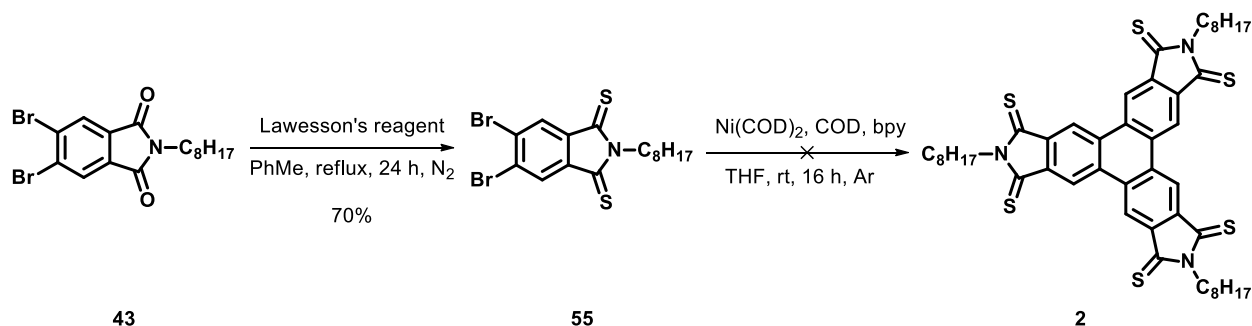


54

Figure 20. Chemical structure of Lawesson's reagent (**54**)

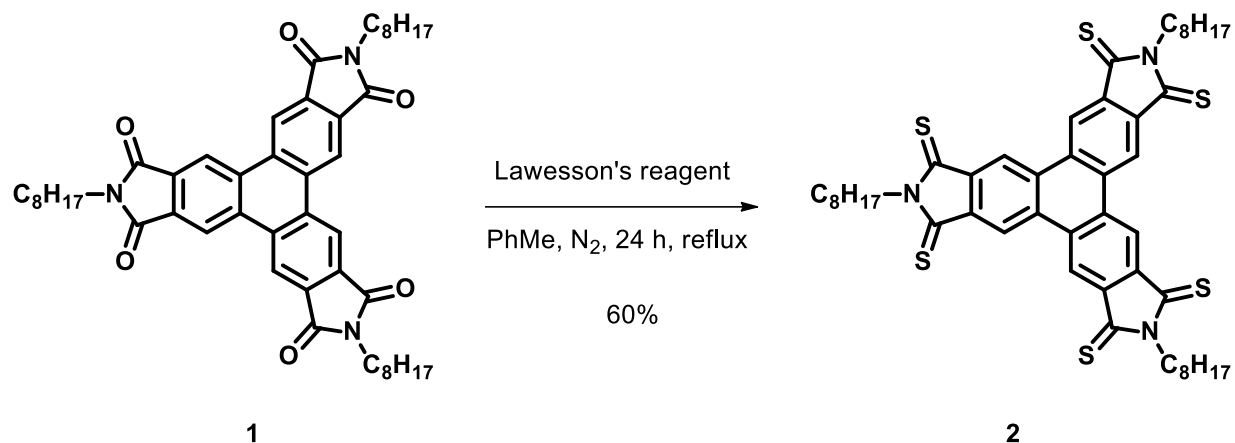
The first attempt at the synthesis of the dicarboxythioimide-substituted triphenylene derivative **2** was by thionation of *o*-dibromoimide **41** using Lawesson's reagent, affording dicarboxythioimide **55** as fine brown needles in 70% yield after column chromatography and recrystallization from a mixture of dichloromethane and methanol (Scheme 18).³⁰ However, the synthesis of dicarboxythioimide-substituted triphenylene **2** was unsuccessful via Yamamoto cyclotrimerization of thionated substrate **55** (Scheme 18). Upon reaction work-up, a crude and intractable mixture was obtained. Proton (¹H) NMR spectroscopy showed no sign of starting material or desired product, but instead showed complex alkyl and aromatic regions with several overlapping signals. The ¹H NMR spectrum obtained suggests that the desired cyclotrimerization may have been hampered by formation of unknown by-products formed from other unproductive reaction pathways. Debromination of the starting material, or linear homo-coupling between molecules as dimers or higher oligomers. Additionally, the failed preparation of triphenylene **2** via the Yamamoto coupling of **55** is also hypothesized to be attributed to the potential poisoning of the nickel(COD)(bpy) complex by the sulfur containing thioimide precursor **55**. In a 1992 paper⁵² published by Marècot *et al.*, it was determined that sulfur-containing compounds and sulfur-containing impurities contaminated nickel catalysts by means of chemisorption.⁵² Unfortunately, sulfur poisoning of nickel catalysts and nickel reagents leads to reduced, or no activity of the nickel

species in solution, and thus is another rationale behind the unsuccessful synthesis of triphenylene **2** via Yamamoto coupling of **55**.



Scheme 18. Unsuccessful synthesis of **2** through Yamamoto coupling of thioimide **55**.

The second attempt at the preparation of the dicarboxylic thioimide triphenylene was through a direct six-fold thionation of dicarboxyimide-substituted triphenylene **1** by refluxing with Lawesson's reagent in toluene for 24 hours (Scheme 19).³⁰ Gratifyingly, this method allowed for the successful synthesis of dicarboxythioimide-substituted triphenylene **2** as a deep-purple solid in a fair 60% yield after purification through a silica column and recrystallization in dichloromethane and methanol. Interestingly, thin-layer chromatography analysis of the reaction's progress over the 24-hour reaction time, as well as the crude reaction mixture, showed several other spots at lower retention factor (R_f) values than compound **2**, suggesting the formation of derivatives that are not fully thionated, and may contain anywhere from 1 to 5 thiocarbonyl functional groups. Moreover, this may be an interesting topic to explore in the future as a comparison between partially thionated derivatives of compound **2** may bring about interesting results, as a varying amount of thioimide groups may have different influences on the mesomorphic, electronic and optoelectronic properties of **1**.



Scheme 19. Successful 6-fold thionation of **1** using Lawesson's reagent.

The liquid crystalline and electronic properties of compound **2** were investigated via polarized optical microscopy, differential scanning calorimetry and UV-Vis spectroscopy. The results were compared to the parent compound **1** as well as previous results from the Maly group to further understand how thionation affects the properties of the liquid crystalline phase as well as the electrochemical and optoelectronic properties of dicarboxyimide-substituted triphenylenes, like compound **1**.

Investigation of the liquid crystalline properties of compound **2** revealed that **2** did exhibit a liquid crystalline phase, and underwent a phase transition to the isotropic liquid phase at approximately 320 °C in comparison to compound **1** with no sulfur atoms that underwent a phase transition to the isotropic liquid phase at 228 °C. Upon cooling, a phase transition from isotropic liquid to a columnar liquid crystalline phase was observed (Figure 21). Furthermore, polarized optical microscopy revealed that compound **2** displays dendritic textures, consistent with that of a hexagonal columnar mesophase (Figure 21). The columnar mesophase was maintained to room

temperature, suggesting the formation of a glass phase. Unfortunately, heating compound **2** above 300 °C seems to have potentially resulted in at least, partial decomposition, as a pungent sulfur smell was detected upon heating above 300 °C. Consequently, due to the suspected partial decomposition of **2**, the phase transition temperature from mesophase to isotropic liquid phase was reduced with each subsequent heating and cooling cycle. Unfortunately, the exact phase transitions were not easily observed qualitatively via polarized optical microscopy, which made it difficult to characterize the mesophase appropriately and accurately or to make a direct comparison of the mesophase with that of parent compound **1**.

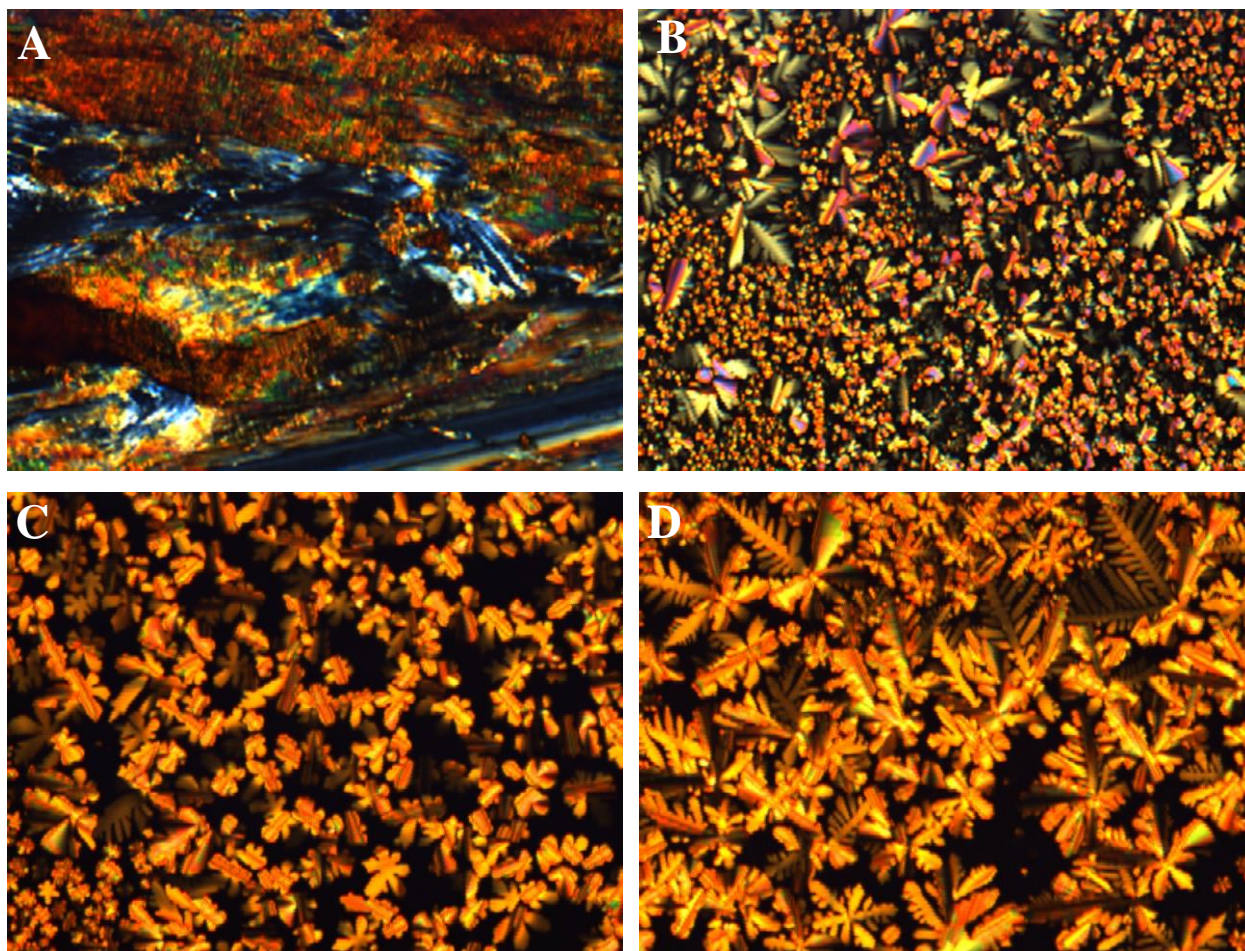


Figure 21. Polarized optical micrographs of **A)** **2** at room temperature before heating, **B)** **2** at 45 °C, **C)** **2** cooling from second heating cycle at 230 °C, **D)** **2** cooling from third heating cycle at 200 °C. All micrographs were taken upon cooling from the isotropic-columnar phase transition.

Differential scanning calorimetry is commonly used to determine precise transition temperatures for liquid crystalline compounds. However, upon running differential scanning calorimetry experiments for compound **2**, it was observed, similar to that of the polarized optical microscopy data, that there was no distinct phase range for the liquid crystalline phase of compound **2**. In the differential scanning spectra for compound **2** (Figure 22), two consecutive heating and cooling cycles were performed at a constant temperature change rate of 5 °C/min. The

first phase transition from crystalline solid to mesophase is observed to be approximately 65 °C and the second transition point, from mesophase to isotropic liquid is at about 325 °C, which is consistent with the results from polarized optical microscopy. However, upon the first cooling cycle and subsequent heating and cooling cycle, no obvious phase transitions were observed in the differential calorimetry scanning trace, suggesting that compound **2** did in fact experience at least partial degradation at the elevated temperature of the first heating cycle.

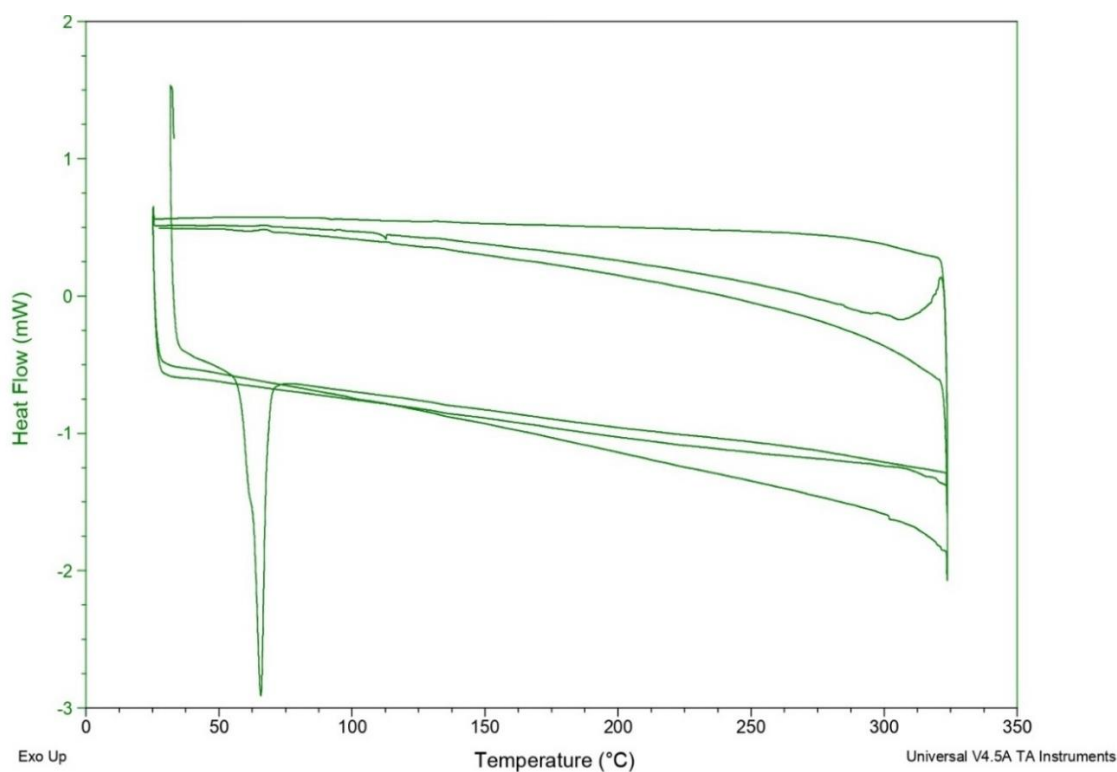


Figure 22. Differential scanning calorimetry plot for triphenylene **2** with a constant scan rate of 5 °C/min on heating.

To further explore the suspected degradation of compound **2**, thermogravimetric analysis was performed. Thermogravimetric analysis is a method of thermal analysis in which the mass of

a sample is measured while the temperature is constantly increasing, as a function of time. Thermogravimetric analysis is commonly employed to provide information regarding physical and chemical properties of the analyte in question, such as phase transitions and thermal decomposition. As such, thermogravimetric analysis of compound **2** revealed that **2** begins to experience complete thermal degradation at approximately 334 °C (Figure 23). The results collected from thermogravimetric analysis are consistent with the qualitative observations observed via polarized optical microscopy and the qualitative observation that compound **2** is indeed experiencing thermal degradation at temperatures above 300 °C.

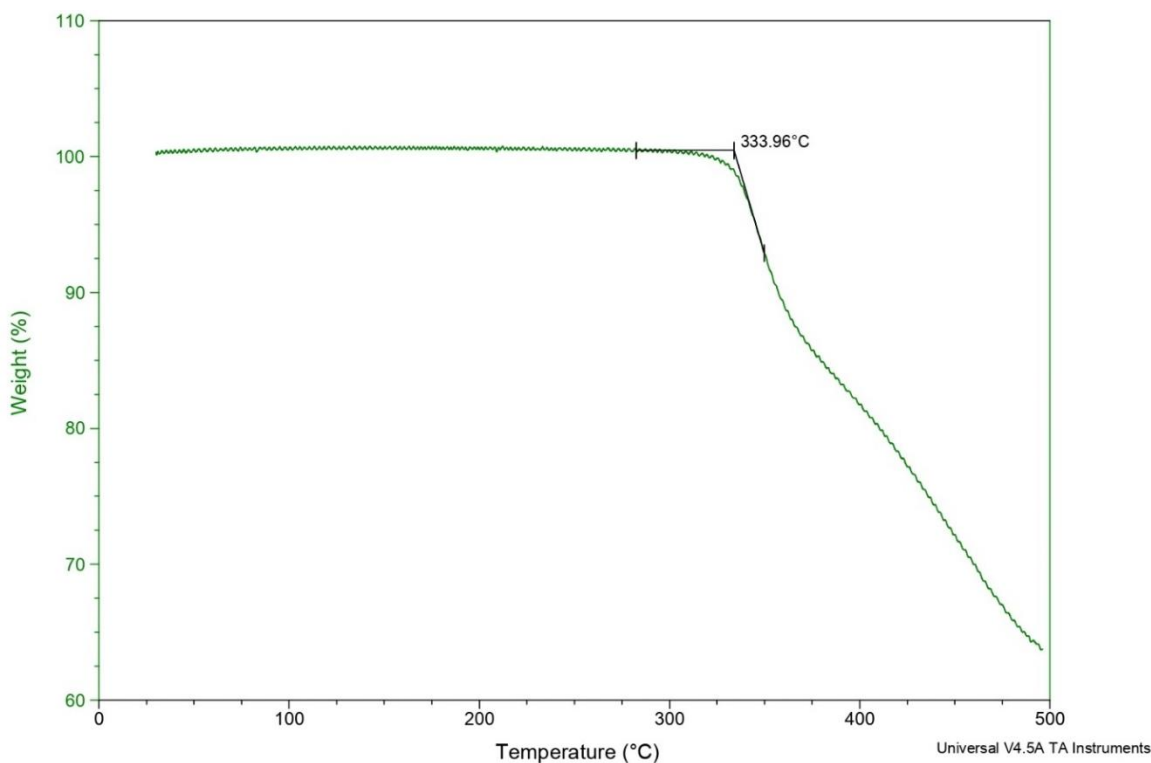


Figure 23. Thermogravimetric analysis plot for triphenylene **2**.

In this particular system, it can be concluded that thionation did in fact influence the liquid crystalline temperature phase range by increasing the clearing point of compound **1** from 228 °C to the point of what is suspected to be partial decomposition at approximately 320 °C for compound **2**. Interestingly, these observations are in direct contrast with what was observed with the dicarboxyimide-substituted dibenzanthracene and triphenylene series previously reported by the Maly group, where thionation only had a subtle impact on the mesophase temperature range of these liquid crystalline compounds.^{29,30} In previous reports from the Maly group, thionation mainly influenced the mesophase temperature range by increasing the melting transition point from crystalline solid to the columnar mesophase (ca. 24 °C increase for dibenzanthracenes and ca. 25 °C for triphenylenes), while have a very little impact on the clearing point from columnar mesophase to isotropic liquid (ranging between ca. 7 °C to 17 °C).^{29,30} In this case, all six carboximide oxygen atoms have been replaced by sulfur atoms via reaction with Lawesson's reagent, which dramatically impacted the phase transition temperatures of **1**. However, if a derivative of **2** was prepared where anywhere from one to five oxygen atoms of the carboximide functionalities are replaced with sulfur, it may not affect the mesophase range as dramatically, to the point where decomposition may not be observed. Conversely, this may potentially be a difficult task, as the regioselectivity of the thionation reaction with Lawesson's reagent will be difficult to predict, and separation of the products via column chromatography may also prove to be cumbersome.

The spectroscopic properties of these materials were also examined as both triphenylenes **1** and **2** displayed different colours in the solid-state and in solution. Triphenylene **1** was a white solid that formed a clear and colourless solution in dichloromethane, while triphenylene **2** was a dark-purple solid and formed a dark orange coloured solution when dissolved in dichloromethane.

The UV-Vis absorbance spectra of triphenylenes **1** and **2** can be seen in Figure 24. Triphenylene **1** shows an absorbance maximum close to 285 nm, while triphenylene **2** has a small absorption maximum at 325 nm and a broad absorbance band around 385 nm that trails into the blue region (400-465 nm). These two distinct absorbance bands for compound **2** suggests that it does go through more than one transitions to different excited states at a lower and higher energy level. With that said, it is common for many organic compounds to exhibit more than one absorbance maximum peak in a UV-Vis absorbance spectrum. When comparing compounds **1** and **2**, there is a distinct red shifting of the absorbance maxima with the thionated derivative **2**. This red shift suggests a narrowing of the HOMO-LUMO energy band gap with increased sulfur content, which is consistent with previously reported observations the Maly group.

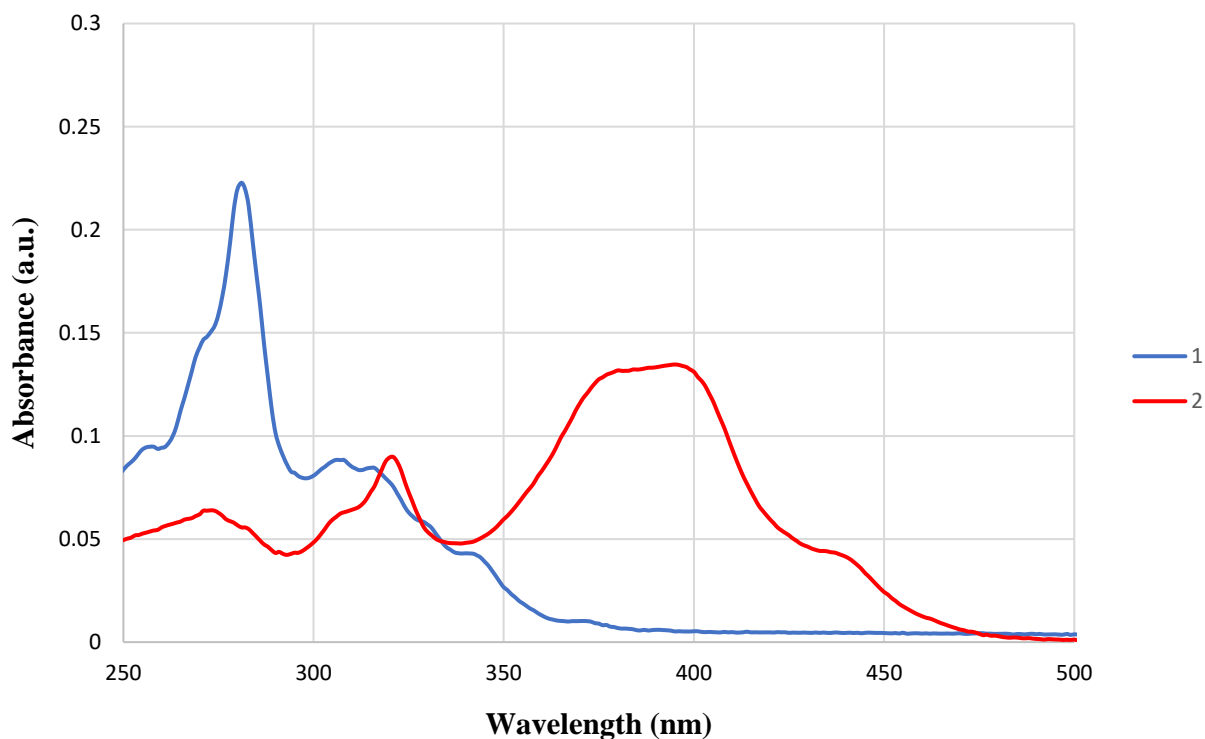


Figure 24. UV-Vis spectra of 2×10^{-6} M solutions of triphenylenes **1** and **2** in CH_2Cl_2 .

2.3 Conclusions and Future Work

In summary, dicarboxyimide-substituted triphenylene **1** was successfully prepared via the nickel-mediated Yamamoto coupling reaction of *o*-dibromoarene **41** in a 65% yield. This approach is more convenient, and higher yielding in comparison to the previously reported approach to triphenylene **1** by Wu and coworkers and avoids purification of compound **1** via column chromatography in the final step. Furthermore, this synthetic route allows for a modular approach to several derivatives of compound **1** with varying *N*-alkyl substituents as the preceding dicarboxyimide-substituted *o*-dibromoarene can easily be prepared with variable *N*-alkyl chains via reaction of anhydride **50** with an amine in the presence of Ni(OAc)₂ and Ac₂O, as previously described in Scheme 11.

Dicarboxythioimide-substituted triphenylene **2** was also successfully prepared in 60% yield following thionation of triphenylene **1** with Lawesson's reagent. Compound **2** shows evidence for a columnar mesophase with a high clearing point and displayed dendritic textures on cooling from the isotropic liquid phase. However, as an unexpected consequence of thionation of **1**, the clearing point of compound **2** was increased to a high enough point where **2** experienced thermal degradation upon reaching the clearing point from mesophase to isotropic liquid. Due to the thermal degradation of compound **2** upon reaching the clearing point temperature, it does not allow for any clear comparisons to the mesophase characteristics of compound **1**. These results are in contrast with previously collected data from studies on the effects of thionation of dicarboxyimide-bearing liquid crystalline trinaphthylenes and triphenylenes,³⁰ where thionation only had a subtle impact on the mesophase range, and more specifically, the clearing point temperature. Additionally, a red-shift in the UV-Vis spectra (Figure 24) was observed for the thionated triphenylene derivative in comparison to triphenylene **1**. This red-shift suggests a

narrowing of the HOMO-LUMO energy band gap with increased thionation which is consistent with what was previously observed by the Maly group.

In the future, it may be interesting to explore the effects of partial thionation on the mesophase and electronic characteristics of compound **1**. It is expected that partial thionation of the dicarboximide functional groups, where anywhere from one to five of the oxygens could be replaced by a sulfur atom would have a more subtle impact on the mesophase and electronic properties of **1** in comparison to the fully thionated derivative **2**.

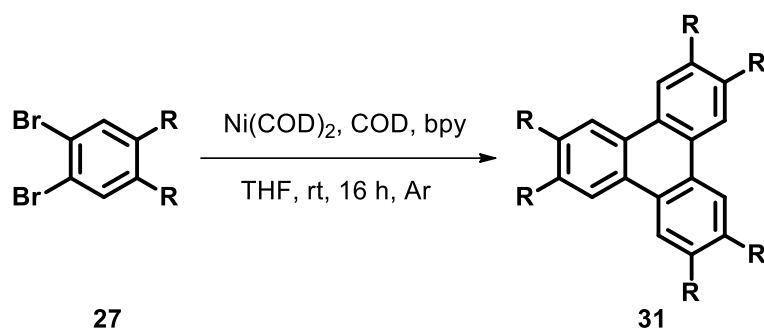
CHAPTER 3: EXPLORATION OF ALTERNATIVE NICKEL-MEDIATED CYCLOTRIMERIZATION REACTION CONDITIONS

3.1 Introduction

Transition metal-catalyzed carbon-carbon bond formation is an extremely important type of reaction in organic chemistry for the synthesis of many compounds. Some important metal-catalyzed carbon-carbon bond formation reactions include the Suzuki-Miyaura coupling, Heck reaction, Sonogashira coupling, Ullman coupling, and the list goes on.⁴¹

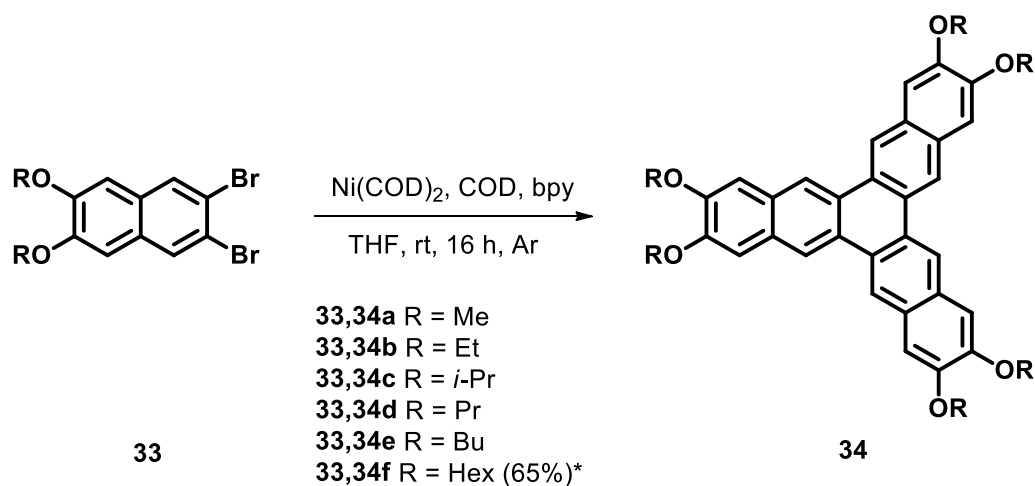
Cross-coupling reactions proceed through a catalytic cycle, where a new carbon-carbon bond is formed between an organometallic intermediate and an organic halide. As such, cross-couplings are commonly used for arylations and employ transition metals such as copper, palladium, and nickel to name a few.⁴¹

The Yamamoto coupling reaction is a nickel-mediated homo-coupling of *o*-dibromoarenes and allows for the concise trimerization of the *o*-dibromoarene starting materials. This reaction is mediated by the *in situ* formation of a 1:1:1 active catalyst species between a stoichiometric amount of a zero valent nickel reagent known as nickel(0)bis(1,5-cyclooctadiene) (Ni(COD)₂), 1,5-cyclooctadiene and 2,2'-bipyridine in solvents such as tetrahydrofuran or dimethylformamide (Scheme 20).



Scheme 20. The Yamamoto cyclotrimerization reaction.

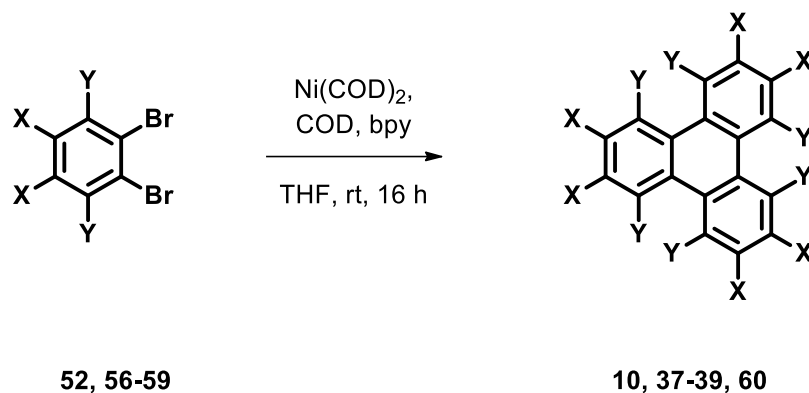
The Yamamoto coupling has been shown to be synthetically useful to access cyclotrimerized starphene-type compounds by several groups. To illustrate, Bunz and coworkers reported the successful synthesis of a series of novel hexakis(alkoxy)trinaphthylenes (**34a-f**) via nickel-mediated Yamamoto coupling reaction of the corresponding *o*-dibromonaphthalenes (**33a-f**) (Scheme 21).⁴⁴ The synthesis of compound **34f** was previously reported by Maly and coworkers using a cumbersome four-step sequence with an overall yield of 23%.²⁵ Using the Yamamoto coupling, Bunz and coworkers dramatically shortened the synthesis of hexakis(alkoxy)trinaphthylene **34f** via an efficient one-step process from **33f** to afford trinaphthylene **34f** in a much improved 65% yield.⁴⁴



Scheme 21. Preparation of a series of novel trinaphthalenes (**34a-f**) via Yamamoto coupling of *o*-dibromonaphthalene precursors, reported by Bunz and coworkers.⁴⁴

Additionally, our group has further displayed the synthetic utility and conciseness of the Yamamoto coupling reaction via the preparation of compounds **10**, **37-39**, and **61** in good yields when compared to their respective, previously reported syntheses. (Table 1).⁵³

Table 1. Summary of Yamamoto coupling results with *o*-dibromoarenes as reported by Maly and coworkers⁵³



Substrate	Product	Yield (%)	Previous Yield (%)
56 (X=Y=H)	10	59	60 ⁴²
52 (X=CH ₃ , Y=H)	60	58	32 ⁵⁴
57 (X=CO ₂ CH ₃ , Y=H)	37	74	13 ⁵⁵
58 (X=F, Y=H)	39	44	52 ⁵⁶
59 (X=Y=F)	38	20	5 ⁵⁷

Overall, Maly and coworkers demonstrated that the nickel-mediated Yamamoto coupling of *o*-dibromoarenes can be used for the preparation of substituted triphenylenes. The approach was shown to be much more concise, and higher yielding in all but two case, in comparison to the existing synthetic methodologies reported. In particular, the yields and synthetic routes for electron-deficient systems (**37-39**), which are difficult to prepare via oxidative cyclization methods were drastically improved.⁵³ Furthermore, in the previous chapter of this thesis, the convenience

of the Yamamoto coupling reaction was also displayed in the improved synthesis of electron-deficient tris(dicarboxyimide)triphenylene **1**.

While the Yamamoto coupling is an effective method for the preparation of triphenylenes and related compounds, it does have a few drawbacks as it requires a stoichiometric amount of Ni(COD)_2 , and the use of an inert atmosphere glove box due to the instability of Ni(COD)_2 in the presence of air, light and moisture. Due to unforeseen circumstances, the glove box was unavailable, and the inability to use the glove box hampered research progress. As such, there was considerable interest in developing alternative nickel-mediated cyclotrimerization methods to access triphenylenes that use catalytic nickel(0) and reagents that are air-stable.

3.1.1 Reductive Polymerization via Nickel(0)-Catalyzed Coupling of Aryl Halides

Our initial investigation into alternative metal-catalyzed trimerizations led us to a publication from 1996,⁵⁸ in which Yang *et al.* reported the synthesis of efficient blue polymer light-emitting diodes from a series of soluble poly(paraphenylene) (PPP) derivatives (Figure 25), by utilizing a reductive polymerization reaction via nickel(0)-catalyzed coupling of bis(aryl halides) with nickel(II) chloride and zinc dust.⁵⁸

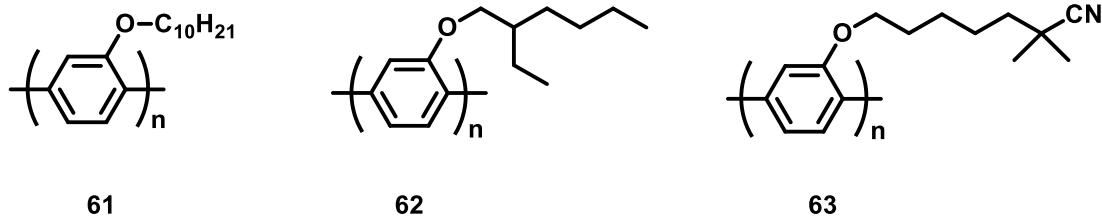
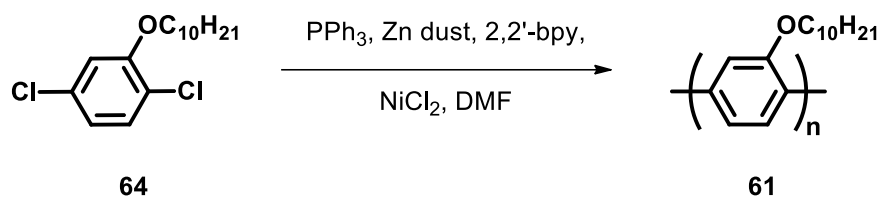


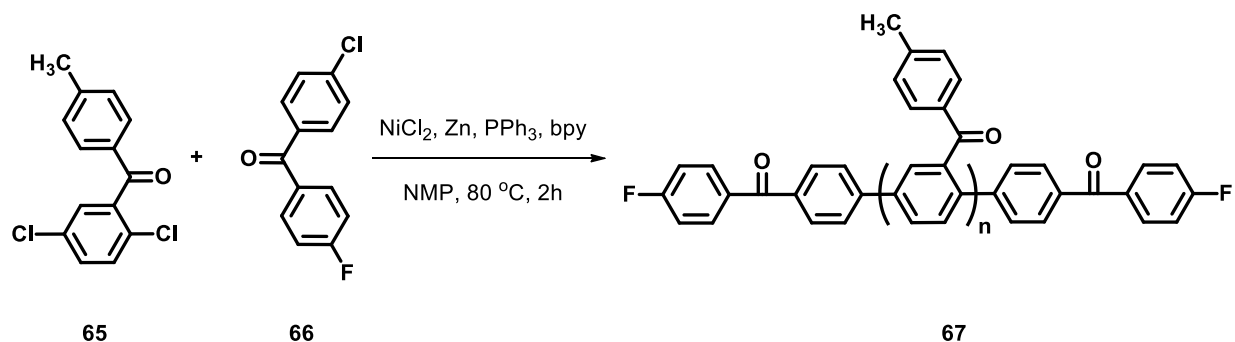
Figure 25. Structures of poly(paraphenylene) derivatives prepared by Yang et al. for blue light-emitting diodes.⁵⁸

In Yang's synthesis of poly(paraphenylene) **61**, 2,5-dichloro-1-decyloxybenzene **64** is first prepared via S_N2 reaction between 2,5-dichlorophenol and 1-bromodecane in the presence of sodium hydroxide.⁵⁸ Poly(2-decyloxy-1,4-phenylene) (DO-PPP) **61**, was then prepared by Ni(0)-catalyzed reductive polymerization reaction of **64** in the presence of nickel(II) chloride (NiCl_2), zinc dust, triphenylphosphine (PPh_3), and dipyriddy (2,2'-bpy) in dimethylformamide (Scheme 22).⁵⁸ Under these reaction conditions, zinc acts as a reducing agent and reduces NiCl_2 to form Ni(0) and ZnCl_2 . Subsequently, an active 1:1:1 catalytic complex will form between Ni(0), triphenylphosphine and 2,2'-bipyridine ($\text{Ni(PPh}_3\text{)(bpy)}$). The formation of this Ni(0)-catalyst results in the homocoupling between bis(aryl chloride) **64** thus forming DO-PPP. The chemical synthesis of the other two poly(paraphenylene) derivatives **62**, and **63** in Figure 25 were performed in analogous fashion to PPP **61** using the conditions in Scheme 22.⁵⁸



Scheme 22. Synthesis of DO-PPP **61** via Ni(0)-catalyzed coupling of **64** as reported by Yang *et al.*⁵⁸

In a subsequent 2001 paper,⁵⁹ Bloom *et al.* reported the synthesis of poly(*p*-phenylene) macromonomers and multiblock copolymers via Ni(0)-catalytic coupling of aromatic dichlorides, similar to that of Yang *et al.* in 1996. In this study, Bloom and coworkers successfully prepared poly(4'-methyl-2,5-benzophenone) **67**, end-capped with 4-chloro-4'-fluorobenzophenone to produce rigid-rod macromonomers (Scheme 23) in the presence of nickel(II) chloride, zinc dust, triphenylphosphine, and 2,2'-bipyridine in *N*-methyl-2-pyrrolidone (NMP).⁵⁹



Scheme 23. Synthesis of poly(4'-methyl-2,5-benzophenone) macromonomers via Ni(0)-catalyzed coupling as reported by Bloom and coworkers.⁵⁹

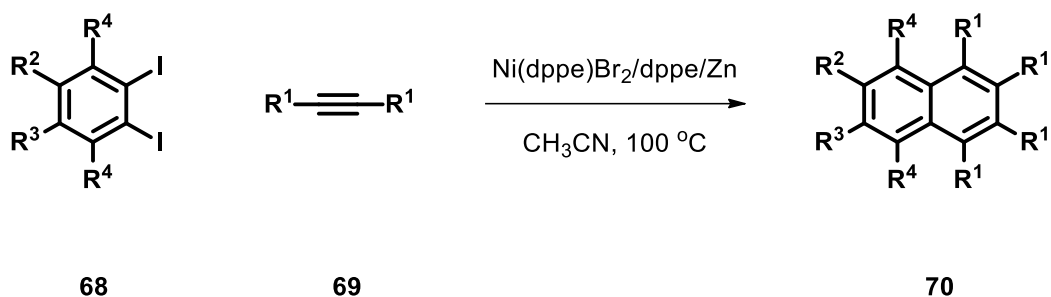
Although the routes reported by Yang *et al.* and Bloom *et al.*, respectively, are towards the synthesis of polymeric materials, and not cyclotrimers, it still served as a good starting point. There are many examples in the literature showing that it is possible to generate an active nickel(0)-species *in situ* without the use of a glove box or harsh conditions. However, it was unknown if the catalytic system of NiCl₂, PPh₃, bpy, and Zn would produce trimers and not polymers. Therefore, the literature was further investigated.

3.1.2 Nickel-catalyzed [2+2+2] Cycloaddition Reactions

In a 2008 publication,⁶⁰ communicated by Cheng *et al.*, *o*-dibromoarenes were employed as aryne precursors for nickel-catalyzed [2+2+2] homo-cycloaddition reactions and cycloaddition reactions with alkynes and nitriles using a similar catalytic system as Yang and Bloom. In this article, *o*-dihaloarenes are used as aryne precursors that react with acetylenes and nitriles catalyzed by the NiBr₂(dppe), 1,2-bis(diphenylphosphino)ethane (dppe) and zinc system to give substituted naphthalene, phenanthridine or triphenylene derivatives depending on the reaction conditions employed.⁶⁰ Moreover, this catalytic reaction is proposed to involve a nickel-assisted generation of benzyne intermediates as a key step in the formation of naphthalene, phenanthridine and triphenylene derivatives.

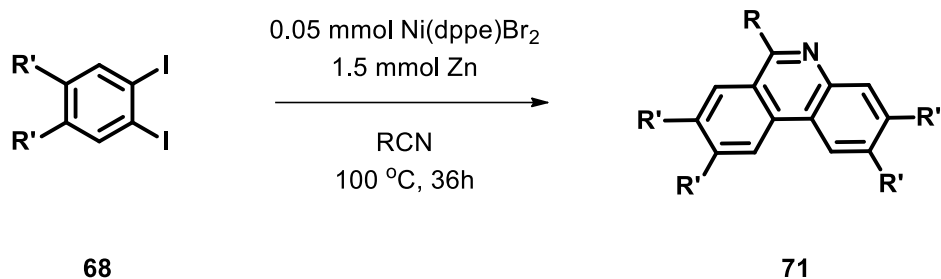
Naphthalene derivatives were synthesized via treatment of 1,2-diiodobenzene **68** with disubstituted alkynes **69** in the presence of Ni(dppe)Br₂, dppe, and zinc powder in acetonitrile at 100 °C for 48 hours in moderate to excellent yields ranging from 51% to 96% (Scheme 17).⁶⁰ Interestingly, it was found that a substantial amount of triphenylene would form in addition to the expected naphthalenes **70**, as a result of homo-cycloaddition of 1,2-diiodobenzene **68** under certain

unoptimized reaction conditions. Under these unoptimized conditions to prepare substituted naphthalenes, one of either NiBr₂(PPh₃) or NiCl₂(PPh₃) was used as the nickel catalyst and triphenylphosphine was used as the ligand.



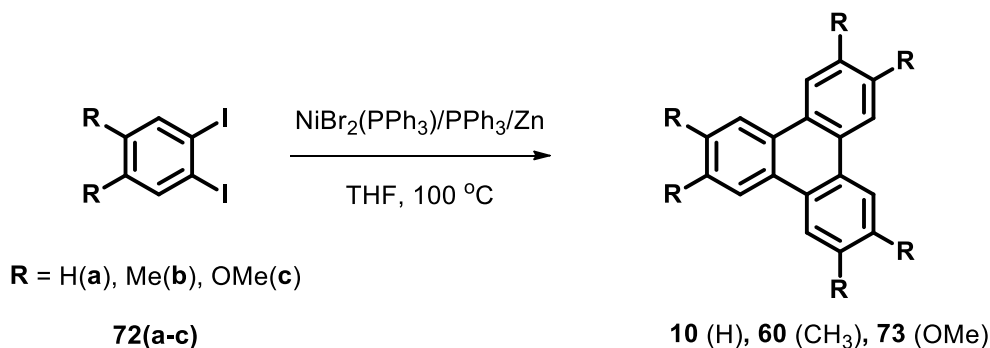
Scheme 24. Nickel-catalyzed cycloaddition of *o*-diiodoarenes with disubstituted alkynes as reported by Cheng and coworkers.⁶⁰

Unexpectedly, it was found that when 1,2-diiodobenzenes **68** were heated in the presence of Ni(dppe)Br₂ and zinc dust, but with no additional dppe in acetonitrile, afforded substituted phenanthridine derivatives **71** were afforded (Scheme 25). Additionally, similar to that of the synthesis of substituted naphthalenes, it was again found that under certain reaction conditions, when less acetonitrile solvent was used, triphenylenes would form as the major product, in addition to the formation of phenanthridines **71**. However, it was found that as the amount of acetonitrile solvent was increased, phenanthridine **71** became the major product of the reaction.



Scheme 25. Synthesis of phenanthridine derivatives in the presence of Ni(dppe)Br_2 and zinc without additional dppe.⁶⁰

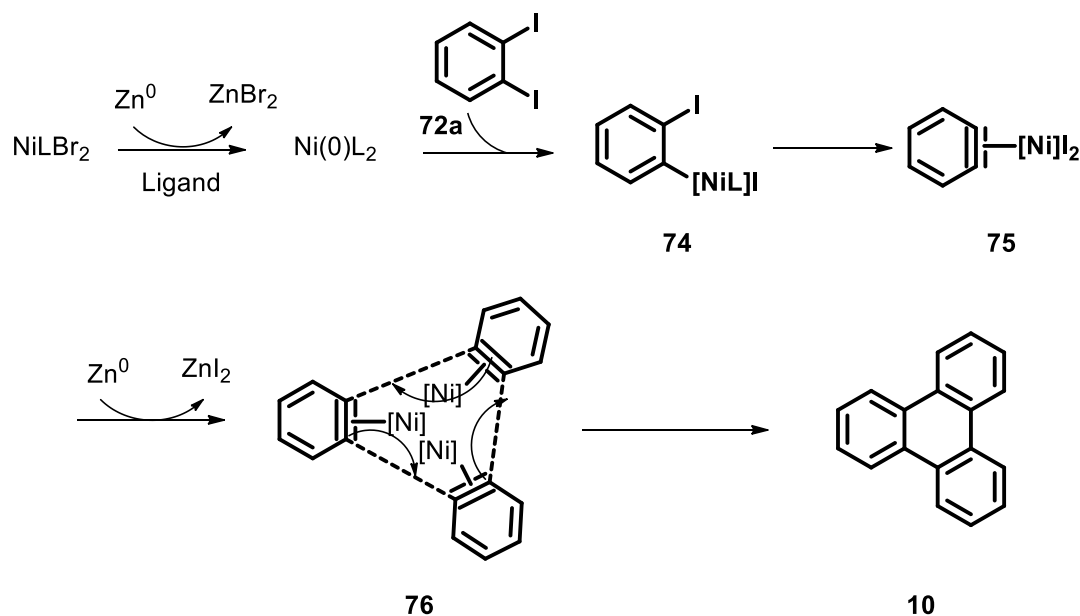
Cheng and coworkers also reported optimized reaction conditions for the formation of three triphenylene derivatives (Scheme 26). It was reported that reaction of 1,2-diiodobenzenes **72(a-c)** in the presence of $\text{NiBr}_2(\text{PPh}_3)_2$, and zinc, with triphenylphosphine in tetrahydrofuran at 100 °C for 48 hours produced triphenylenes **10**, **60** and **73**.⁶⁰



Scheme 26. Synthesis of triphenylenes using $\text{NiBr}_2(\text{PPh}_3)_2$ in tetrahydrofuran.⁶⁰

The results obtained by Cheng *et al.* in this article strongly suggest that the nickel-catalyzed reactions producing naphthalenes, triphenylenes and phenanthridines are likely due to a [2+2+2]

cycloaddition of arynes, alkynes or nitriles. As shown in Scheme 27, the active nickel(0) species is generated via reduction of the Ni(II) catalyst with zinc. The aryne intermediate is likely generated from the oxidative addition of *o*-dihaloarene **72a** to the nickel(0) complex to give **74**, followed by β -halogen elimination to afford **75**.⁶⁰ Reduction of **75** gives Ni-aryne complex **76** and subsequent [2+2+2] cycloaddition gives, in this case, triphenylene **10**. Additionally, [2+2+2] cycloaddition of **76** with nitriles or disubstituted alkynes will give phenanthridines and naphthalenes, respectively.



Scheme 27. Proposed nickel(0)-catalyzed mechanism for the [2+2+2] homo-cycloaddition of Ni(0)-assisted generation of benzyne to form triphenylene.⁶⁰

3.1.3 Air-Stable Binary Nickel(0)-Olefin Precatalysts

A 2020 publication⁶¹ reported by Tran and coworkers, discusses the preparation, and use of an air-stable binary nickel(0)-olefin precatalyst, nickel(0)(1,5-cyclooctadiene)(duroquinone) [Ni(COD)(DQ)]. Research on homogeneous nickel catalysis has recently been gaining a lot of interest as nickel can serve as an inexpensive alternative to precious metals used in many catalytic transformations, including palladium-catalyzed cross-couplings (e.g., Suzuki coupling). Ni(COD)₂ is a Ni(0)-olefin complex that has been extensively used as a precatalyst.⁶¹ However, the use of Ni(COD)₂ is limited by its sensitivity to air and moisture, and its use requires an inert atmosphere glovebox for storage and reaction setup.⁴² These limitations have inspired the development of new Ni(0)-olefin precatalysts with increased stability that may offer advantages over the previously used precatalysts.

Consequently, Tran and coworkers have worked to expand upon the current portfolio of nickel(0)-olefin precatalysts and describe the catalytic activity of Ni(COD)(DQ). Moreover, Ni(COD)(DQ) is isostructural and isoelectronic to Ni(COD)₂, both of which are 18-electron Ni(0)-olefin complexes.⁶¹ However, in contrast to Ni(COD)₂, Ni(COD)(DQ) is air and moisture stable in both solid and solution states, and possesses high thermal stability, which allows it to be conveniently stored at room temperature.⁶¹ The scope of the catalytic activity of Ni(COD)(DQ) was investigated using reactions that have been previously reported in the literature to proceed with different nickel precatalysts with the hope of establishing Ni(COD)(DQ) as a competent nickel precatalyst source. The reactions investigated using Ni(COD)(DQ) included the Suzuki-Miyaura coupling, Buchwald-Hartwig amination, borylation of aryl halides, C-H activation, alkene hydroarylation and decarboxylative cycloaddition.⁶¹ Notably, all reactions were setup outside of a glovebox and followed procedures using reaction conditions that were otherwise

identical to previously reported synthetic protocols. Furthermore, all reactions tested using Ni(COD)(DQ) as the replacement nickel precatalyst were successful, and provided yields of desired products that were comparable to those using the antecedent nickel precatalyst.

Overall, Tran and coworkers determined that Ni(COD)(DQ) successfully acted as a nickel-olefin precatalyst for a variety of distinct catalytic processes previously reported in the literature using other nickel precatalysts like, Ni(COD)₂. In all cases, *in situ* ligation with a variety of ligands was successful in generating an active nickel catalyst without optimization of the original reported conditions.⁶¹ Furthermore, the promise of Ni(COD)(DQ) as a new and reliable nickel precatalyst is due to its undeniable stability, and would be particularly ideal for handling in situations where it is not possible to completely exclude air and moisture.

3.2 Results and Discussion

To explore alternative nickel-catalyzed cyclotrimerization reaction conditions, a series of electron-rich and electron-deficient *o*-dibromoarenes were selected and included electron-rich 4,5-dibromo-*o*-xylene **52**, and electron-deficient substrates, dimethyl 4,5-phthalate **57** and 5,6-dibromo-2-octylisoindoline-1,3-dione **41**.

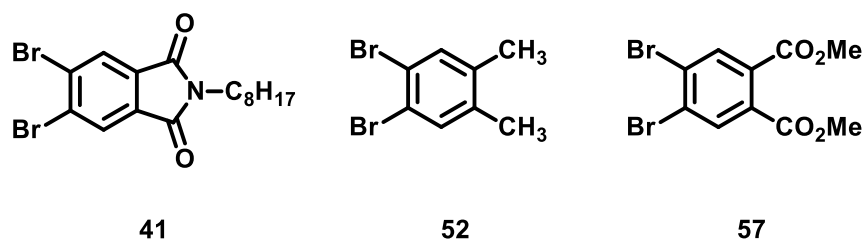
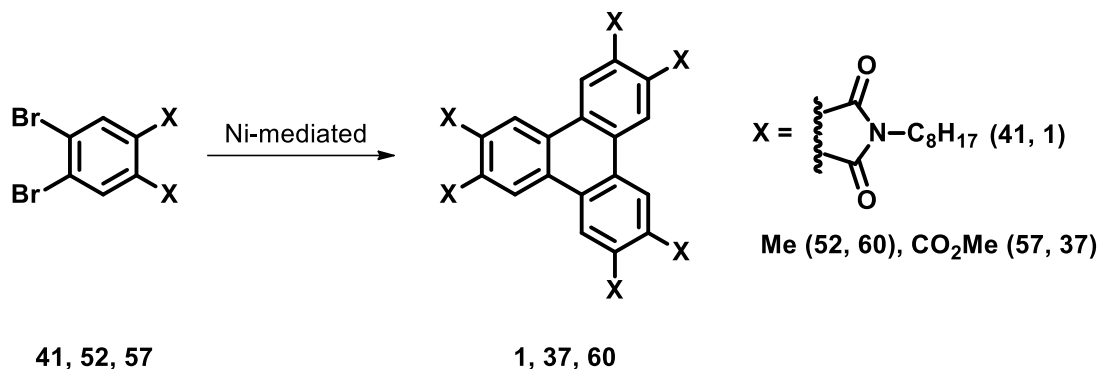


Figure 26. Structures of *o*-dibromoarene substrates tested.

Triphenylenes **1**, **37**, and **60** were chosen as target molecules because they have all been previously prepared in good yields by our group via the Yamamoto coupling reaction. Additionally, this allowed for a direct comparison of alternative nickel-catalyzed homocyclotrimerization conditions with the Yamamoto coupling approach. Notably, all reactions were run outside of a glovebox and under an atmosphere of nitrogen, as opposed to the Yamamoto coupling conditions which calls for reaction set-up under inert glovebox conditions to accommodate for the instability of Ni(COD)_2 in the presence of air and moisture.

First, Compound **41** was subjected to conditions similar to that of the Yamamoto coupling procedure however, using Ni(COD)(DQ) as the precatalyst. Additionally, compounds **52** and **57** were each subjected to nickel-catalyzed cycloaddition reactions with zinc dust, as reported by Cheng and coworkers.⁶⁰ Unfortunately, the alternative nickel-catalyzed conditions employed to prepare triphenylenes **1**, **37**, and **60** from their respective *o*-dibromoarene substrates were unsuccessful (Table 2).

Table 2. Summary of alternative Ni-catalyzed cyclotrimerization reactions vs Yamamoto coupling



Entry	Substrate	Method	Product	Yield (%)
1	41	Yamamoto ^a	1	65
2	41	Ni(COD)(DQ) ^b	1	0
3	52	Yamamoto ^a	60	58
4	52	Ni(II) and Zn ^c	60	0
5	52	Ni(II) and Zn ^d	60	Mixture
6	52	Ni(II) and Zn ^e	60	Mixture
7	57	Yamamoto ^a	37	70
8	57	Ni(II) and Zn ^e	37	Mixture
9	57	Ni(II) and Zn ^c	37	0

^aNi(COD)₂ (1.25 eq), 2,2'-bpy (1.25 eq), COD (2.05 eq), THF, rt, 24 h

^bNi(COD)(DQ) (1.25 eq), 2,2'-bpy (1.25 eq), COD (2.05 eq), THF, rt --> reflux, 48 h

^cNiBr₂(PPh₃)₂ (10 mol%), Zn (3.0 eq), THF, 100 °C, 48 h

^dNiBr₂(PPh₃)₂ (10 mol%), dppe (10 mol%), Zn (3.0 eq), THF, 100 °C, 48 h

^eNiBr₂(PPh₃)₂ (10 mol%), PPh₃ (10 mol%), Zn (3.0 eq), DMF, 85 °C, 22 h

3.2.1 Yamamoto coupling reaction using Ni(0) precatalyst Ni(COD)(DQ)

Triphenylene **1** has been prepared via the Yamamoto coupling reaction of *o*-dibromoarene substrate **41** in 65% yield using conditions developed in our lab. Moreover, to test whether the Yamamoto coupling reaction could be replicated outside of a glovebox, we employed Ni(COD)(DQ) as substitute nickel precatalyst for Ni(COD)₂. As previously mentioned, Tran and coworkers reported that Ni(COD)(DQ) was an air and moisture stable nickel(0)-precatalyst that is isostructural and isoelectronic to Ni(COD)₂.⁶¹ Additionally, Tran demonstrated that Ni(COD)(DQ) was able to act as a nickel-olefin precatalyst for a variety of distinct catalytic processes previously reported in the literature using other nickel precatalysts (e.g., Suzuki-Miyaura coupling, Buchwald-Hartwig coupling).⁶¹ With this in mind, we hypothesized that Ni(COD)(DQ) could be used to replace Ni(COD)₂ as the Ni(0)-species for the cyclotrimerization reaction. Unfortunately, subjecting **41** to the reaction conditions (Table 2, entry 2), with Ni(COD)(DQ) in the presence of COD, bpy in THF at room temperature for 24 hours yielded no reaction. Subsequently, the reaction temperature was increased to reflux which caused the solution to change colour from red to green. The reaction was then left for an additional 24 hours, by which point the colour of the solution had turned opaque black. Thin-layer chromatography and ¹H NMR spectroscopy revealed that indeed no reaction had occurred and compound **41** was recovered.

3.2.2 Nickel-catalyzed [2+2+2] cycloaddition reactions

Hexamethyltriphenylene **60** has been prepared by our group in 58% yield using the Yamamoto coupling reaction. Cheng and coworkers have also reported the synthesis of hexamethyltriphenylene via nickel-catalyzed [2+2+2] cycloaddition in the presence of zinc dust and a Ni(II) precatalyst (Scheme 19).⁶⁰ To evaluate if **60** could be prepared using a method other

than the Yamamoto coupling, Ni(II)-catalyzed cycloaddition conditions reported by Cheng and coworkers were employed.⁶⁰ The first attempt at preparing triphenylene **60** involved reaction of *o*-dibromoarene **52** with NiBr₂(PPh₃)₂ in the presence of zinc dust in THF at 100 °C for 48 hours (Table 2, entry 4). Under these conditions, the reaction was unsuccessful and only starting material was recovered. This is most likely because no ligand was present. Consequently, the Ni(0)-catalyst species that was formed *in situ* was not stabilized and was unable to undergo oxidative addition with **52**.

In the second approach to prepare triphenylene **60** via Ni-catalyzed [2+2+2] cycloaddition, **52** was reacted in the presence of NiBr₂(PPh₃)₂, zinc dust and 1,2-bis(diphenylphosphino)ethane in THF at 100 °C for 48 hours (Table 2, entry 5). Following the 48-hour reaction time, the crude mixture was filtered through a plug of silica, yielding an orange oil as the crude product. ¹H NMR showed that a small amount of hexamethyl triphenylene was present in the crude mixture as evidenced by a pair of singlets at 2.49 ppm and 8.32 ppm for methyl protons and the triphenylene protons, respectively. Notably, the ¹H NMR spectrum of the crude product also contained several other peaks for unknown by-products as well as unreacted starting material. Purification of hexamethyltriphenylene from the crude reaction mixture via column chromatographic separation was attempted. However, separation of dppe from hexamethyltriphenylene proved to be difficult due to similar polarities exhibited by both compounds and overlapping spots via TLC analysis, resulting in poor separation. Overall, a crude white solid was obtained containing an approximately 1:1 mixture of triphenylene and dppe at a mass less than that of 50% of the theoretical yield of pure triphenylene **60**. Due to low conversion of starting material, and difficulty in purification, the conditions were not pursued further.

In another attempt to prepare hexamethyltriphenylene (**60**), subjecting *o*-dibromoarene **52** to Cheng and coworkers' initial conditions was assessed (Table 2, entry 6). Under these conditions, DMF was used as the reaction solvent, and triphenylphosphine was employed as the ligand rather than 1,2-(diphenylphosphino)ethane. After the first 22 hours of reaction time, disappearance of starting material **52** was confirmed via thin-layer chromatography. The crude reaction mixture was filtered through a pad of celite with dichloromethane and concentrated to yield a crude yellow oil. Moreover, purification via column chromatography was attempted, resulting in the collection of a white solid containing a mixture of triphenylphosphine and hexamethyltriphenylene in approximately an 18:1 ratio and with a crude mass that was 50% of the theoretical mass of pure hexamethyltriphenylene. It is possible that a significant amount of hexamethyltriphenylene may have remained in the column due to poor solubility in the eluting solvent hexanes, and because the column may have been too long. No further purification of hexamethyltriphenylene or investigation of the synthesis of **60** under these reaction conditions was attempted due to low conversion of starting material **52** and difficulty in purification.

In addition to hexamethyltriphenylene **60**, investigation into the preparation of hexa(methyl ester)triphenylene **37** was examined using two similar approaches used to examine the potential preparation of hexamethyltriphenylene **60**. Both approaches are iterations of what was reported by Cheng and coworkers in their 2008 communication.⁶⁰

In the first approach, phthalic ester **57** was subjected to the [2+2+2] cycloaddition reaction conditions in the presence of NiBr₂(PPh₃)₂, zinc dust and triphenylphosphine in THF at 80 °C (Table 2, entry 8) as reported by Cheng *et al.*⁶⁰ Thin-layer chromatography and ¹H NMR spectroscopy showed that for the first 22 hours no product was present and a significant amount of starting material remained in the reaction mixture. Since no product had yet formed, the reaction

temperature was increased from 80 °C to 100 °C and the reaction was allowed to stir for an additional 26 hours. Following the additional allotted reaction time and separation of the organics from insoluble nickel salts, thin-layer chromatography showed the formation of several new spots and ¹H NMR showed a small aromatic singlet approximately at 9.04 ppm, representative of the hexa(methyl ester)triphenylene proton, among several other proton signals from unknown by-products and starting material. Unfortunately, further purification of **37** was not pursued as the amount of triphenylene formed was extremely miniscule and separation via column chromatography would have proved to be cumbersome as several spots with similar R_f values were present on the TLC plate.

In the second approach to access hexa(methyl ester) triphenylene **37**, *o*-dibromoarene **57** was subjected to [2+2+2] cycloaddition reaction conditions in the presence of NiBr₂(PPh₃)₂, zinc dust in THF at 100 °C for 48 hours (Table 3, entry 9). Notably, no ligand was present in this reaction and just like that of 4,5-dibromo-*o*-xylene, phthalic ester **57** did not undergo trimerization via [2+2+2] cycloaddition. Analysis of the crude reaction mixture via thin-layer chromatography and ¹H NMR showed that starting material was still present, among other unknown by-products that were not further investigated.

Because the reactions of *o*-dibromoarenes **52** and **57** were unsuccessful under the Ni-catalyzed [2+2+2] cycloaddition conditions, and due to time constraints, further investigation of these reactions of **52** and **57** were not pursued. Additionally, Cheng and coworkers did not report any yields, purification conditions or ¹H NMR spectra for triphenylenes **10**, **60**, and **73** prepared under the reported conditions (Scheme 26), which made it difficult to compare results and assess if the triphenylenes prepared were purified. With that being said, it is clear that the Yamamoto coupling reaction conditions are superior to that of the [2+2+2] cycloaddition reaction conditions.

3.3 Summary and Future Work

In summary, we have demonstrated that the Yamamoto coupling reaction is a superior and more reliable approach to access a variety of electron-rich and electron-deficient triphenylenes such as **1**, **37** and **60** in comparison to other synthetic methods tested. In this study, we sought to develop an alternative method to access triphenylenes via a nickel-assisted cyclotrimerization that did not require nickel(0)bis(1,5-cyclooctadiene) or reaction set-up under inert glove box conditions. We tested two promising methods using two distinct stable nickel-precatalysts in attempts to prepare triphenylenes **1**, **37** and **60** from the respective *o*-dibromoarene precursor. The first of two methods assessed included Yamamoto coupling type reaction employing the use of an air and moisture stable nickel(0)-precatalyst, Ni(COD)(DQ) as a replacement for Ni(COD)₂ and reaction set-up outside of a glove box. The second cyclotrimerization conditions tested was a nickel-assisted [2+2+2] cycloaddition reaction of *o*-dibromoarenes that had been previously reported by Cheng *et al.*⁶⁰

Synthesis of electron-deficient triphenylene **1** has been successfully completed via the Yamamoto coupling reaction of *o*-dibromoarene **41** in 65% yield. However, this same reaction was not successful when Ni(COD)(DQ) was employed as the nickel(0)-precatalyst as a substitute for Ni(COD)₂. Although conditions identical to that of the Yamamoto coupling, with the exception of Ni(COD)(DQ) and reaction set-up outside of a glove box, were employed, the reaction did not produce triphenylene **1**. It is possible that the active Ni(0)-species, Ni(COD)(bpy) was not formed *in situ* and therefore no reaction would take place. Moreover, a full screening and optimizing of the conditions has yet to be performed due to time constraints. Additionally, Tran and coworkers reported the use of Ni(COD)(DQ) as a replacement nickel-precatalyst without any optimization or change in conditions when assessing the catalytic scope of Ni(COD)(DQ), so it was to our

disappointment that Ni(COD)(DQ) did not serve as an effective substituted for Ni(COD)₂ for the Yamamoto coupling reaction. In the future, various reaction screening trials may be assessed. These will include adjustment of reaction concentration, solvent, and reaction temperature. It is also important to note that Ni(COD)(DQ) is quite expensive and can only be purchased in small quantities so it may not be economically feasible to further investigate this route, especially considering a stoichiometric amount of nickel(0) is needed for the reaction. Conversely, gram-scale synthesis of Ni(COD)(DQ) is reported by Tran *et al.* from air-stable Ni(II) precursor nickel(II) acetylacetonate [Ni(acac)₂] in the presence of diisobutylaluminum hydride (DIBAL-H) in 60%.⁶¹ In terms of cost, the synthesis of Ni(COD)(DQ) from Ni(acac)₂ is a much cheaper option than directly purchasing Ni(COD)(DQ), additionally, this allows for preparation of Ni(COD)(DQ) on a much larger scale. If this potential alternative Yamamoto coupling route is further investigated, the synthesis of Ni(COD)(DQ) allows for the investigation to be more cost-efficient.

Furthermore, triphenylenes **37** and **60** have both been previously prepared by our group via the Yamamoto coupling reaction in 58% and 70% yields, respectively. Cheng and coworkers also reported the synthesis of hexamethyltriphenylene **60** when *o*-diiodoarene **72b** was subjected to nickel-catalyzed [2+2+2] cycloaddition in the presence of NiBr₂(PPh₃)₂, PPh₃ or dppe, and zinc dust in THF (Scheme 26).⁶⁰ The conditions employed by Cheng and coworkers to synthesize triphenylenes was of interest because it utilized a stable, cheap and readily available Ni(II)-complex and the reaction could be set-up outside of a glovebox. On the other hand, Cheng did not report yields, purification strategies or NMR spectra for the three triphenylenes prepared, which made it difficult to make any comparisons to what Cheng and coworkers had done following the reaction. Nonetheless, *o*-dibromoarenes **52** and **57** were each subjected to the nickel-assisted [2+2+2] cycloaddition reaction conditions resulting in the formation of complex and intractable

mixtures of starting material, ligand, unknown by-products, and small amounts of the desired triphenylene. Several attempts were made to purify the crude products of **37** and **60**, however, the low yields and poor separations via chromatographic separation made it extremely difficult and time consuming. It is unclear if the triphenylene products obtained by Cheng and coworkers were fully purified or if they were characterized as crude mixtures. Consequently, the poor results obtained from this study led to a pause in any further investigation into the nickel-catalyzed [2+2+2] cycloaddition method as reported by Cheng and coworkers.

CHAPTER 4: TOWARDS THE SYNTHESIS OF A NOVEL COVALENT ORGANIC FRAMEWORK

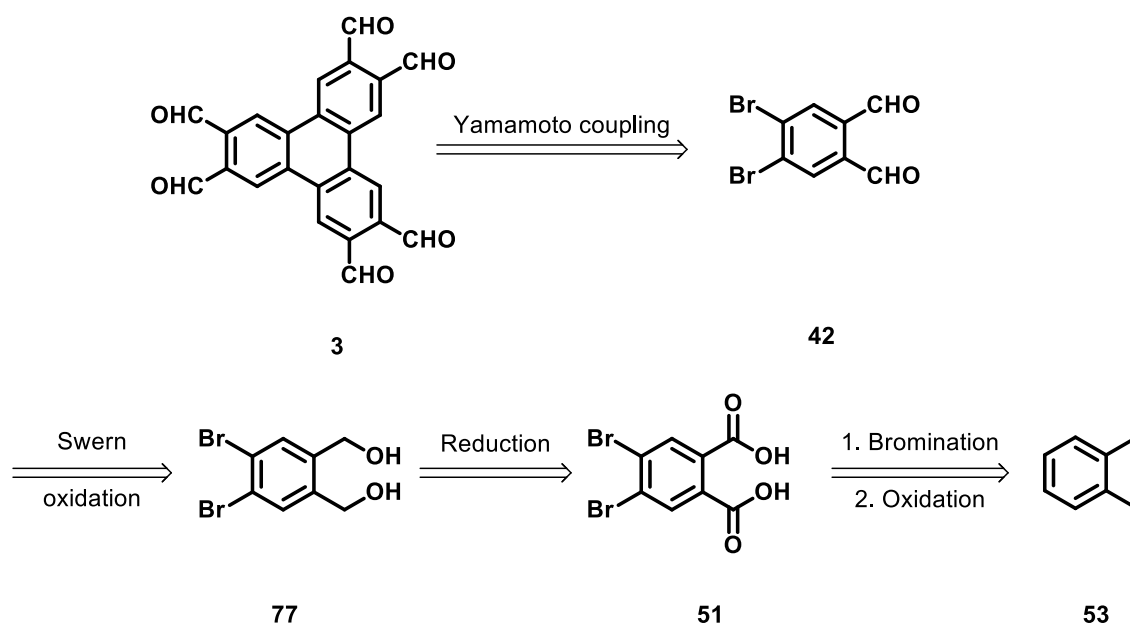
4.1 Introduction

Intense efforts are being made in the field of materials science to better understand the structure-property relationships of microporous materials with the goal of being able to manipulate their structures to elicit desired functions for specific applications. The development of porous materials has lead to the development of materials like, metal-organic frameworks (MOFs),^{32,33} which are held together by coordination bonds of metal atoms to ligands, and covalent organic frameworks (COFs), which are constructed of carbon and other light elements in a covalently linked framework.³¹ In particular, covalent organic frameworks have garnered much interest as functional microporous structures due to their potential design opportunities and various applications such as gas storage and separations, catalysis, environmental remediation, sensing, enzyme and drug uptake and materials science.^{31,34}

Covalent organic frameworks are primarily constructed using a bottom-up approach, as smaller subunits are designed and linked together through reversible covalent bond formations. Slightly reversible condensation reactions of organic linkers are utilized to build COFs,^{31,34} and as a result of this, the covalent bonds formed establish a thermally stable framework in which the reversible nature of the coupling reactions permits for error correction and rearrangement of the network, allowing the for the formation of a crystalline structure.³⁴ To date, covalent organic frameworks have been prepared utilizing a variety of linking groups like boroxines, boronic esters, imines, hydrazones and others.³⁴ However, these linking groups can be subjected to unwanted hydrolysis reactions, thus, corrupting the integrity of the framework via bond breakages.

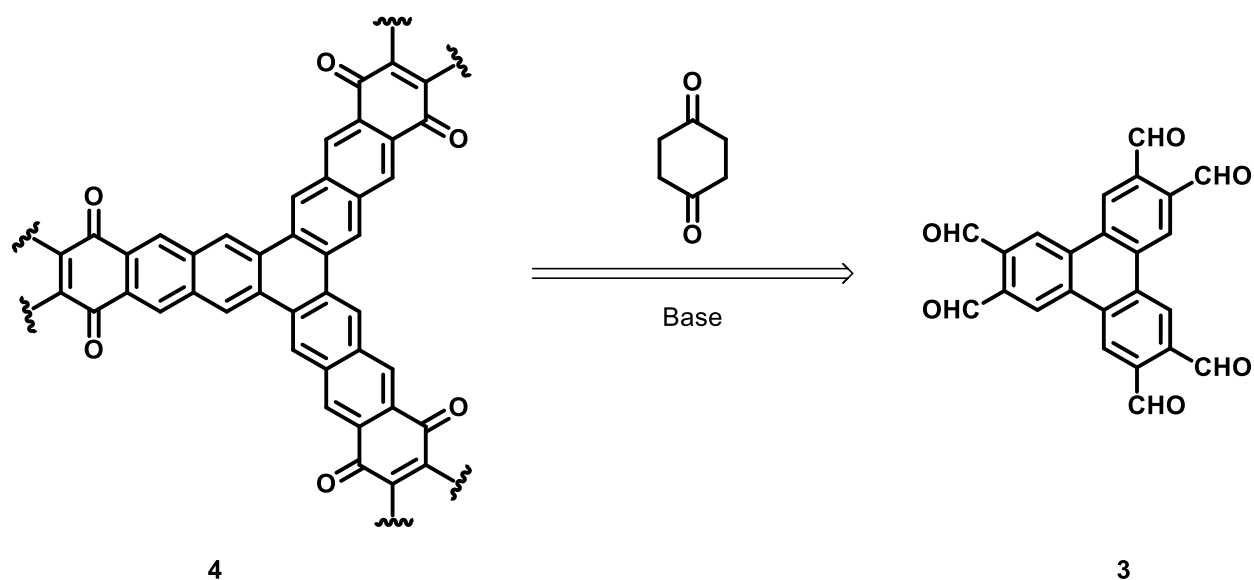
In this approach, aldol condensation of hexa(formyl)triphenylene and 1,4-cyclohexadione will produce a covalent organic framework linked by rigid rings consisting of carbon-carbon bonds. Aldol condensations are reversible acid-base reactions. However, if the thermodynamics of the reaction are in favour forming covalent organic framework **4** (Scheme 29), it will produce an extended 2-dimensional network linked via rigid carbon-carbon bonds. In addition, the quinone units within the extended network offer potential opportunities to perform functional group transformations using appropriate reagents. For example, reduction of the quinone units installed in the framework will yield a pure, extended polycyclic aromatic hydrocarbon framework, like that of graphene.

The desired hexa(formyl)triphenylene **3** can be synthesized starting from *o*-xylene **53** (Scheme 28). Through consecutive steps, *o*-xylene will undergo a two-fold bromination followed by a two-fold oxidation to access *o*-dibromophthalic acid **51** as reported by Zhang *et al.*⁵¹ *o*-Dibromophthalic acid **51** then undergoes reduction in the presence of a borane-tetrahydrofuran complex, followed by a subsequent Swern oxidation via a procedure adapted from Kozmin *et al.* to access phthalaldehyde **42**.⁶² Hexa(formyl)triphenylene **3** can then potentially be obtained following the Yamamoto cyclotrimerization of **42**.



Scheme 28. Proposed retrosynthetic approach to hexaaldehyde-substituted triphenylene **3**.

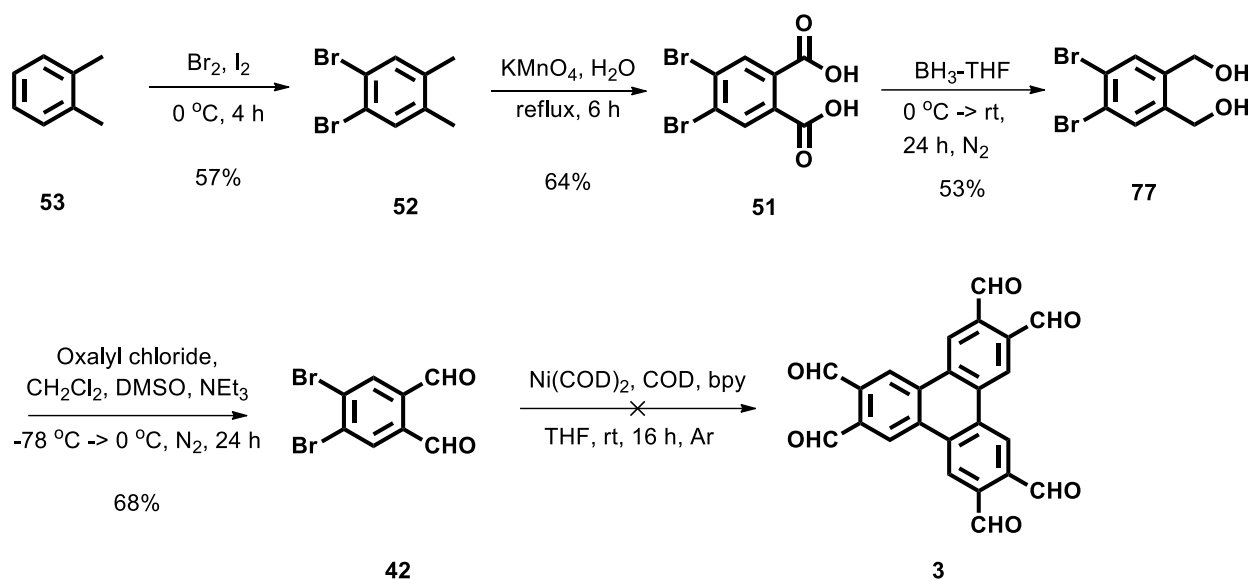
Moreover, novel covalent organic framework **4** may potentially be synthesized via the aldol condensation of hexa(formyl)triphenylene **3** and 1,4-cyclohexadione using an appropriate solvent and base (Scheme 29).



Scheme 29. Retrosynthetic approach to COF 4 from aldehyde 3.

4.2 Results and Discussion

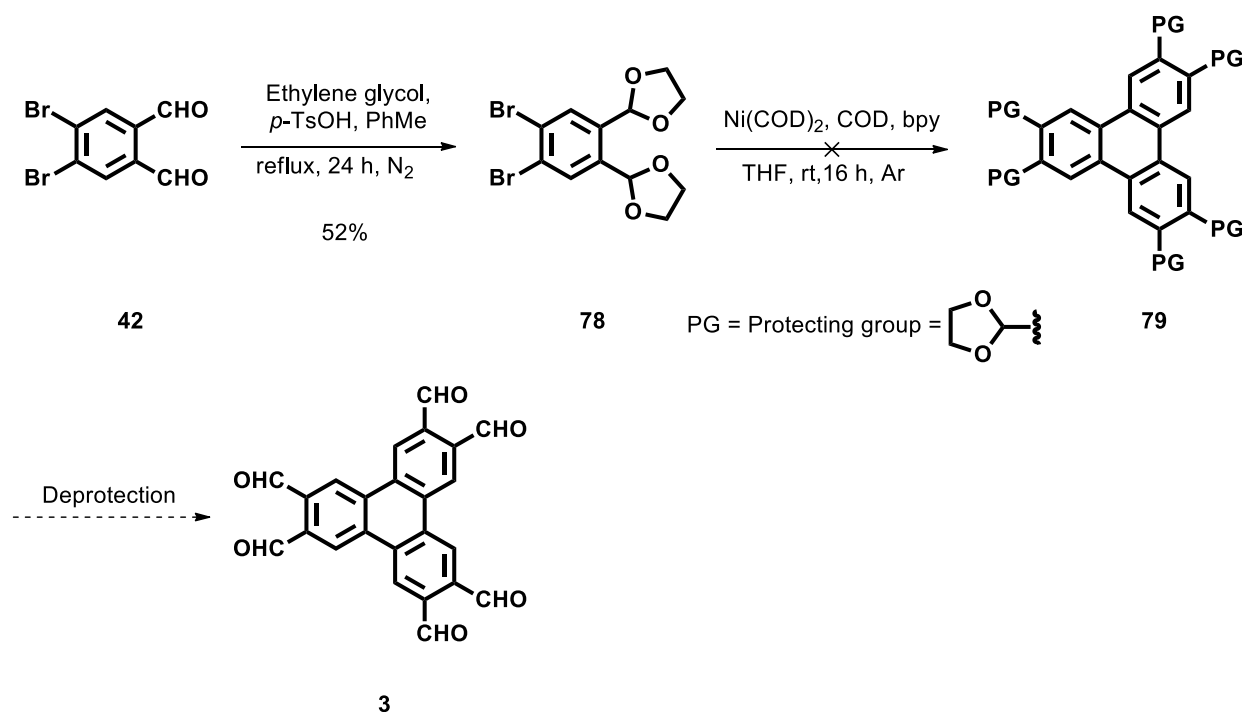
The initial synthetic approach that was explored in attempts to access hexa(formyl)triphenylene **3** is represented by schemes 30. The preparation of 4,5-dibromophthalic acid **51** was achieved through bromination of *o*-xylene **53** and subsequent benzylic oxidation of **52** as reported by Zhang *et al.*⁵¹ Following this, (4,5-dibromo-1,2-phenylene)dimethanol **78** was prepared in 53% yield via the reduction of phthalic acid **51** with a borane tetrahydrofuran (THF) complex as the reducing agent, adapted from a procedure reported by Kozmin *et al.*⁶² Alcohol **77** was then subjected to Swern oxidation conditions using a procedure adapted from one reported by Kozmin *et al.*,⁶² affording desired aldehyde substrate **42** in a 68% yield (Scheme 30). Since aldehydes are known to oxidize in the presence of oxygen at ambient conditions, **42** was stored in an air-tight container, flushed with nitrogen gas, and sealed with parafilm.



Scheme 30. Initial synthetic route attempted to prepare hexa(aldehyde)triphenylene **3**.

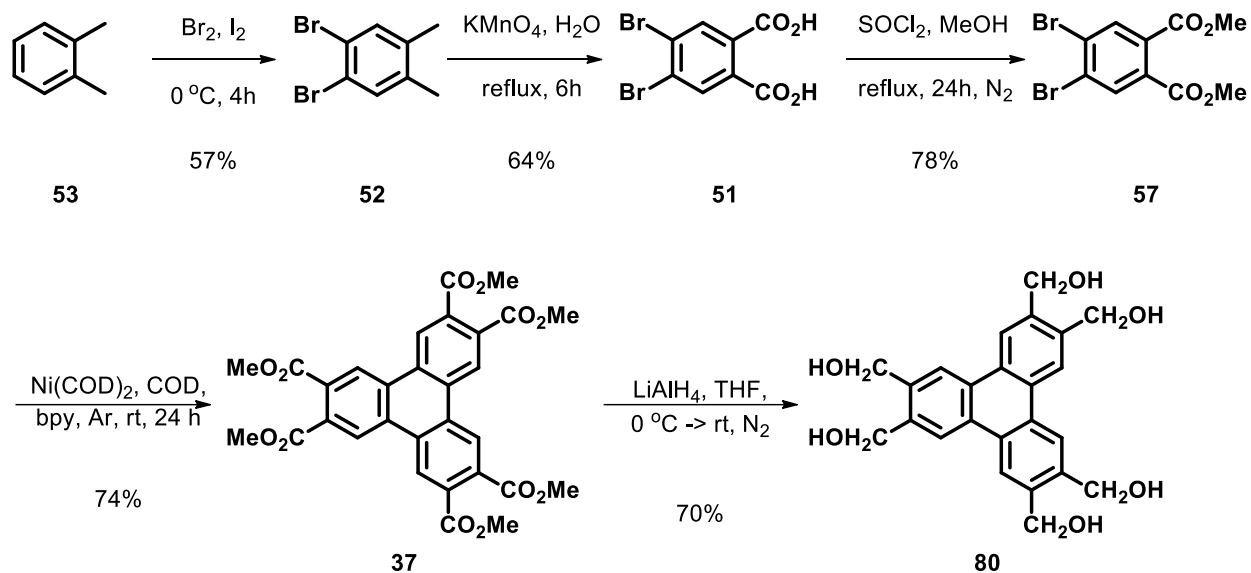
Next, the synthesis of hexa(formyl)triphenylene **3** was attempted via the direct Yamamoto cyclotrimerization of phthalaldehyde substrate **42** (Scheme 30). Unfortunately, this approach was unsuccessful and no triphenylene product was obtained. There is literature precedent for the activation of aldehydes via the coordination of zerovalent nickel catalysts like Ni(COD)_2 which can lead to unwanted by-products and side reactions. As reported by Ogoshi *et al.*, benzylic aldehydes and aliphatic aldehyde species are activated by zerovalent nickel catalysts to undergo homodimerization reactions to form esters.⁶⁴ The unwanted activation of the benzylic aldehydes of substrate **42** by zero-valent Ni(COD)_2 , may attribute to the unsuccessful formation hexa(formyl)triphenylene **3** under Yamamoto coupling conditions. Consequently, the failed formation of hexa(formyl)triphenylene **3** illustrates a limitation in the scope of the Yamamoto coupling reaction when other reactive functional groups like aldehydes are present within the starting material.

To potentially overcome this complication, cyclic acetal groups were installed to replace phthalaldehyde **42** with diacetal **78** (Scheme 31). The protected substrate was formed as a yellow oil in 52% yield via the reaction of phthalaldehyde **42** in the presence of ethylene glycol and a catalytic amount of *p*-toluenesulfonic acid (*p*-TsOH), while refluxing in toluene with a Dean-Stark apparatus equipped to remove the water formed, thus pushing the reaction to completion.⁶³ Similarly, efforts to prepare hexa(formyl)triphenylene **3** from the protected *o*-dibromoarene precursor **78** were unsuccessful, resulting in the formation of a complex mixture with no evidence of the desired product **79**. It is suspected that a similar issue to that observed with phthalaldehyde **42** arises when **78** is subjected to Yamamoto coupling conditions.



Scheme 31. Attempted synthesis of hexa(formyl)triphenylene **3** via protection of aldehyde **42**.

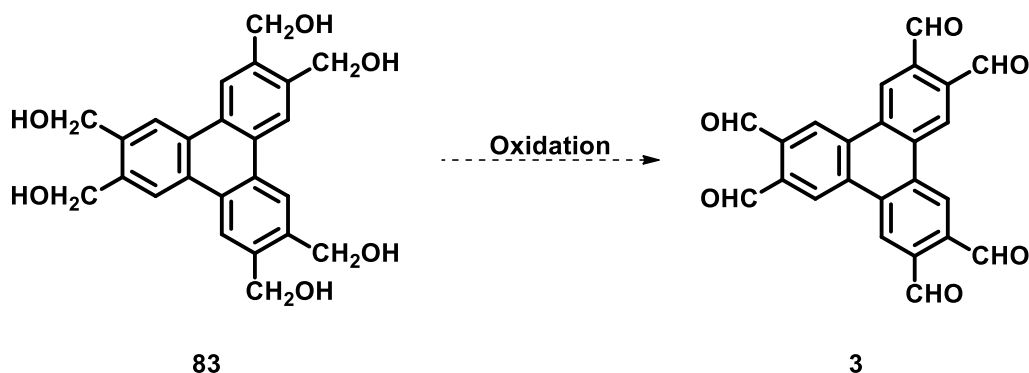
Following the observation of the limitations of the Yamamoto coupling reaction when reactive functional groups like benzylic aldehydes are used in the presence of zero-valent Ni(COD)₂, a new approach to access hexa(formyl)triphenylene was needed. We envisioned that we could potentially access hexa(formyl)triphenylene **3** via reduction of hexa(methyl ester)triphenylene **37**, to form the benzylic alcohol derivative **80**, followed by subsequent oxidation. Fortunately, our lab had already previously developed a synthesis of hexa(methyl ester)triphenylene **37** in good yields.⁵³ In Scheme 32, the synthesis of hexa(methyl ester)triphenylene is described starting with a 2-fold bromination of cheap and readily available *o*-xylene to access 4,5-dibromo-*o*-xylene **52** in 57% yield as reported by Chen *et al.*⁵¹ 4,5-Dibromo-*o*-xylene **52** is subsequently oxidized in the presence of potassium permanganate in water at refluxing temperatures to afford phthalic acid **51** in 64% yield as reported by Zhang *et al.*⁵¹ Phthalic acid **51** then undergoes Fisher esterification in the presence of thionyl chloride and methanol, allowing access to the corresponding phthalate **57** in 78% yield, as reported by Zhang *et al.*⁶⁵ Yamamoto coupling of phthalate **57**, using conditions reported by Yamamoto *et al.* in the presence of Ni(COD)₂, 1,5-cyclooctadiene and 2,2'-bipyridine in tetrahydrofuran under inert glove box conditions proceeds to give hexa(methyl ester)triphenylene **37** in 74% yield.⁴² With hexa(methyl ester)triphenylene in hand, the synthesis of hexa(methanol)triphenylene **80** was achieved adapting from a procedure reported by Yuan and coworkers via lithium aluminum hydride reduction of **37** in tetrahydrofuran at 0 °C, followed by acidic workup with 1 M HCl and recrystallization of the crude product using a 2:1 mixture of water and dimethyl sulfoxide giving **80** as a pale-yellow powder in 70% yield.⁶⁶



Scheme 32. Synthesis of hexa(methanol)triphenylene **80** from hexa(methyl ester)triphenylene **37**.

After the successful synthesis of hexa(methanol)triphenylene **80** in good yield, several attempts to prepare the corresponding hexa(formyl)triphenylene **3** under oxidizing conditions were made (Table 3). Hexa(formyl)triphenylene **3** is an unknown compound in the chemical literature databases and therefore no synthetic or characterization data currently exists for **3**. Table 3 summarizes the multiple oxidation conditions employed in attempts to prepare **3** from alcohol **80**. Unfortunately, all conditions tested thus far have had limited to no success in the preparation of aldehyde **3**.

Table 3. Summary of oxidation trials of hexa(methanol)triphenylene **80**.



Substrate	Method	Expected Product	Yield (%)
80	Swern oxidation	3	0
80	PCC	3	0
80	Dess-Martin	3	Mixture
80	Burgess reagent	3	Mixture

First, oxidation of **80** was attempted using Swern oxidation conditions as reported by Yuan and coworkers.⁶⁶ In Yuan's work, a Swern oxidation was performed on a relatively larger acene-type system containing four benzyl alcohol functional groups. Successful 4-fold Swern oxidation of this molecule afforded the corresponding tetraformyl-substituted derivative in good yields.⁶⁶ Although most Swern oxidation conditions are quite consistent over a broad range of alcohols, these particular conditions reported by Yuan and coworkers were chosen because it was the closest representative example of a Swern oxidation performed on a molecule containing several benzylic alcohol groups. Using the same conditions, hexa(methanol)triphenylene **80** was subjected to Yuan's Swern oxidation protocol in the presence of oxalyl chloride, and dimethyl sulfoxide in dichloromethane at -78 °C for 6 hours, followed by addition of triethylamine at -78 °C. Upon

workup, a brown solid was collected from the reaction mixture. Both the organic and aqueous layers were analyzed via ^1H NMR spectroscopy which surprisingly revealed that neither starting material or product were present. This result is extremely perplexing, and there is no logical explanation to reason why this occurred. Notably, further Swern oxidation trials were performed with adjustments made to reaction time, the ratio of DMSO to dichloromethane to account for the poor solubility of **80** in dichloromethane, as well as the stoichiometry of the reagents used. However, the results were consistent with the first trial, and no trace of starting material or product was found in the precipitate formed, the organic layers or the aqueous layers.

The disappointing results obtained via the attempted Swern oxidations of hexa(methanol)triphenylene **80** led to the investigation of several other oxidation conditions known to selectively oxidize primary alcohols to the corresponding aldehyde without over-oxidizing to the carboxylic acid. The attempted oxidation reactions of alcohol **80** explored are summarized in Table 3, and include oxidation with pyridinium chlorochromate (PCC), Dess-Martin oxidation, and oxidation with Burgess reagent.

Oxidation of hexa(methanol)triphenylene with pyridinium chlorochromate (PCC) was attempted using a representative procedure for the oxidation of benzylic alcohols as reported by Bialecki and coworkers.⁶⁷ Solid pyridinium chlorochromate was slowly added to a stirring heterogeneous mixture of alcohol **80** in dry dichloromethane. The orange-coloured mixture was left to react overnight, and the dark-brown solution found the following day was filtered through a celite plug. Thin-layer chromatography revealed two spots with similar retention factors near and on the baseline. Excess solvent was subsequently removed, and the crude solid was subjected to column chromatographic purification, resulting in the loss of one the spots seen on the TLC plate. The other spot was collected and analyzed via ^1H NMR spectroscopy and was neither starting

material nor desired product. The loss of starting material can be attributed to the insolubility of **80** in most organic solvents, except for DMSO and it may have been lost during the first filtration through celite or could have been lost during column chromatography. In a second oxidation trial of **80** using PCC, ^1H NMR analysis of the crude reaction mixture in deuterated dimethyl sulfoxide showed proton peaks representative of the starting material but did not any peaks for the expected aldehyde product **3**. Again, poor solubility of alcohol **80** in dichloromethane and the formation of a heterogeneous mixture could have caused the reaction to fail. Upon further investigation of solvents reported to be used for PCC oxidations, it was found that chlorinated solvents like dichloromethane and chloroform were the most common solvents used, with no reports of DMSO being used.

With the results obtained from the prior oxidation trials of alcohol **80**, we began to exclusively look for oxidation reactions that employed DMSO as the reaction solvent primarily because a solvent that could solubilize **80** was needed. Our investigation led us to investigate the oxidation of hexa(methanol)triphenylene **80** via Dess-Martin oxidation. Dess-Martin oxidation employs a hypervalent iodine reagent called Dess-Martin periodinane that is known to oxidize primary alcohols to the corresponding aldehyde, and can be performed in dichloromethane, dimethyl sulfoxide, or a combination of the two solvents.⁶⁸ In the first oxidation trial of **80** following Dess-Martin oxidation protocol as reported by Holsworth,⁶⁸ **80** was suspended in dry dichloromethane at 0 °C under an atmosphere of nitrogen. Dess-Martin periodinane was then added quickly to the reaction flask and left to stir for 2 hours. Analysis of the reaction mixture by thin-layer chromatography and ^1H NMR spectroscopy revealed that no reaction occurred. Dimethyl sulfoxide was then added to the reaction mixture to solubilize alcohol **80**, resulting in a clear yellow solution. After approximately 10 minutes, following the addition of DMSO, a yellow

precipitate had formed in the reaction mixture. The yellow solid was collected via suction filtration and analyzed via ^1H NMR spectroscopy. Gratifyingly, the ^1H NMR spectrum showed that no starting material was present, and the expected peaks for the desired aldehyde **3** were observed. However, the ^1H NMR also revealed an impurity corresponding to either unreacted Dess-Martin periodinane or one of the iodo-compound by-products iodosobenzoic acid (IBA) or 2-iodoxybenzoic acid (IBX). Many attempts were made to separate **3** from the crude mixture containing Dess-Martin oxidation by-products, but these efforts were met with no success. In many reported oxidation procedures of alcohols employing DMP as the oxidant, the reaction is easily quenched with aqueous sodium bicarbonate or sodium thiosulfate followed by removal of the insoluble DMP by-products via filtration.⁶⁸ The filtrates are then extracted with an organic solvent such as diethyl ether or dichloromethane and the products are purified via column chromatography.⁶⁸ However, in our case, the resulting aldehyde is extremely insoluble in all organic solvents, apart from dimethyl sulfoxide which also inconveniently dissolves DMP and reaction by-products. With the inability to perform filtration and extraction of the aldehyde from an organic solvent as well as being unable to perform chromatographic separation of the crude product, another oxidation protocol for **80** was needed.

The final oxidation protocol investigated for the oxidation of alcohol **80** used a procedure reported by Sultane and coworkers.⁶⁹ Sultane reported the efficient and rapid oxidation of alcohols facilitated by Burgess reagent ([methoxycarbonyl-sulfamoyl]triethylamine hydroxide) in dimethyl sulfoxide to the corresponding aldehydes and ketones in excellent yields.⁶⁹ This protocol was also an attractive oxidation method as it is performed under mild conditions (e.g., room temperature) in comparison to the Swern oxidation and requires short reaction times. Adapting from the oxidation protocol reported by Sultane *et al.*,⁶⁹ hexa(methanol)triphenylene **80** was dissolved in

anhydrous DMSO and stirred at room temperature under an atmosphere of nitrogen, forming a yellow transparent solution. Next, Burgess reagent was quickly added, and the resulting reaction mixture was left to stir overnight. The following day, an orange and slightly opaque reaction mixture was found. The crude reaction mixture was poured over ice water resulting in the formation of a dark-orange precipitate that was collected via suction filtration. Analysis of the crude product via ^1H NMR spectroscopy in deuterated DMSO revealed that a mixture of partially oxidized products was potentially formed. Several overlapping singlet peaks were observed between 8.43-9.13 ppm on the NMR spectrum, characteristic of a triphenylene proton. Additionally, a broad peak with several overlapping singlets was also observed between 10.38-10.63 ppm, which is where the expected aldehyde proton signal should exist on the spectrum. These results suggest that the reaction was unable to reach completion as several triphenylene products containing an unknown number of aldehyde functional groups seemed to be present within the sample. Assessment of longer reaction times (>24 hours) and increased amounts of Burgess reagent (>1.3 equivalents per alcohol) may be investigated in the future. Although, the use of increased amounts of Burgess reagent is not economically feasible, as it is quite expensive and can only be purchased in a package size of 1 gram.

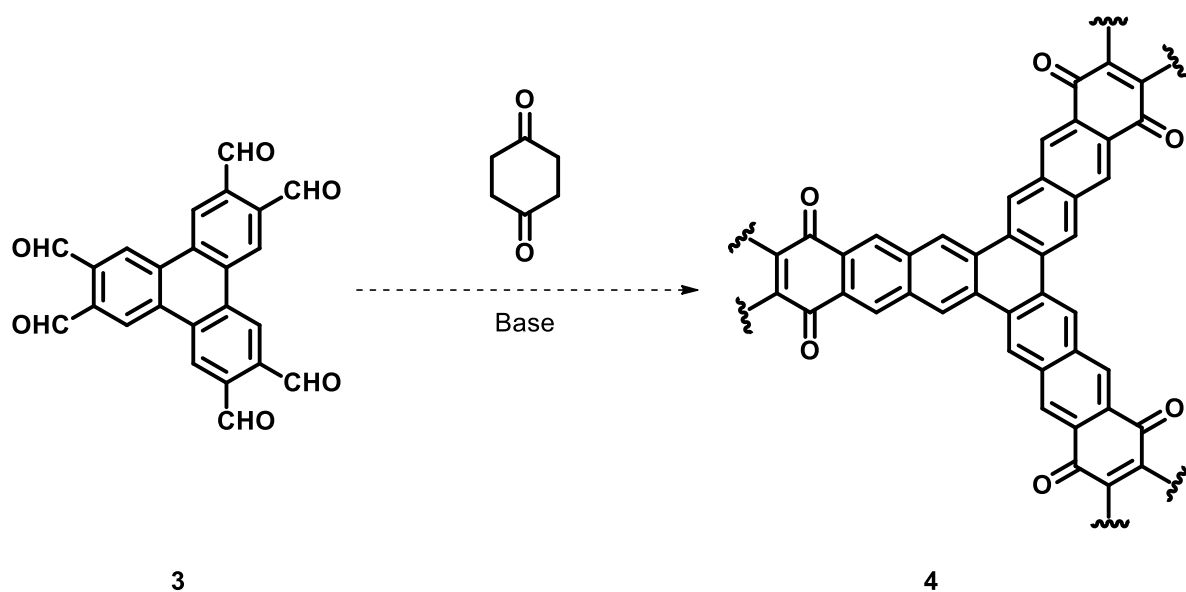
4.3 Summary and Future Work

In summary, the synthesis of hexa(formyl)triphenylene **3** via the Yamamoto coupling of either one of phthalaldehyde substrate **42** or aldehyde-protected substrate **77** was unsuccessful due to the high reactivity of these functional groups in the presence of zero-valent Ni(COD)_2 , leading to unwanted side reactions and complex mixtures. Moreover, these results have highlighted a

limitation of the Yamamoto coupling reactions substrate scope as *o*-dibromoarenes containing aldehydes or 1,3-dioxolane functional groups are incompatible with the reaction conditions.

Novel compound hexa(methanol)triphenylene **80** was prepared in 70% yield via lithium aluminum hydride reduction of hexa(methyl ester)triphenylene **37** for the purposes of accessing target aldehyde **3** by reduction. Unfortunately, oxidation of alcohol **80** was unsuccessful using several different oxidation protocols including, the Swern oxidation, oxidation with pyridinium chlorochromate, Dess-Martin oxidation, and oxidation with Burgess reagent. Although oxidation of **80** with Dess-Martin periodinane afforded the desired aldehyde **3**, a complex mixture was obtained, and separation and purification has proved to be extremely difficult.

In future attempts to access hexa(formyl)triphenylene, Parikh-Doering oxidation and oxidation with manganese dioxide may be attempted as both conditions have been reported using dimethyl sulfoxide as a solvent, which is an extremely important requirement for the success of the oxidation as hexa(methanol)triphenylene is observed to only be soluble in DMSO. Furthermore, an oxidation protocol reported by Zhang and coworkers to oxidize benzylic alcohols to the corresponding aldehyde in the presence of 9-fluorenone and blue LED light in DMSO may be investigated in hopes to transform alcohol **80** to the desired aldehyde **3**.⁷⁰



Scheme 33. Proposed synthetic approach to novel covalent organic framework (**4**) via the aldol condensation of hexa(formyl)-substituted triphenylene **3** and cyclohexanedione.

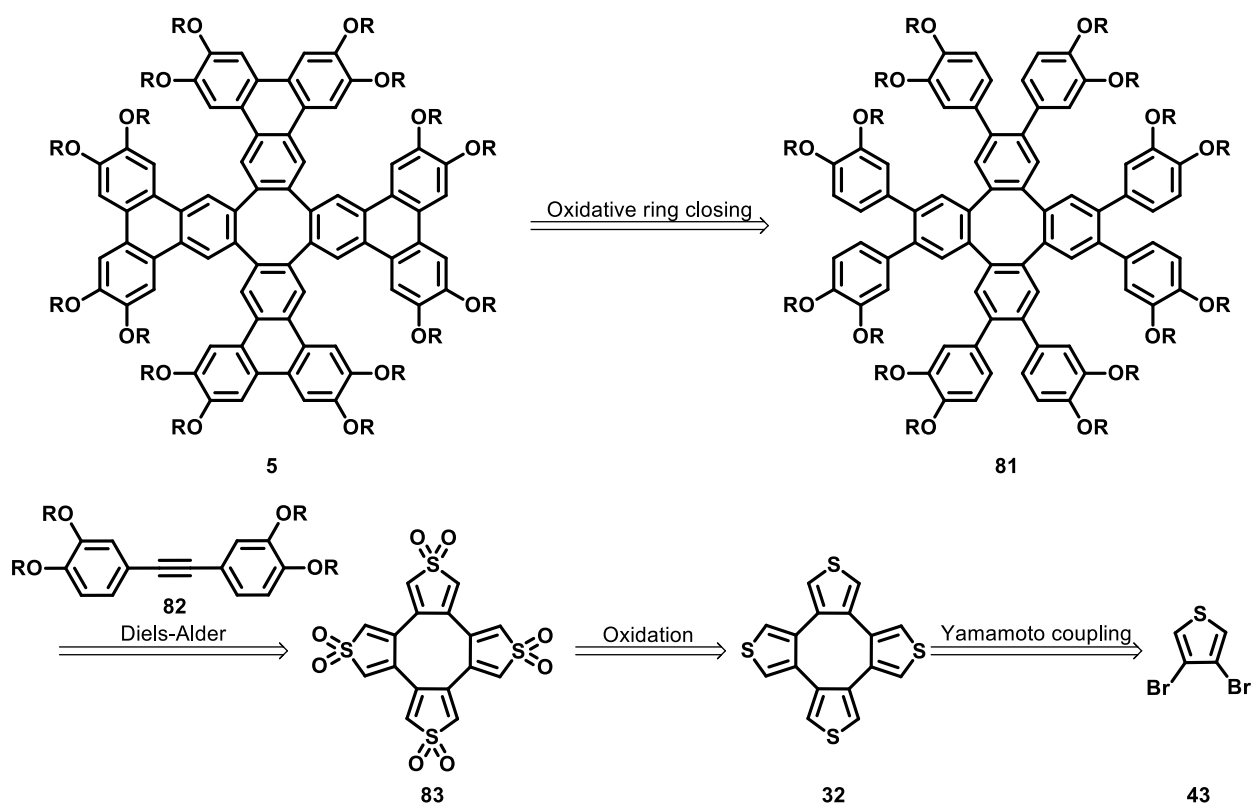
Following the successful preparation of hexa(formyl)triphenylene, novel covalent organic framework **4** may be accessed via the aldol condensation of hexa(formyl)-substituted triphenylene **3** and 1,4-cyclohexanedione in the presence of an appropriate solvent and base (Scheme 33).

CHAPTER 5: TOWARDS THE SYNTHESIS OF NOVEL TETRAPHENYLENES

5.1 Introduction

Small, nonplanar polycyclic aromatic compounds like tetraphenylenes and other related curved architectures are of high interest in supramolecular chemistry research due to their potential applications in guest-host binding chemistry, supramolecular chemistry, biological chemistry and materials science.^{36,37} Tetraphenylenes are characteristically non-planar aromatic structures, allowing them to adopt a saddle-shaped conformation and interact with smaller curved guest molecules.^{37,40} Tetraphenylene's adoption of a saddle-shaped conformation makes it an interesting target as a host-molecule for applications in supramolecular chemistry as a binding-host for smaller guest compounds.

The third and final major objective of this research is to employ a novel synthetic approach to construct extended tetraphenylene **5**. In our retrosynthetic approach (Scheme 38), novel target extended tetraphenylene **5** may be accessed via oxidative ring closing of terphenyl-derivative **81** using Scholl reaction conditions with iron (III) chloride or oxidation with DDQ. Cycloadduct **81** can be prepared by oxidation of tetrathiophene **32** with 3-chloroperoxybenzoic acid (*m*-CPBA) or trifluoroacetic anhydride and hydrogen peroxide to give diene **83** followed by subsequent [4+2] Diels-Alder cycloaddition with bi(aryl)acetylene **82**. Tetrathiophene **32** can easily be prepared via Yamamoto coupling of 3,4-dibromothiophene **43** as reported by Yamamoto *et al.*⁴² 3,4-dibromothiophene **43** can be accessed via 4-fold bromination of thiophene with bromine and subsequent α -carbon debromination of 2,3,4,5-tetrabromothiophene with zinc in acetic acid and water.⁷¹

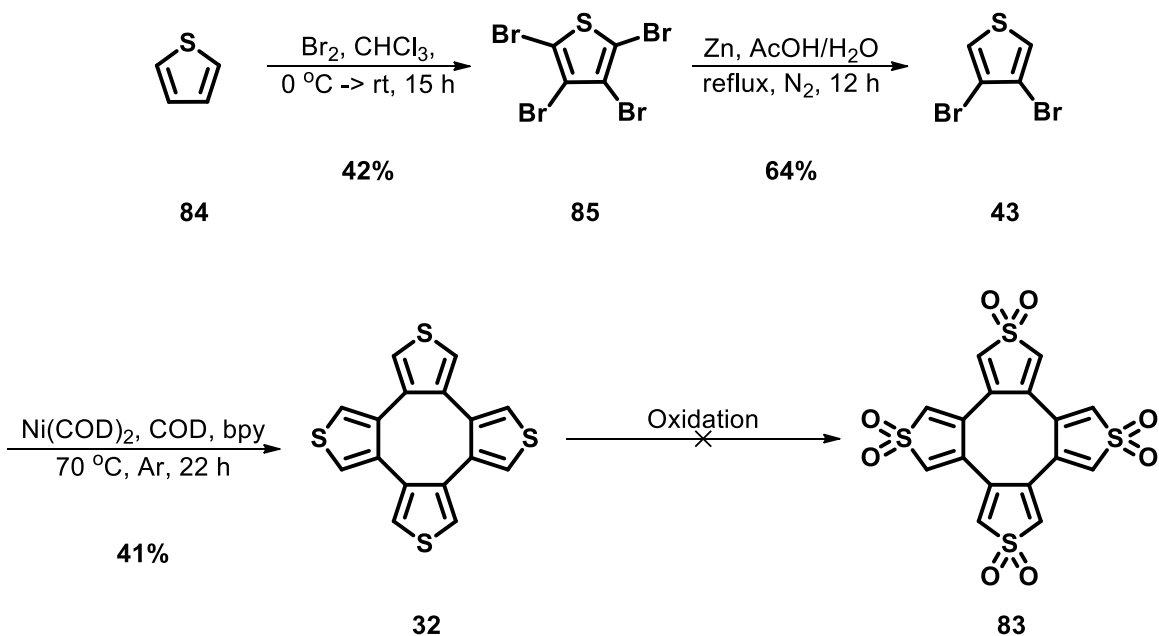


Scheme 34. Retrosynthetic approach to tetraphenylene **5** starting from 3,4-dibromothiophene **43**.

It is anticipated that by replacing the benzene units of tetraphenylene with extended triphenylene units, a larger π -surface will be formed and thus, increase the capability of binding larger guest molecules like fullerenes and electron-deficient materials. Furthermore, additional dienophiles such as 1,4-naphthaquinone and acenaphthylene may be explored as potential building blocks towards novel extended tetraphenylenes.

5.2 Results and Discussion

Synthesis towards novel extended tetraphenylene **5** began with attempts to access oxidized tetrathiophene **83**. In Scheme 35, thiophene was subjected to bromination using excess bromine in chloroform, to afford 2,3,4,5-tetrabromothiophene **85** in 42% yield following a procedure reported by Wang and coworkers.⁷¹ Subsequently, 2,3,4,5-tetrabromothiophene underwent debromination at the α -positions in the presence of activated zinc dust in a mixture of glacial acetic acid and water to afford 3,4-dibromothiophene **43** in 64% yield, again using a procedure from Wang and coworkers.⁷¹ 3,4-Dibromothiophene was then subjected to Yamamoto coupling conditions using $\text{Ni}(\text{COD})_2$, 1,5-cyclooctadiene and 2,2'-bipyridine in dimethylformamide to furnish tetrathiophene **32**, as reported by Yamamoto and coworkers in 41% yield.⁴² Thus far, efforts to prepare **83** via oxidation of tetrathiophene **32** have been unsuccessful, resulting in loss of starting material and no sign of desired product.



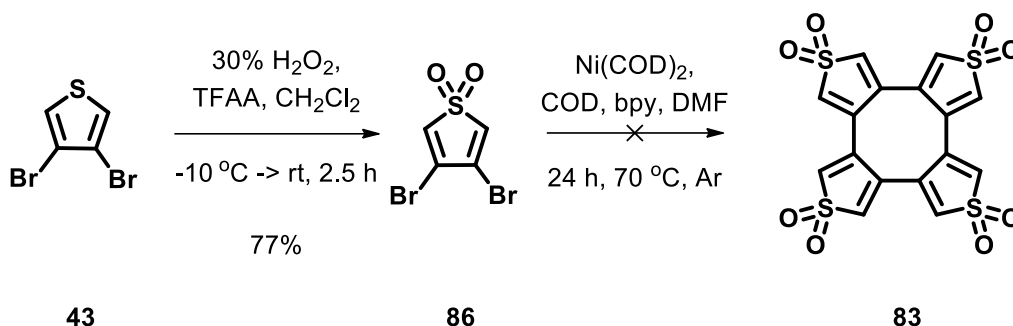
Scheme 35. Synthesis of tetrathiophene 32.

The first attempted oxidation of tetrathiophene employed trifluoroacetic anhydride and 35% hydrogen peroxide in dichloromethane, adapting from a procedure reported by Sanchez and coworkers.⁷² Trifluoroacetic anhydride and hydrogen peroxide were combined in the reaction flask at -10 °C to form trifluoroperacetic acid *in situ*. A solution of tetrathiophene in dichloromethane was added and the reaction mixture was allowed to stir for 3 hours followed by quenching with aqueous sodium carbonate. The organic layer was separated, and the aqueous layer was extracted with dichloromethane. The combined organic layers were concentrated to yield a crude material. Unfortunately, upon analysis of the crude material collected from the organic and the aqueous layer via ¹H NMR, it was clear that no product was present. However, starting material **32** was completely consumed under the reaction conditions. Further investigation into the progress of the reaction and what exactly is causing tetrathiophene to be consumed is needed before any concrete conclusions can be formed.

Oxidation of tetrathiophene was also attempted using 3-chloroperoxybenzoic acid (*m*-CPBA), but the reaction was unsuccessful. In a 2017 publication,⁷³ Nagata and coworkers reported the successful oxidation of tetrathia[8]circulenes, containing four thiophene moieties embedded within the core with *m*-CPBA. Adapting from the procedure reported by Nagata and coworkers,⁷³ tetrathiophene was subjected to oxidation in the presence of excess 77% *m*-CPBA in chloroform at reflux for 3 hours, resulting in a clear and yellow solution. Disappearance of starting material **32** was observed via analysis of the reaction mixture by thin-layer chromatography and ¹H NMR spectroscopy. However, no product was found in the crude reaction mixture before and after workup with aqueous sodium bicarbonate. Similar to that of the oxidation of tetrathiophene with trifluoroacetic anhydride and hydrogen peroxide, a more in-depth investigation into why

tetrathiophene is completely consumed under these reaction conditions, and product is not detected by ^1H NMR spectroscopy is needed.

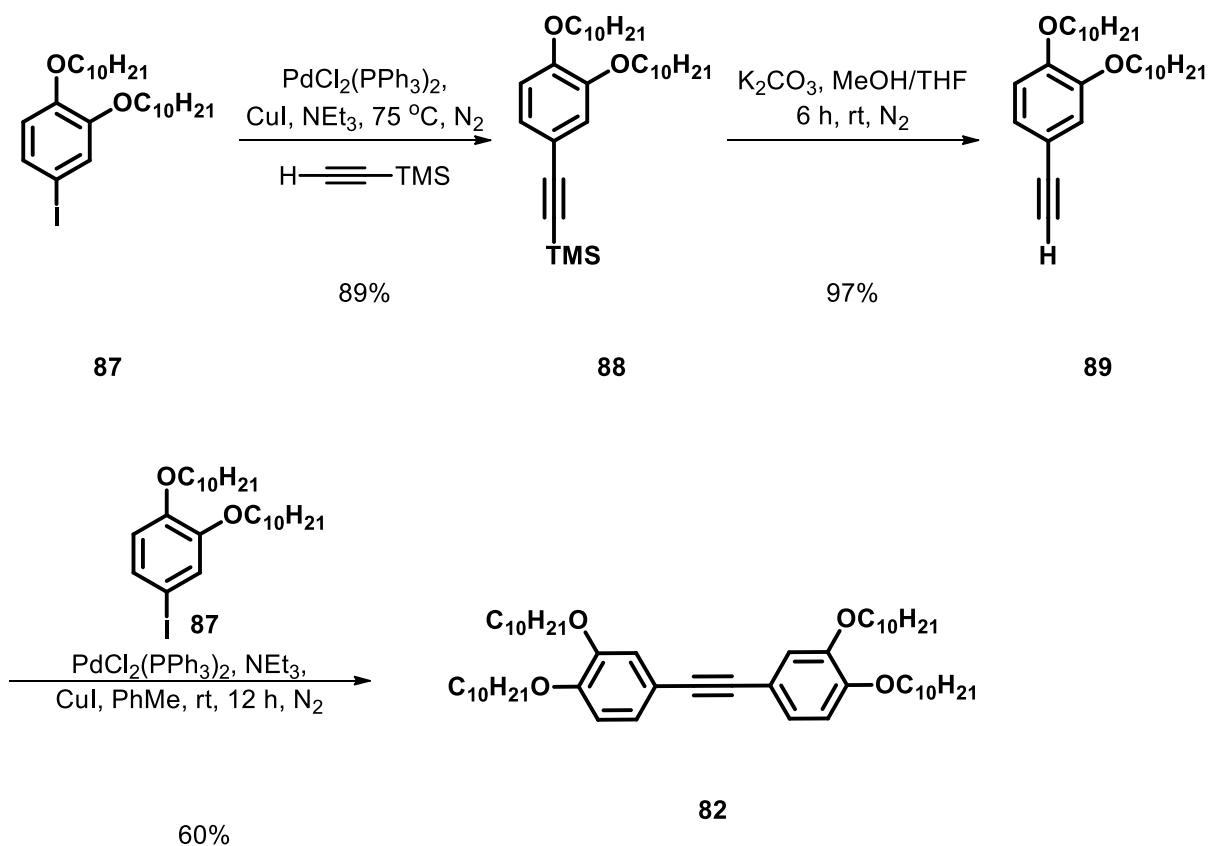
Having failed to directly oxidize tetrathiophene **32** using well known oxidation methods, an alternative method for the potential synthesis of **83** was pursued (Scheme 36). We turned our attention to a potential Yamamoto coupling of 3,4-dibromothiophene-1,1-dioxide **86**, which is easily prepared via oxidation of 3,4-dibromothiophene **43** with hydrogen peroxide and trifluoroacetic anhydride in dichloromethane in 77% yield, following a procedure reported by Sanchez *et al.*⁷² Compound **86** was then subjected to reaction with $\text{Ni}(\text{COD})_2$, COD, and 2,2'-bipyridine in THF at 70 °C, adapting from a procedure published by Yamamoto and coworkers.⁴² Upon analyzing the crude reaction mixture following reaction workup and filtration through a 5 cm silica column, both the expected product and starting material were unobservable in the ^1H NMR spectrum. It is clear that starting material **86** was consumed under the reaction conditions. However, it is not clear if **83** formed during the reaction, or if another product formed. Furthermore, if **83** was formed, the potential for poor solubility in common organic solvents may have resulted in the loss of **83** during initial filtration through a silica plug. To our disappointment, oxidized tetrathiophene **83** has yet to be prepared which has greatly hindered the progress of this final research objective.



Scheme 36. Attempted synthesis of oxidized tetrathiophene **83** via Yamamoto coupling of 3,4-dibromothiophene-1,1-oxide **86**.

In addition to the synthesis of tetrathiophene **32** and attempted synthesis of **83**, the desired bis(aryl) acetylene dienophile has been successfully prepared in good yield starting from 1,2-didecyloxy-4-iodobenzene **87**, which had been previously prepared in our lab (Scheme 37). First, employing conditions reported by Yu and coworkers,⁷⁴ Sonogashira cross-coupling of 1,2-didecyloxy-4-iodobenzene **87** and trimethylsilyl acetylene in the presence of bis(triphenylphosphine)palladium chloride [PdCl₂(PPh₃)₂], copper (I) iodide (CuI) and triethylamine at 75 °C afforded trimethylsilyl- (TMS) protected acetylene derivative **88** in a very good 89% yield following chromatographic purification. The trimethylsilyl-protecting group was subsequently cleaved in the presence of solid potassium carbonate and methanol in tetrahydrofuran, as reported by Yu and coworkers,⁷⁴ giving **89** in an almost quantitative yield of 97%. Finally, adapting from a procedure reported by Elangovan and coworkers,⁷⁵ 1,2-di(decyloxy)-4-ethynylbenzene **89** was subjected to Sonogashira cross-coupling with 1,2-di(decyloxy)-4-iodobenzene **87** in the presence of PdCl₂(PPh₃)₂, CuI and triethylamine in toluene at room temperature, furnishing the desired bi(aryl)acetylene **82** in 60% yield after recrystallization from acetone. Notably, the final Sonogashira coupling to access **82** avoids elevated temperatures

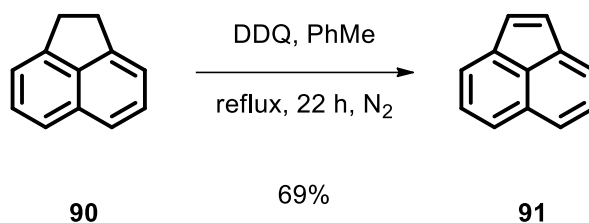
and final purification via column chromatography, as reported by Williams and coworkers for the synthesis of analogous bi(aryl)acetylene materials, only differing by the length of the alkoxy chains.⁷⁶ Although compound **82** has been prepared towards the synthesis of novel, extended tetraphenylene **5**, its use has been thwarted by the failure to synthesize oxidized tetrathienophene **83**.



Scheme 37. Synthesis of dienophile **82**, towards the preparation of an extended tetraphenylene.

In addition to dienophile **82**, other compatible dienophiles like acenaphthylene may be explored as potential building blocks for the preparation of novel tetraphenylenes from [4+2] cycloaddition with oxidized tetrathienophene **83**. In anticipation of the successful synthesis of the all

important diene **83**, another potential dienophile building block, acenaphthylene **90** was readily oxidized via treatment with 2,3-dichloro-5,6-dicyano-1,4-benzoquinone (DDQ) in toluene at reflux (Scheme 42), giving **91** as a yellow crystalline solid in 69% yield, similar to that reported by Kotha and coworkers.⁷⁷

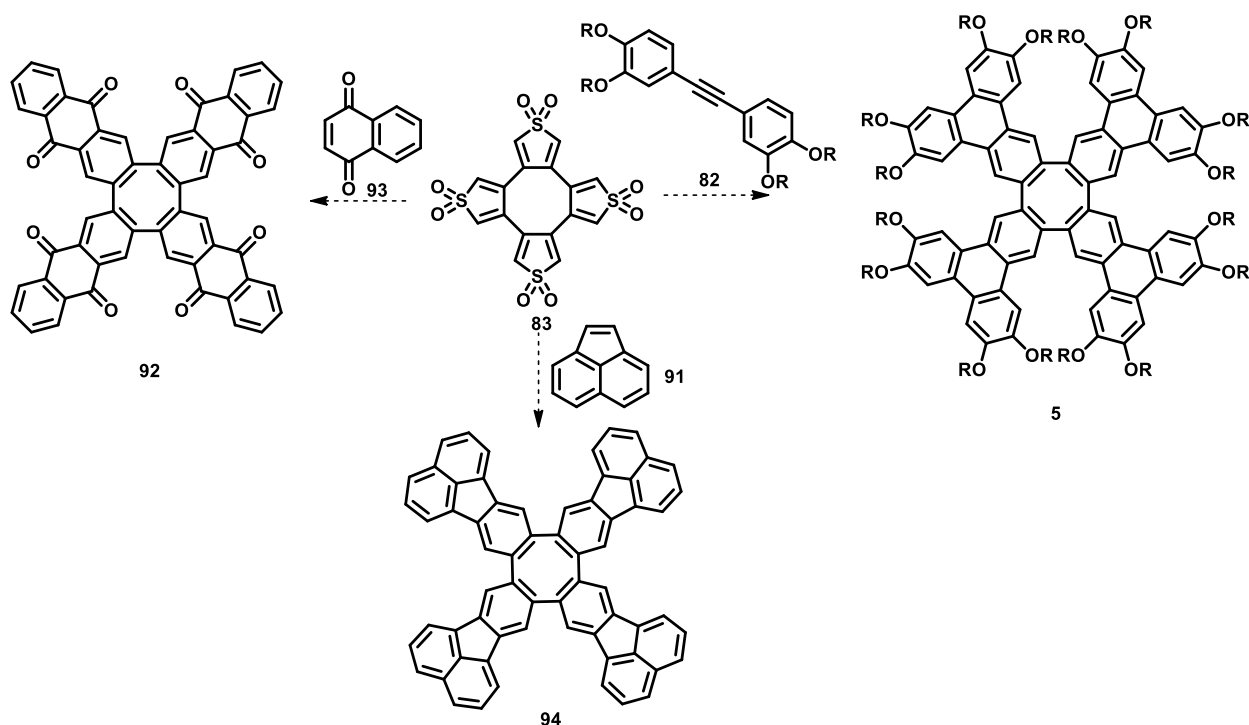


Scheme 38. *Synthesis of dienophile acenaphthylene as a building block towards a novel tetraphenylene by treatment of acenaphthene with DDQ.*

5.3 Summary and Future Work

In summary, the third and final objective of this thesis has yet to be completed. However, important intermediates towards the preparation of extended tetraphenylene **5** have been prepared in good yields. Notably, tetrathiophene has been prepared via Yamamoto coupling of 3,4-dibromothiophene in 41% yield. Dienophile building blocks, 1,2-bis(3,4-bis(decyloxy)phenyl)ethyne **82** and acenaphthylene **91** have also both been prepared in 60% and 69% yields, respectfully, in anticipation of the successful preparation of oxidized tetrathiophene **83** for purpose of [4+2] cycloaddition reactions to afford the extended tetraphenylene cycloadducts (Scheme 39). In addition to cycloadditions of **82** and **91**, respectively, Diels-Alder reaction of **83** with 1,4-naphthaquinone may be explored in the future to access another novel tetraphenylene

derivative (Scheme 39). Unfortunately, oxidized tetrathiphene **83** has yet to be successfully prepared using the oxidation methods described, which has greatly hindered the progress of this final research objective. Further investigation into the oxidation reactions of tetrathiphene **32** with either *m*-CPBA or TFAA and H₂O₂ is needed. Specifically, the reason for the consumption and loss of starting material, as well as ideal workup and purification conditions to collect product must be determined. Moreover, investigation of alternative oxidation conditions to access dioxide **83** will be apart of future work



Scheme 39. Future work, synthesis of extended tetraphenylene derivatives via [4+2] cycloaddition reaction.

CHAPTER 6: CONCLUSIONS AND FUTURE WORK

The overall goal of this research was to synthesize and study the structure-property relationships of novel polycyclic aromatic compounds capable of self-assembling to form liquid crystalline, and microporous structures, as well as molecules capable of molecular recognition. The unifying theme that connects this research is the utilization of the Yamamoto coupling reaction to access the desired polycyclic aromatic hydrocarbon targets. More specifically, the scope of the Yamamoto coupling reaction was explored for the synthesis of electron-deficient triphenylene derivatives that are otherwise difficult to prepare. The molecules prepared via the Yamamoto coupling reaction are expected to be further utilized as intermediates for the synthesis of novel target materials.

Tris(dicarboxyimide)-substituted triphenylene **1** was successfully prepared via the Yamamoto coupling reaction of *o*-dibromoarene **41** in a 65% yield. This approach is more convenient, and higher yielding in comparison to the previously reported approach to triphenylene **1** by Wu and coworkers. Furthermore, this synthetic route allows for a modular approach to several derivatives of compound **1** with varying *N*-alkyl substituents as the preceding dicarboximide-substituted *o*-dibromoarene can easily be prepared with variable *N*-alkyl chains.

Additionally, tris(dicarboxythioimide)-substituted triphenylene **2** was also successfully prepared in 60% yield via thionation of triphenylene **1** with Lawesson's reagent. Compound **2** shows evidence for a columnar mesophase with a high clearing point and displayed dendritic textures on cooling from the isotropic liquid phase. However, as an unexpected consequence of thionation of **1**, the clearing point of compound **2** was increased to a high enough point where **2** experienced thermal degradation upon reaching the clearing point from mesophase to isotropic

liquid. Due to the thermal degradation of compound **2** upon reaching the clearing point temperature, it does not allow for any clear comparisons to the mesophase characteristics of compound **1**. Furthermore, these results are in contrast with previously collected data from studies on the effects of thionation of dicarboximide-bearing liquid crystalline trinaphthylenes and triphenylenes,³⁰ where thionation only had a subtle impact on the mesophase range, and more specifically, the clearing point temperature. Additionally, a red-shift in the UV-Vis spectra was observed for the thionated triphenylene **2** in comparison to triphenylene **1**. This red-shift suggests a narrowing of the HOMO-LUMO energy band gap with increased thionation which is consistent with what was previously observed by our group for related compounds.

We have demonstrated that the Yamamoto coupling reaction is a superior and more reliable approach to access a variety of electron-rich and electron-deficient triphenylenes, in comparison to other synthetic methods tested. In this study, we sought to develop an alternative method to access triphenylenes via a nickel-assisted cyclotrimerization that did not require nickel(0)bis(1,5-cyclooctadiene) or reaction set-up under inert glove box conditions. We tested two promising methods using two distinct stable nickel-precatalysts in attempts to prepare triphenylenes **1**, **37** and **60** from the respective *o*-dibromoarene precursor. The first of two methods assessed included a Yamamoto coupling type reaction employing the use of an air and moisture stable nickel(0)-precatalyst, Ni(COD)(DQ) as a replacement for Ni(COD)₂ and reaction set-up outside of a glove box. The second cyclotrimerization conditions tested was a nickel-assisted [2+2+2] cycloaddition reaction of *o*-dibromoarenes that had been previously reported by Cheng *et al.*⁶⁰ Ultimately, we showed that the Yamamoto coupling reaction was superior to the alternative homocyclotrimerization conditions explored as they were ineffective at producing the desired triphenylenes, leading to no product or complex and inseparable mixtures.

The second major objective of this thesis was to prepare electron deficient triphenylene **3** via the Yamamoto coupling reaction and use it as a building block towards the preparation of a novel organic framework. The synthesis of hexa(formyl)triphenylene **3** via the Yamamoto coupling of either one of phthalaldehyde substrate **42** or aldehyde-protected substrate **78** was unsuccessful due to the high reactivity of the functional groups in the presence of zero-valent Ni(COD)₂, which potentially led to unwanted side reactions, resulting in complex mixtures. These results have highlighted a limitation in the scope of the Yamamoto coupling as *o*-dibromoarenes containing aldehydes or 1,3-dioxolane functional groups are incompatible with the reaction conditions. Furthermore, novel compound hexa(methanol)triphenylene **80** was prepared in 70% yield via lithium aluminum hydride reduction of hexa(methyl ester)triphenylene **37** for the purposes of accessing target aldehyde **3** by oxidation of **80**. Unfortunately, oxidation of alcohol **80** was unsuccessful using several different oxidation protocols including the Swern oxidation, oxidation with pyridinium chlorochromate, Dess-Martin oxidation, and oxidation with Burgess reagent. Notably, oxidation of **80** with Dess-Martin periodinane afforded the desired aldehyde **3**, however a complex mixture was obtained, and separation and purification of **3** has proved to be extremely difficult. In the future, following the successful preparation of hexa(formyl)triphenylene **3**, novel covalent organic framework **4** may be accessed via the aldol condensation of **3** and 1,4-cyclohexanedione.

In the final objective of this thesis, we investigated a route to access a novel extended tetraphenylene derivative. Unfortunately, the final objective has yet to be completed. However, important intermediates towards the preparation of extended tetraphenylene **5** have been prepared in good yields. Notably, tetrathiophene has been prepared via Yamamoto coupling of 3,4-dibromothiophene in 41% yield. Dienophile building blocks, 1,2-bis(3,4-

bis(decyloxy)phenyl)ethyne **82** and acenaphthylene **91** have also both been prepared in 60% and 69% yields, respectfully, in anticipation of the successful preparation of oxidized tetrathiophene **83** for purpose of [4+2] cycloaddition reactions to afford novel extended tetraphenylene cycloadducts. Unfortunately, oxidized tetrathiophene **83** has yet to be successfully prepared using the oxidation methods described. Unfortunately, this has greatly hindered the progress of this final research objective. Further investigation into the oxidation reactions of tetrathiophene **32** with either *m*-CPBA or TFAA and H₂O₂ is needed. Moreover, investigation of alternative oxidation conditions to access dioxide **83** is ongoing and will be apart of the future work for this objective.

In conclusion, we have further demonstrated that the Yamamoto coupling reaction can be used as a viable method to access 3-fold symmetric electron-deficient triphenylene derivatives that are not readily accessible using other methods in. Unfortunately, the thionated triphenylene derivative **2** degrades at elevated temperatures, thus, making it an unsuitable material for use as an n-type semiconductor. Although the target covalent organic framework **4** and target tetraphenylene derivative **5** were not successfully prepared, significant progress was made towards their preparation which will aid in future work.

CHAPTER 7: METHODOLOGY AND EXPERIMENTAL PROCEDURES

7.1 Materials and Methods of Characterization

7.1.1 NMR Spectroscopy

^1H and ^{13}C NMR spectra were recorded on an Agilent Technologies Varian 300 MHz Unity Inova NMR spectrometer or 400 MHz NMR Spectrometer using deuterated chloroform or deuterated dimethyl sulfoxide purchased from Sigma-Aldrich and used as received. Chemical shifts are reported in δ scale downfield from the peak for tetramethylsilane.

7.1.2 High Resolution Mass Spectrometry

High resolution mass spectra were recorded at the Regional Mass Spectrometry Centre facility at the University of Montreal using an Agilent LC-MSD TOF spectrometer.

7.1.3 Melting Points

Melting points were determined on a Mel-Temp® Electrothermal melting point apparatus and are uncorrected.

7.1.4 Mesophase Characterization Techniques

Polarized optical microscopy studies were performed using an Olympus BX-51 polarized optical microscope equipped with a Linkam LTS 350 heating stage and a digital camera. *Differential scanning calorimetry* studies were carried out using a TA Instruments DSC Q200 with a scanning rate of 5 °C/min.

7.1.5 Thermogravimetric Analysis

Thermogravimetric analysis (TGA) was performed on TA Instruments TGA Q50.

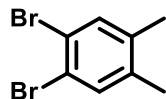
7.1.6 Ultraviolet-visible (UV-Vis) Spectroscopy

UV-Vis spectra were recorded on a Varian Carey 50 Bio UV-visible spectrophotometer using quartz cuvettes ($l = 1.0$ cm).

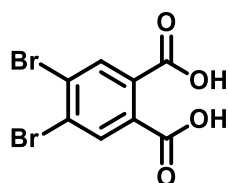
7.1.7 Chemicals and Solvents

All reagents and starting materials were purchased from Sigma-Aldrich and used as purchased. Anhydrous solvents were dispensed using a custom-built solvent system from Glass-contour (Irvine, CA) which used purification columns packed with activated alumina and supported copper catalyst. Oven-dried glassware was used for all reactions and all reactions were performed under nitrogen unless otherwise stated. Column chromatography was performed using silica gel (60 Å, 230-400 mesh, 40-63 μm particle size) purchased from Sigma-Aldrich as the adsorbent and used as received. All Yamamoto cyclotrimerization reactions were performed under inert atmosphere using glove box conditions due to the reaction requiring the air, temperature and water sensitive reagent, bis(1,5-cyclooctadiene) nickel(0) complex.⁴² Consistency of the Yamamoto cyclotrimerization reactions were maintained via the adherence to a general procedure in the probing of functional group tolerance. Invariable conditions allowed for the direct comparison of previous and current results collected.

7.2 Experimental Procedures

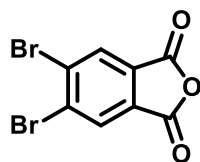


1,2-dibromo-4,5-dimethylbenzene (52): *o*-Xylene (25 mL, 200 mmol, 1.0 eq.) and iodine (0.1g, 0.44 mmol, 0.002 eq.) were combined in a 250 mL round bottom flask equipped with a stir bar and cooled to 0 °C. Bromine (22 mL, 400 mmol, 2.04 eq.) was added dropwise via an addition funnel. The solution was left overnight and allowed to gradually warm to room temperature. The resulting orange solid was dissolved in ether and washed with 2 M sodium hydroxide (3x30 mL). The organic layer was dried with magnesium sulfate and subjected to gravity filtration. The solvent was removed under reduced pressure to yield a white solid as the crude product. The crude product was recrystallized from methanol to yield **52** as a white solid (23.5 g, 43%). m.p. = 85.7-87.8 °C; ^1H NMR (400 MHz, CDCl_3) δ : 2.35 (6H, s), 7.72 (2H, s). The ^1H NMR data collected is consistent with the values reported in the literature.⁷⁸

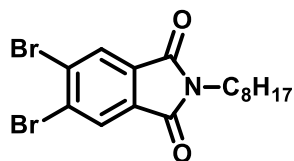


4,5-dibromophthalic acid (51): 1,2-dibromo-4,5-dimethylbenzene (6.44 g, 20 mmol, 1.0 eq.), potassium permanganate (15.79 g, 100 mmol, 4.0 eq.) and deionized water (200 mL) were combined in a 500 mL round bottom flask equipped with a reflux condenser and a stir bar. The solution was stirring at reflux for 6 hours. Sodium bisulfite (8 g) was added to the solution to

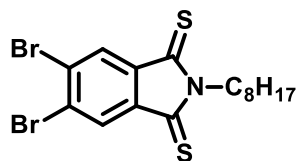
reduce any unreacted potassium permanganate. 3M sodium hydroxide (120 mL) was added to increase the pH of the solution to >12. The reaction mixture was filtered to collect a clear and colourless filtrate which was then acidified with 6M hydrochloric acid (80 mL) to achieve pH 2. After acidification, the product precipitated out of solution as a white solid, and was collected via suction filtration, to yield **51** as a brittle, white solid (4.22 g, 53%). m.p. = >260 °C; ¹H NMR (400 MHz, DMSO-*d*₆) δ: 8.80 (2H, *s*). The ¹H NMR data collected is consistent with the values reported in the literature.⁵¹



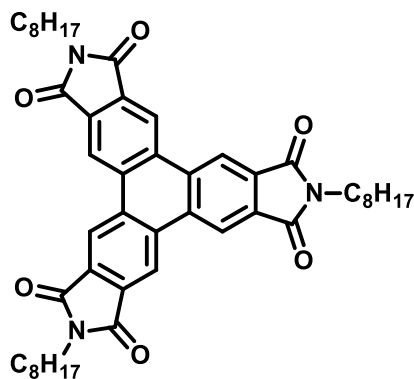
5,6-dibromoisobenzofuran-1,3-dione (50): To an oven-dried 25 mL, 2-neck round bottom flask equipped with a stir bar, reflux condenser and nitrogen inlet, was added 4,5-dibromophthalic acid (2.00 g, 6. mmol, 1.0 eq.). The flask was warmed to 60 °C in an oil bath followed by the slow dropwise addition of thionyl chloride via syringe (1 drop/second). The resulting mixture was refluxed at 90 °C and stirred under nitrogen for 16 hours. The crude mixture was cooled to room temperature and subsequently concentrated under reduced pressure to yield **50** as a white solid (1.88 g, 100%). m.p. = 220 °C (decomp.); ¹H NMR (400 MHz, DMSO-*d*₆) δ: 3.30 (sharp H₂O *s*), 8.50 (*s*, 2H). HRMS (ESI+) *m/z*: [M+H]⁺ calc. for C₈H₂[⁷⁹Br]₂O₃ 304.84435, found 304.84542. This compound was used without any further purification.



5,6-dibromo-2-octylisobenzofuran-1,3-dione (41): To an oven-dried, 100 mL, 2-neck round bottom flask equipped with a stir bar, reflux condenser and nitrogen inlet was added 5,6-dibromoisobenzofuran-1,3-dione (1.08 g, 3.52 mmol, 1.0 eq.), anhydrous dimethylformamide (35 mL) and octylamine (1.2 mL, 7.3 mmol, 2.0 eq.). The mixture was stirred under nitrogen at 90 °C for 30 minutes followed by the addition of acetic anhydride (0.64 mL, 6.8 mmol, 1.93 eq.), triethylamine (2.5 mL, 18 mmol, 5.0 eq.) and nickel acetate (0.101 g, 0.405 mmol, 0.115 eq.). The resulting mixture was stirred at 90 °C under nitrogen for 24 hours. Following the allotted reaction time, the reaction mixture was then cooled to room temperature, poured into an ice/water mixture (350 mL), and stirred for 1 hour. The resulting beige-coloured precipitate was collected via suction filtration. The brown solid was then dissolved in chloroform (40 mL), washed with deionized water (3x40 mL), and brine (2x40 mL), dried over magnesium sulfate, filtered, and concentrated under reduced pressure to yield **41** as a dark brown oil that upon standing in ambient conditions, solidified into a crystalline solid. A white crystalline solid was isolated after column chromatography (silica gel; 98:2, hexanes/ethyl acetate, 0.82 g, 56%). m.p. = 63.4-64 °C; ¹H NMR (400 MHz, CDCl₃) δ: 0.91 (*t*, *J* = 8 Hz, 3H), 1.32 (*m*, 10H), 1.69 (*m*, 2H), 3.70 (*t*, *J* = 6 Hz, 2H), 8.11(*s*, 2H); ¹³C NMR (100 MHz, CDCl₃) δ: 14.00, 22.55, 26.77, 28.39, 29.04, 29.08, 31.69, 38.50, 128.28, 131.18, 131.84, 166.41; HRMS (ESI+) *m/z*: [M+H]⁺ calc. for C₁₆H₁₉[⁷⁹Br]₂NO₂ 415.98553, found 415.98745.

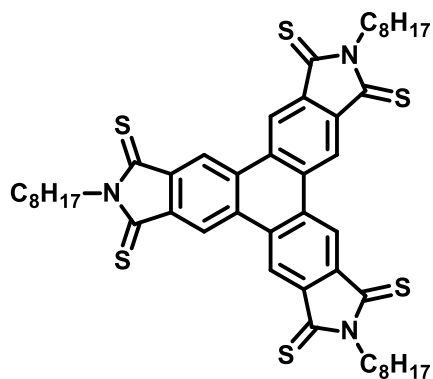


5,6-dibromo-2-octylisoindoline-1,3-dithione (55): To an oven-dried, 2-neck, 25 mL round bottom flask equipped with a stir bar, reflux condenser and nitrogen inlet was added 5,6-dibromo-2-octylisoindoline-1,3-dione (0.100 g, 0.239 mmol, 1.0 eq.), anhydrous toluene (5 mL) and Lawesson's Reagent (0.242 g, 0.599 mmol, 2.5 eq.). The reaction was left to reflux overnight under N₂. The subsequent solution was concentrated under reduced pressure yielding a crude solid. The crude solid was purified through a silica column (SiO₂, 98:2 hexanes/ethyl acetate). The excess solvent was removed under reduced pressure affording **55** as a brown solid. **55** was recrystallized from dichloromethane/methanol, affording **55** as fine brown needles (75.6 mg, 70%). ¹H NMR (400 MHz, CDCl₃) δ : 0.86 (*t*, *J* = 8 Hz, 3H), 1.29 (*m*, 10H), 1.69 (*quintet*, *J* = 8 Hz, 2H), 4.36 (*t*, *J* = 8 Hz, 2H), 8.06 (*s*, 2H); ¹³C NMR (100 MHz, CDCl₃) δ : 14.03, 22.58, 26.78, 27.59, 29.07, 31.71, 44.37, 77.16, 127.99, 130.17, 134.17, 194.61.



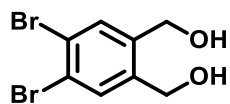
2,7,12-trioctyl-1H-benzo [1,2-*f*:3,4-*f'*:5,6-*f''*] triisoindole-1,3,6,8,11,13 (2H,7H,12H)-hexaone (1): Under inert glove box conditions an oven-dried (single-neck) 50 mL round bottom flask

equipped with a stir bar was charged with 2,2'-bipyridyl (0.047 g, 0.299 mmol, 1.25 eq.), 1,5-cyclooctadiene (0.053 g, 0.491 mmol, 2.05 eq.), anhydrous tetrahydrofuran (2.267 g) and bis(1,5-cyclooctadiene)nickel(0) (0.082 g, 0.299 mmol, 1.25 eq.), resulting in a deep-purple coloured solution. Subsequently, a solution of 5,6-dibromo-2-octylisoindoline-1,3-dione (**41**) (0.100 g, 0.239 mmol, 1.0 eq.) and tetrahydrofuran (2.267 g) was slowly added drop wise via Pasteur pipette (1 drop/second). The resulting solution was sealed with a rubber septum, parafilm and wrapped in tinfoil. The reaction flask was removed from the glove box and transferred to a fume hood where it was stirred under nitrogen for 16 hours. The crude mixture was filtered through a silica plug column (100% chloroform). The filtrate was concentrated under reduced pressure and the resulting crude solid was recrystallized from chloroform/methanol, affording **1** as a white solid (40.3 mg, 65%). m.p. = 220.7-237.6 °C; ¹H NMR (400 MHz, CDCl₃) δ: 0.86 (*t*, *J* = 8 Hz, 9H), 1.30 (*m*, 30H), 1.79 (*quintet*, *J* = 8 Hz, 6H), 3.81 (*t*, *J* = 8 Hz, 6H), 9.26 (*s*, 6H); ¹³C NMR (100 MHz, CDCl₃) δ: 14.03, 22.59, 26.92, 28.56, 29.12, 29.14, 31.73, 38.75, 119.91, 131.65, 134.21, 167.28. The ¹H and ¹³C NMR data collected is consistent with the values reported in the literature.⁴⁶

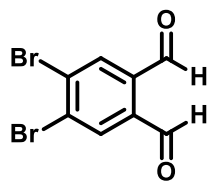


2,7,12-trioctyl-1H-benzo[1,2-f:3,4-f':5,6-f'']trisoindole-1,3,6,8,11,13(2H,7H,12H)-

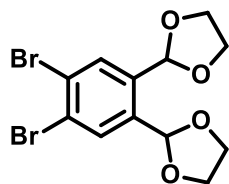
hexathione (2): To an oven-dried 2-neck 25 mL round bottom flask equipped with a stir bar, reflux condenser and nitrogen inlet was added triphenylenedicarboxyimide (**1**) (0.050 g, 0.065 mmol, 1.0 eq.), anhydrous toluene (2.5 mL) and Lawesson's reagent (0.196 g, 0.486 mmol, 7.5 eq.). The mixture was heated to reflux in an oil bath and left to react under nitrogen gas for 24 hours. The reaction mixture was then cooled to room temperature and the solvent was removed under reduced pressure yielding a crude mixture. The crude mixture was purified through a silica column (SiO₂, 1:1 hexanes/dichloromethane). The excess solvent was removed under reduced pressure affording (**2**) as a black-purple solid. **2** was recrystallized from dichloromethane/ methanol affording **2** as a deep purple solid (33.5 mg, 60%). m.p. = 333.9 °C (decomp.); ¹H NMR (400 MHz, CDCl₃) δ: 0.92 (*t*, *J* = 8 Hz, 9H), 1.41 (*m*, 30H), 1.88 (*quintet*, *J* = 8 Hz, 6H), 4.49 (*t*, *J* = 8 Hz, 6H), 8.52 (*s*, 6H); ¹³C NMR (100 MHz, CDCl₃) δ: 14.24, 22.80, 27.17, 27.88, 29.29, 29.39, 31.94, 44.76, 118.32, 131.86, 133.34, 194.05; HRMS (ESI⁺) *m/z*: [M+H]⁺ calc. for C₄₈H₅₇N₃S₆ 868.29495, found 868.29332.



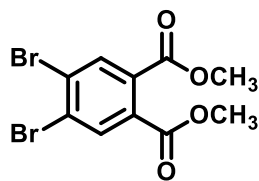
(4,5-dibromo-1,2-phenylene)dimethanol (77): To an oven-dried 25 mL 2-neck round bottom flask equipped with a stir bar and nitrogen inlet was added 4,5-dibromophthalic acid (0.250 g, 0.8 mmol, 1.0 eq.) and dry tetrahydrofuran (2.5 mL). The suspension was stirred under nitrogen gas and cooled to 0 °C in an ice bath. Subsequently, a 1.0 molar borane-tetrahydrofuran solution complex (2.31 mL, 2.31 mmol, 3.0 eq.) was slowly added dropwise via syringe (1 drop/second) to the flask. The reaction mixture was stirred under nitrogen for 24 hours and warmed to room temperature. The reaction was cooled back down to 0 °C in an ice bath and slowly quenched via dropwise addition of a 1:1 solution of tetrahydrofuran and deionized water (8 mL). The reaction mixture was warmed back up to room temperature followed by the addition of potassium carbonate until an aqueous layer formed. The solution was transferred to a separatory funnel, and the organic layer was extracted. The aqueous layer was then extracted with tetrahydrofuran (2x10 mL) and the combined organic layers were dried over magnesium sulfate, filtered, and concentrated via rotary evaporation to yield **78** as a white solid (156 mg, 68%). m.p. = 165.4-170 °C; ¹H NMR (400 MHz, DMSO-_d₆) δ: 4.43 (*d*, *J* = 5.6 Hz, 4H), 5.27 (*t*, *J* = 5.6 Hz, 2H), 7.66 (*s*, 2H); ¹³C NMR (100 MHz, DMSO-_d₆) δ: 59.36, 121.84, 131.53, 141.47; HRMS (ESI+) *m/z*: [M+Na]⁺ calc. for C₈H₈Br₂O₂ 318.87631, found 318.87734.



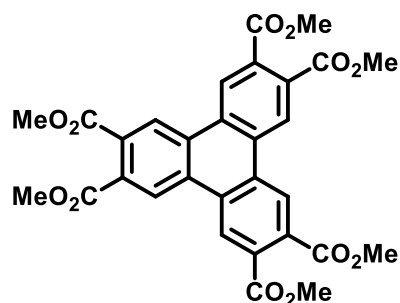
4,5-dibromophthalaldehyde (42): An oven-dried, 2-neck 25mL round bottom flask equipped with a stir bar and nitrogen inlet was charged with oxalyl chloride (0.064 mL, 0.74 mmol, 2.2 eq.) and dichloromethane (2 mL). The resulting mixture was stirred under nitrogen and cooled to -78 °C in an isopropyl alcohol/dry ice bath. To this mixture was added dropwise a solution of dimethyl sulfoxide (0.121 mL, 1.71 mmol, 4.4 eq.) and dichloromethane (2 mL) via syringe (1 drop/s). The resulting solution was stirred for 10 minutes under nitrogen at -78 °C. Subsequently, a solution of (4,5-dibromo-1,2-phenylene)dimethanol (0.100 g, 0.338 mmol, 1.0 eq.), dichloromethane (2 mL) and dimethyl sulfoxide (1 mL) was slowly added dropwise via syringe (1 drop/ s) to the reaction flask at -78 °C. The reaction mixture was stirred for an additional 30 minutes followed by the dropwise addition via syringe (1 drop/second) of triethylamine (0.824 mL, 5.92 mmol, 17.5 eq.). The mixture was stirred for 15 minutes at -78 °C and then allowed to stir overnight while warming up to room temperature. The reaction was quenched with cold deionized water (9 mL), transferred to a separatory funnel and the organic layer was extracted. The aqueous layer was extracted with dichloromethane (2x10 mL). The combined organic layers were washed with sodium bicarbonate (1x10 mL) and brine (1x20 mL), dried over magnesium sulfate, filtered, and concentrated under reduced pressure to yield an orange-brown solid. The solid was washed with hexanes and dried via suction filtration to afford the desired product (64.5 mg, 65%). m.p. = 143 °C (decomp.); ¹H NMR (400 MHz, CDCl₃) δ: 8.18 (s, 2H), 10.44 (s, 2H); ¹³C NMR (100 MHz, CDCl₃) δ: 131.73, 135.51, 136.05, 189.87; HRMS (APCI) m/z: [M+H]⁺ calc. for C₈H₅Br₂O₂ 290.8651, found 290.8937.



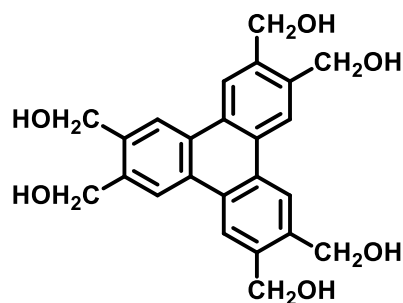
2,2'-(4,5-dibromo-1,2-phenylene)bis(1,3-dioxolane) (78): To an oven-dried, 2-neck, 25 mL round bottom flask equipped with a stir bar, Dean-Stark apparatus and nitrogen inlet was added 4,5-dibromophthalaldehyde (0.10 g, 0.34 mmol, 1.0 eq.) and anhydrous toluene (2.0 mL). To this stirring mixture was added ethylene glycol (0.191 mL, 3.43 mmol, 10.0 eq.) and *p*-toluenesulfonic acid (0.0023 g, 0.012 mmol, 0.035 eq.). The resulting mixture was refluxed with a Dean-Stark apparatus under N₂ overnight. The reaction flask was cooled to room temperature and the reaction was quenched with triethylamine (0.17 mL, 1.2 mmol, 3.52 eq.). The subsequent solution was concentrated via rotary evaporation under reduced pressure. The resulting oil was dissolved in ethyl acetate and washed with sodium bicarbonate (1x5 mL) and brine (1x5 mL), dried over sodium sulfate, filtered, and concentrated under reduced pressure to yield a crude brown oil. The crude mixture was purified through a silica column (SiO₂, 8:2 Hexanes/Ethyl acetate). The excess solvent was removed under reduced pressure affording **77** as a light-yellow oil (68 mg, 52%). ¹H NMR (400 MHz, CDCl₃) δ : 4.01-4.09 (*m*, 8H), 6.13 (*s*, 2H), 7.84 (*s*, 2H).



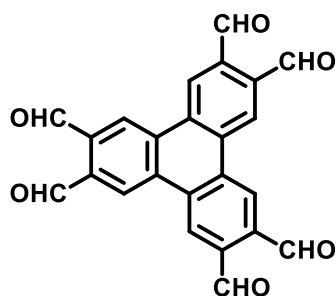
Dimethyl-4,5-dibromophthalate (57): To an oven-dried, 2-neck, 100 mL round bottom flask equipped with a stir bar and reflux condenser was added 4,5-dibromophthalic acid (5.0 g, 15 mmol, 1.0 eq.) and dry methanol (50 mL, 80 eq.). The mixture was stirred under a nitrogen atmosphere and cooled to 0 °C in an ice/water bath. Next, thionyl chloride (6.0 mL, 83 mmol, 5.35 eq.) was slowly added dropwise (1 drop/second) via syringe. The resulting mixture was warmed to room temperature and then refluxed under nitrogen for 36 hours. Following the allotted reaction time, the flask was removed from the heat source and cooled to room temperature. The crude reaction mixture was diluted with dichloromethane and the resulting insoluble by-product was removed via suction filtration. The filtrate was then concentrated under reduced pressure to yield **57** as a brittle, white solid. The crude material was then purified through a silica column (SiO₂, 9:1 hexanes/ethyl acetate) to yield **57** as a fluffy, white solid (4.22 g, 78%). m.p. = 79.2-80.1 °C; ¹H NMR (400 MHz, CDCl₃) δ: 3.89 (s, 6H), 7.95 (s, 2H). The ¹H NMR data collected is consistent with the values reported in the literature.⁶⁵



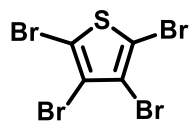
Hexamethyl-triphenylene-2,3,6,7,10,11-hexacarboxylate (37): Under glove box conditions an oven-dried, single-neck, 250 mL round bottom flask equipped with a stir bar was charged with 2,2'-bipyridyl (1.11 g, 7.13 mmol, 1.25 eq.), 1,5-cyclooctadiene (1.27 g, 11.7 mmol, 2.05 eq.), anhydrous tetrahydrofuran (54 g) and bis(1,5-cyclooctadiene)nickel(0) (1.96 g, 7.13 mmol, 1.25 eq.), resulting in a deep-purple coloured solution. Subsequently, a solution of **57** (2.00 g, 5.70 mmol, 1.0 eq.) in anhydrous tetrahydrofuran (54 g) was added dropwise via Pasteur pipette. The resulting solution was sealed with a rubber septum, parafilm and wrapped in tinfoil. The reaction flask was removed from the glove box and transferred to a fume hood where it was stirred under nitrogen for 16 hours. The reaction mixture was then poured over a 1:1 mixture of methanol and 1 molar hydrochloric acid (100 mL) in a 500 mL Erlenmeyer flask and left in the fridge overnight. The resulting white precipitate was collected via suction filtration and wash with methanol and 1 molar hydrochloric acid to yield **37** as a white solid (813 mg, 74%). m.p. = >260 °C; ¹H NMR (400 MHz, CDCl₃) δ: 4.03 (s, 18H), 9.01 (s, 6H). The ¹H NMR data collected is consistent with the values reported in the literature.⁵⁵



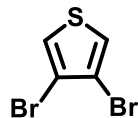
Triphenylene-2,3,6,7,10,11-hexaylhexamethanol (80): To an oven dried 250 mL round bottom flask equipped with a stir bar was added solid lithium aluminum hydride (0.553 g, 14.6 mmol, 12 eq.) and anhydrous tetrahydrofuran (21 mL). The reaction mixture was stirred under nitrogen and cooled to 0 °C in an ice/water bath. Next, a suspension of hexamethyl-triphenylene-2,3,6,7,10,11-hexacarboxylate (**37**) (0.700 g, 1.21 mmol, 1.0 eq.) in anhydrous tetrahydrofuran (35 mL) was slowly added dropwise via syringe at 0 °C. The resulting mixture was stirred for 12 hours and allowed to gradually warm up to room temperature. The reaction was cooled to 0 °C in an ice/water bath and quenched with a saturated aqueous solution of sodium sulfate until bubbling stopped. The reaction was further diluted with deionized water (30 mL) and tetrahydrofuran was removed via rotatory evaporation, leaving behind a white slurry. 1 molar hydrochloric acid was then added until pH 2 was achieved. The crude white solid was collected and dried via suction filtration, followed by recrystallization from dimethyl sulfoxide/ H₂O to yield **80** as an off-white powder (342 g, 69%). m.p. = >260 °C; ¹H NMR (400 MHz, DMSO-*d*₆) δ: 4.77 (*d*, *J* = 5.6 Hz, 12H), 5.33 (*t*, *J* = 6 Hz, 6H), 8.71 (*s*, 6H); ¹³C NMR (100 MHz, DMSO-*d*₆) δ: 61.02, 121.49, 128.11, 139.15; HRMS (ESI+) *m/z*: [M+Na]⁺ calc. for C₂₄H₂₄O₆ 431.14651, found 431.14574.



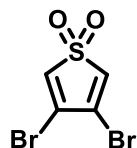
Triphenylene-2,3,6,7,10,11-hexacarbaldehyde (3): To an oven-dried, 2-neck, 50 mL round bottom flask was added triphenylene-2,3,6,7,10,11-hexaylhexamethanol (**80**) (0.05 g, 0.1 mmol, 1.0 eq.) and a 1:1 mixture of anhydrous dichloromethane and dimethyl sulfoxide (20 mL). The mixture was stirred under nitrogen and cooled to 0 °C in an ice/water bath. Next, Dess-Martin periodinane (0.467 g, 1.17 mmol, 9.0 eq.) was added all at once to the flask. The ice bath was removed, and the reaction was stirred at room temperature for 2 hours, during which time the reaction went from clear and colourless to a yellow slurry. Following the allotted reaction time, the reaction was quenched with a saturated aqueous sodium bicarbonate solution, diluted, and extracted with dichloromethane (3x15 mL), and then transferred to a separatory funnel. The organic layer was washed with saturated aqueous sodium bicarbonate (2x35 mL) and brine (2x35 mL), dried over sodium sulfate, filtered, and concentrated to yield a crude white solid (mixture of DMP, IBA/IBX and aldehyde). A pale-yellow solid was also collected from the aqueous layer via suction filtration (47 mg, crude aldehyde). ^1H NMR (400 MHz, $\text{DMSO-}d_6$) δ : 9.18 (s, 6H), 10.58 (s, 6H); HRMS (ESI+) m/z: $[\text{M}+\text{H}]^+$ calc. for $\text{C}_{24}\text{H}_{12}\text{O}_6$ 397.07066, found 397.07130.



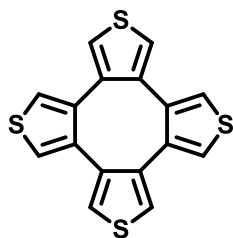
2,3,4,5-tetrabromothiophene (85): To an oven-dried, 3-neck, 250 mL round bottom flask equipped with a stir bar, dropping funnel and base trap (saturated aqueous sodium hydroxide) was added thiophene (8.0 mL, 100 mmol, 1.0 eq.), and chloroform (10 mL). The reaction flask was cooled to 0 °C in an ice/water bath and a mixture of bromine (25.6 mL, 500 mmol, 5.0 eq.) and chloroform (30 mL) was slowly added dropwise via addition funnel over a period of 2 hours. Following the completion of bromine addition, the reaction was stirred for 1.5 hours while gradually warming up to room temperature. The reaction mixture was then refluxed at 65 °C in an oil bath for the next 16 hours. Following the allotted reaction time, the mixture was cooled to 0 °C in an ice/water bath and excess bromine was quenched with 40 mL of a 20% w/v aqueous solution of sodium hydroxide. The crude solid was collected via suction filtration and washed with methanol to yield **85** as a fluffy, off-white solid (16.8 g, 42%). m.p. = 111.3-114.7 °C; ¹³C NMR (100 MHz, CHCl₃) δ: 110.25, 116.91. The ¹³C NMR data collected is consistent with the values reported in the literature.⁷¹



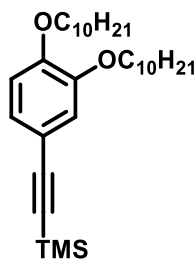
3,4-dibromothiophene (43): To an oven-dried, 100 mL round bottom flask equipped with a stir bar, reflux condenser and glass stopper was added glacial acetic acid (12 mL), deionized water (3 mL) and 2,3,4,5-tetrabromothiophene (7.2 g, 18 mmol, 1.0 eq.). The resulting mixture was stirred under nitrogen at room temperature and activated zinc dust (7.0 g, 107 mmol, 6.0 eq.) was slowly added to the reaction mixture in spatula tip portions. Following the addition of zinc dust, the reaction was stirred at room temperature under a nitrogen atmosphere for 12 hours. The reaction was then gravity filtered to remove excess zinc and by-products to yield a colourless filtrate. The filtrate was extracted with ethyl acetate (3x20 mL), and the organic layer was washed with brine (3x20 mL), dried over magnesium sulfate, filtered, and concentrated to yield **43** as a pale-yellow oil (2.8 g, 64%). ^1H NMR (400 MHz, CDCl_3) δ : 7.29 (s, 2H). The ^1H NMR data collected is consistent with the values reported in the literature.⁷¹



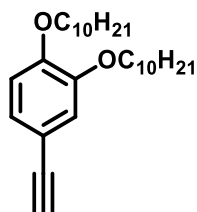
3,4-dibromothiophene 1,1-dioxide (86): To an oven-dried 2-neck 50 mL round bottom flask equipped with a stir bar, internal thermometer and addition funnel was added 30% H₂O₂ (1.7 mL, 8.0 eq.). The reaction flask was cooled to -10 °C in a dry ice/acetone bath and trifluoroacetic anhydride (TFAA) (4.2 mL, 30 mmol, 14.33 eq.) was slowly added dropwise via addition funnel. It is important to note that the addition of TFAA to H₂O₂ is extremely exothermic, and the addition of TFAA must be carefully controlled to maintain the temperature of the solution between -10 °C and 0 °C. Following the addition of TFAA, the mixture was allowed to stir and warm up to room temperature over 30 minutes. A solution of 3,4-dibromothiophene (0.500 g, 2.07 mmol, 1.0 eq.) (**43**) in dichloromethane (3 mL) was then quickly added all at once. The reaction mixture was allowed to stir at room temperature and open to air for 3 hours. Following the allotted reaction time, the mixture was transferred to a 250 mL Erlenmeyer flask and cooled to 0 °C in an ice/water bath. The reaction mixture was quenched with a saturated aqueous solution of sodium carbonate until a pH of 8 or greater was achieved (tested via pH paper). The organic layer was extracted with dichloromethane (3x30 mL), dried over MgSO₄, filtered, and concentrated via rotary evaporation to yield **86** as a pale-yellow powder (435 mg, 77%). m.p. = 102.9-105.9 °C (decomp.); ¹H NMR (400 MHz, CDCl₃) δ: 6.81 (s, 2H). The ¹H NMR data collected is consistent with the values reported in the literature.⁷²



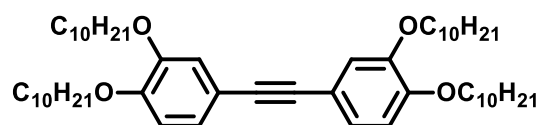
Cycloocta[1,2-*c'*:5,6-*c''*:7,8-*c'''*]tetrathiophene (32): Under glove box conditions an oven-dried, single-neck, 50 mL round bottom flask equipped with a stir bar was charged with 2,2'-bipyridyl (1.03 g, 6.61 mmol, 1.25 eq.), 1,5-cyclooctadiene (1.17 g, 10.8 mmol, 2.05 eq.), anhydrous dimethylformamide (11.0 g) and bis(1,5-cyclooctadiene)nickel(0) (1.82 g, 6.61 mmol, 1.25 eq.), resulting in a deep-purple coloured solution. Subsequently, a solution of **43** (1.30 g, 5.28 mmol, 1.0 eq.) in anhydrous dimethylformamide (11.0 g) was added dropwise via Pasteur pipette. The resulting solution was sealed with a rubber septum, parafilm and wrapped in tinfoil. The reaction flask was removed from the glove box and transferred to a fume hood where it was stirred under nitrogen at 70 °C in an oil bath for 24 hours. The flask was then removed from the oil bath and cooled to room temperature. The resulting crude reaction mixture was filtered through a pad of celite and washed with chloroform. The resulting filtrate was poured over ice cold deionized water and stirred for 30 minutes, transferred to a separatory funnel, and extracted with chloroform (3x50 mL). The organic layers were combined and washed with deionized water (3x100 mL), dried over magnesium sulfate, filtered, and concentrated to yield a crude yellow oil that crystallized upon cooling. The crude material was adsorbed onto silica gel and purified via column chromatography (SiO₂, 5cm, 100% hexanes) to yield **32** as a pale-yellow solid (0.177 g, 41%). m.p. = >260 °C; ¹H NMR (400 MHz, CDCl₃) δ: 7.20 (s, 8H). The ¹H NMR data collected is consistent with the values reported in the literature.⁷⁹



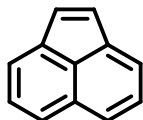
((3,4-bis(decyloxy)phenyl)ethynyl)trimethylsilane (88): To an oven-dried, 2-neck, 25 mL round bottom flask equipped with a stir bar and reflux condenser was added 1,2-didecyloxy-4-iodobenzene (1.50 g, 2.90 mmol, 1.0 eq.), and triethylamine (8 mL). The mixture was sparged with nitrogen for 20 minutes followed by addition of bis(triphenylphosphine)palladium(II) dichloride (0.102 g, 0.145 mmol, 0.05 eq.), and copper(I) iodide (0.055 g, 0.29 mmol, 0.10 eq.), resulting in an opaque yellow solution. Finally, ethynyltrimethylsilane (0.46 mL, 0.71 mmol, 1.14 eq.) was quickly added via syringe resulting in a red coloured solution. The reaction mixture was then heated to 50 °C in an oil bath and stirred under nitrogen for 18 hours. The reaction was then removed from the oil bath and cooled to room temperature followed by dilution with deionized water (10 mL) and extraction with ethyl acetate (3x20 mL). The organic layers were combined and washed with deionized water (2x20 mL) and brine (2x20 mL), dried over magnesium sulfate, filtered, and concentrated to yield a crude dark-brown oil. The crude material was then purified through a silica column (SiO₂, 85:15 hexanes/dichloromethane) to yield **88** as an orange oil (1.26 g, 89%). ¹H NMR (400 MHz, CDCl₃) δ: 0.22 (*s*, 9H), 0.87 (*t*, *J* = 6.8 Hz, 6H), 1.25-1.29 (*m*, 24H), 1.44 (*m*, 4H), 1.79 (*m*, 4H), 3.93-3.98 (*m*, 4H), 6.74-6.76 (*d*, *J* = 4 Hz, 1H), *6.87 (*s*, 1,2-bis(decyloxy)benzene impurity), 6.94-6.95 (*d*, *J* = 1.6 Hz, 1H), 6.99-7.02 (*dd*, *J* = 1.6 Hz, 1H); ¹³C NMR (100 MHz, CDCl₃) δ: 0.04, 14.07, 22.65, 25.95-25.93, 29.12-29.58, 31.88, 69.1-69.2, 92.02, 105.47, 113.08, 115.18, 116.99, 125.41, 148.58, 149.88; HRMS (APCI+) *m/z*: [M+H]⁺ calc. for C₃₁H₅₄O₂Si 487.3966, found 487.3979.



1,2-bis(decyloxy)-4-ethynylbenzene (89): To an oven-dried 100 mL round bottom flask was added a solution of ((3,4-bis(decyloxy)phenyl)ethynyl)trimethylsilane (**88**) (1.256 g, 2.579 mmol, 1.0 eq.), in a 1:1 mixture of tetrahydrofuran and methanol (26 mL). Solid potassium carbonate (0.929 g, 6.72 mmol, 2.6 eq.) was then added all at once, and the resulting mixture was stirred under nitrogen at room temperature for 24 hours. The reaction mixture was then passed through a short silica plug (5 cm SiO₂) using dichloromethane (100%) as the eluting solvent. Excess solvent was removed via rotatory evaporation to yield a crude yellow oil, which upon standing in ambient conditions, solidified into a crystalline yellow solid. The crude material was then purified through a silica column (SiO₂, 85:15 hexanes/dichloromethane) to yield **89** as a clear yellow oil that solidifies to a grey-green solid (0.983 g, 92%). m.p. = 32-33.4 °C; ¹H NMR (400 MHz, CDCl₃) δ: 0.86 (*t*, *J* = 6.8 Hz, 6H), 1.25-1.40 (*m*, 24H), 1.42-1.53 (*m*, 4H), 1.75-1.83 (*m*, 4H), 2.96 (*s*, 1H), 3.93-3.99 (*m*, 4H), 6.76-6.78 (*d*, *J* = 8.8 Hz, 1H), *6.87 (*s*, 1,2-bis(decyloxy)benzene impurity), 6.97 (*d*, *J* = 1.2 Hz, 1H), 7.02-7.05 (*dd*, *J* = 1.6 Hz, 1H). The ¹H NMR data collected is consistent with the values reported in the literature.⁷⁶



1,2-bis(3,4-bis(decyloxy)phenyl)ethyne (82): To an oven-dried, 2-neck, 50 mL round bottom flask equipped with a stir bar was added 1,2-bis(decyloxy)-4-iodobenzene **87** (0.200 g, 0.387 mmol, 1.0 eq.), bis(triphenylphosphine)palladium(II) dichloride (0.014 g, 0.019 mmol, 0.05 eq.), and copper(I) iodide (0.008 g, 0.04 mmol, 0.10 eq.). The flask was degassed with nitrogen for 20 minutes, followed by the addition of both anhydrous toluene (6 mL) and triethylamine (4 mL, 6 eq.) via syringe. A solution of 1,2-bis(decyloxy)-4-ethynylbenzene **89** (0.169 g, 0.407 mmol, 1.05 eq.) in anhydrous toluene (6 mL) was then slowly added dropwise (1 drop/s) via syringe, and the reaction was left to stir at room temperature for 24 hours under an atmosphere of nitrogen. The crude mixture was diluted with dichloromethane and filtered through a 5 cm silica plug, using a 1:1 mixture of dichloromethane and ethyl acetate as the eluting solvents. Excess solvents were then removed under reduced pressure to yield a crude, yellow-orange solid. The crude material was recrystallized from acetone, and the resulting precipitate was collected via suction filtration, washed with ice cold acetone, and dried to yield **82** as a fluffy off-white solid (0.185 g, 60%). m.p. = 98-98.3 °C; ^1H NMR (400 MHz, CDCl_3) δ : 0.87 (*t*, $J = 7.2$ Hz, 12H), 1.22-1.38(*m*, 54H), 1.45 (*m*, 8H), 1.80 (*quintet*, $J = 6.4$ Hz, 8H), 3.99 (*t*, $J = 6.8$ Hz, 8H), 6.79-6.81 (*d*, $J = 8.4$ Hz, 2H), 7.00 (*d*, $J = 2$ Hz, 2H), 7.04-7.06 (*dd*, $J = 6$ Hz, 2H); ^{13}C NMR (100 MHz, CDCl_3) δ : 14.07, 22.66, 25.98, 29.19, 29.32-29.39, 29.55-29.59, 31.88, 69.17, 69.22, 87.94, 113.34, 115.64, 116.61, 124.71, 148.72, 149.46; HRMS (APCI+) m/z : $[\text{M}+\text{H}]^+$ calc. for $\text{C}_{54}\text{H}_{90}\text{O}_4$ 803.69119, found 803.69236.



Acenaphthylene (91): To an oven-dried 2-neck 250 mL round bottom flask equipped with a stir bar and reflux condenser was added acenaphthene (2.00 g, 12.9 mmol, 1.0 eq.) and anhydrous toluene (105 mL) under an atmosphere of nitrogen. Next, 2,3-dichloro-5,6-dicyano-1,4-benzoquinone (DDQ) (3.53 g, 15.6 mmol, 1.2 eq.) was added all at once to the reaction flask and the resulting mixture was stirred under nitrogen at reflux for 22 hours. The reaction was cooled to room temperature and quenched with deionized water. The crude reaction mixture was filtered via suction filtration, transferred to a separatory funnel and to it was added 150 mL of deionized water. The organic materials were extracted with dichloromethane (4x50 mL) and the organic layer was washed with DI H₂O (2x100 mL). The organic layer was dried over MgSO₄, filtered, and concentrated to yield a dark red oil as the crude product. The crude material was adsorbed onto silica gel and purified via column chromatography (SiO₂, 95:5 hexanes: ethyl acetate) to yield **91** as a yellow crystalline solid (1.36 g, 69%). m.p. = 91-93 °C; ¹H NMR (400 MHz, CDCl₃) δ : 7.07 (s, 2H), 7.51-7.55 (m, 2H), 7.67-7.68 (d, *J* = 6.8 Hz, 2H), 7.78-7.81 (d, *J* = 8.4 Hz, 2H); HRMS (APCI+) *m/z*: [M+H]⁺ calc. for C₁₂H₈ 153.06988, found 153.06940. The ¹H NMR data collected is consistent with that of a sample obtained from Sigma Aldrich.

REFERENCES

- (1) Brusso, J. L.; Hirst, O. D.; Dadvand, A.; Ganesan, S.; Cicoira, F.; Robertsons, C. M.; Oakley, R. T.; Rosei, F.; Perepichka, D. F. Two-Dimensional Structural Motif in Thienoacene Semiconductors: Synthesis, Structure, and Properties of Tetrathienoanthracene Isomers. *Chem. Mater.* **2008**, *20* (7), 2484–2494.
<https://doi.org/10.1021/cm7030653>.
- (2) Roncali, J.; Leriche, P.; Blanchard, P. Molecular Materials for Organic Photovoltaics : Small Is Beautiful. *Adv. Mater.* **2014**, *26*, 3821–3838.
<https://doi.org/10.1002/adma.201305999>.
- (3) Peumans, P.; Yakimov, A.; Forrest, S. R. Small Molecular Weight Organic Thin-Film Photodetectors and Solar Cells. *J. Appl. Phys.* **2003**, *93* (7), 3693–3723.
<https://doi.org/10.1063/1.1534621>.
- (4) Palilis, L. C.; Lane, P. A.; Kushto, G. P.; Purushothaman, B.; Anthony, J. E.; Kafafi, Z. H. Organic Photovoltaic Cells with High Open Circuit Voltages Based on Pentacene Derivatives. *Org. Electron. Physics, Mater. Appl.* **2008**, *9* (5), 747–752.
<https://doi.org/10.1016/j.orgel.2008.05.015>.
- (5) Sheraw, C. D.; Jackson, T. N.; Eaton, D. L.; Anthony, J. E. Functionalized Pentacene Active Layer Organic Thin-Film Transistors. *Adv. Mater.* **2003**, *15* (23), 2009–2011.
<https://doi.org/10.1002/adma.200305393>.
- (6) Katz, H. E.; Bao, Z.; Gilat, S. L. Synthetic Chemistry for Ultrapure, Processable, and High-Mobility Organic Transistor Semiconductors. *Acc. Chem. Res.* **2001**, *34* (5), 359–

369. <https://doi.org/10.1021/ar990114j>.
- (7) Bruzek, M. J.; Anthony, J. E. Synthesis and Optical Properties of Dioxolane-Functionalized Hexacenes and Heptacenes. *Org. Lett.* **2014**, *16* (13), 3608–3610. <https://doi.org/10.1021/ol501373s>.
- (8) Yoo, S.; Domercq, B.; Kippelen, B. Efficient Thin-Film Organic Solar Cells Based on Pentacene/C 60 Heterojunctions. *Appl. Phys. Lett.* **2004**, *85* (22), 5427–5429. <https://doi.org/10.1063/1.1829777>.
- (9) Shi, X.; Chi, C. Different Strategies for the Stabilization of Acenes and Acene Analogues. *Chem. Rec.* **2016**, *16* (3), 1690–1700. <https://doi.org/10.1002/tcr.201600031>.
- (10) Sun, Z.; Ye, Q.; Chi, C.; Wu, J. Low Band Gap Polycyclic Hydrocarbons: From Closed-Shell near Infrared Dyes and Semiconductors to Open-Shell Radicals. *Chem. Soc. Rev.* **2012**, *41* (23), 7857–7889. <https://doi.org/10.1039/c2cs35211g>.
- (11) Ye, Q.; Chi, C. Recent Highlights and Perspectives on Acene Based Molecules and Materials. *Chem. Mater.* **2014**, *26* (14), 4046–4056. <https://doi.org/10.1021/cm501536p>.
- (12) Anthony, J. E. Functionalized Acenes and Heteroacenes for Organic Electronics. *Chem. Rev.* **2006**, *106* (12), 5028–5048. <https://doi.org/10.1021/cr050966z>.
- (13) Balaban, A. T. Clar Formulas: How to Draw and How Not to Draw Formulas of Polycyclic Aromatic Hydrocarbons. *Polycycl. Aromat. Compd.* **2004**, *24* (2), 83–89. <https://doi.org/10.1080/10406630490424124>.
- (14) Watson, M. D.; Fechtenkötter, A.; Müllen, K. Big Is Beautiful - “Aromaticity” Revisited from the Viewpoint of Macromolecular and Supramolecular Benzene Chemistry. *Chem.*

- Rev.* **2001**, *101* (5), 1267–1300. <https://doi.org/10.1021/cr990322p>.
- (15) Würthner, F.; Schmidt, R. Electronic and Crystal Engineering of Acenes for Solution-Processible Self-Assembling Organic Semiconductors. *ChemPhysChem.* **2006**, *7* (4), 793–797. <https://doi.org/10.1002/cphc.200600078>.
- (16) Anthony, J. E.; Brooks, J. S.; Eaton, D. L.; Parkin, S. R. Functionalized Pentacene: Improved Electronic Properties from Control of Solid-State Order . *J. Am. Chem. Soc.* **2001**, *123* (38), 9482–9483. <https://doi.org/10.1021/ja0162459>.
- (17) Kumar, S. Self-Organization of Disc-like Molecules: Chemical Aspects. *Chem. Soc. Rev.* **2006**, *35* (1), 83–109. <https://doi.org/10.1039/b506619k>.
- (18) Laschat, S.; Baro, A.; Steinke, N.; Giesselmann, F.; Hägele, C.; Scalia, G.; Judele, R.; Kapatsina, E.; Sauer, S.; Schreivogel, A.; et al. Discotic Liquid Crystals: From Tailor-Made Synthesis to Plastic Electronics. *Angew. Chemie - Int. Ed.* **2007**, *46* (26), 4832–4887. <https://doi.org/10.1002/anie.200604203>.
- (19) Park, C. Il; Seong, M.; Kim, M. A.; Kim, D.; Jung, H.; Cho, M.; Lee, S. H.; Lee, H.; Min, S.; Kim, J.; et al. World's First Large Size 77-Inch Transparent Flexible OLED Display. *J. Soc. Inf. Disp.* **2018**, *26* (5), 287–295. <https://doi.org/10.1002/jsid.663>.
- (20) Chandrasekhar, S.; Ranganath, G. S. Discotic Liquid Crystals. *Reports Prog. Phys.* **1990**, *53* (1), 57–84. <https://doi.org/10.1088/0034-4885/53/1/002>.
- (21) Boden, N.; Borner, R. C.; Bushby, R. J.; Cammidge, A. N.; Jesudason, M. V. The Synthesis of Triphenylene-Based Discotic Mesogens New and Improved Routes. *Liq. Cryst.* **1993**, *15* (6), 851–858. <https://doi.org/10.1080/02678299308036504>.

- (22) Boden, N.; Bushby, R. J.; Clements, J.; Movaghar, B.; Donovan, K. J.; Kreouzis, T. Mechanism of Charge Transport in Discotic Liquid Crystals. *Phys. Rev. B* **1995**, 52 (18), 13274–13280. <https://doi.org/10.1103/PhysRevB.52.13274>.
- (23) Paquette, J. A.; Yardley, C. J.; Psutka, K. M.; Cochran, M. A.; Calderon, O.; Williams, V. E.; Maly, K. E. Dibenz[*a,c*]anthracene Derivatives Exhibiting Columnar Mesophases over Broad Temperature Ranges. *Chem. Commun.* **2012**, 48 (66), 8210–8212. <https://doi.org/10.1039/c2cc33407k>.
- (24) Paquette, J. A.; Psutka, K. M.; Yardley, C. J.; Maly, K. E. Probing the Structural Features That Influence the Mesomorphic Properties of Substituted Dibenz[*a,c*]anthracenes. *Can. J. Chem.* **2017**, 95 (4), 399–409. <https://doi.org/10.1139/cjc-2016-0505>.
- (25) Psutka, K. M.; Williams, J.; Paquette, J. A.; Calderon, O.; Bozek, K. J. A.; Williams, V. E.; Maly, K. E. Synthesis of Substituted Dibenz[*a,c*]anthracenes and an Investigation of Their Liquid-Crystalline Properties. *European J. Org. Chem.* **2015**, 2015 (7), 1456–1463. <https://doi.org/10.1002/ejoc.201403504>.
- (26) Foster, E. J.; Jones, R. B.; Lavigueur, C.; Williams, V. E. Structural Factors Controlling the Self-Assembly of Columnar Liquid Crystals. *J. Am. Chem. Soc.* **2006**, 128 (26), 8569–8574. <https://doi.org/10.1021/ja0613198>.
- (27) Psutka, K. M.; Bozek, K. J. A.; Maly, K. E. Synthesis and Mesomorphic Properties of Novel Dibenz[*a,c*]Anthracenedicarboximides. *Org. Lett.* **2014**, 16 (20), 5442–5445. <https://doi.org/10.1021/ol502678m>.
- (28) Kozma, E.; Catellani, M. Perylene Diimides Based Materials for Organic Solar Cells. *Dye. Pigment.* **2013**, 98 (1), 160–179. <https://doi.org/10.1016/j.dyepig.2013.01.020>.

- (29) Psutka, K. M.; Maly, K. E. Synthesis and Characterization of Novel Dibenz[*a,c*]anthracenedicarboxythioimides: The Effect of Thionation on Self-Assembly. *RSC Adv.* **2016**, *6* (82), 78784–78790. <https://doi.org/10.1039/c6ra16890f>.
- (30) Psutka, K. M.; Ledrew, J.; Taing, H.; Eichhorn, S. H.; Maly, K. E. Synthesis and Self-Assembly of Liquid Crystalline Triphenylenedicarboxythioimides. *J. Org. Chem.* **2019**, *84*, 10796–10804. <https://doi.org/10.1021/acs.joc.9b01330>.
- (31) Song, Y.; Sun, Q.; Aguila, B.; Ma, S. Opportunities of Covalent Organic Frameworks for Advanced Applications. *Adv. Sci.* **2019**, *6* (2). <https://doi.org/10.1002/advs.201801410>.
- (32) Furukawa, H.; Cordova, K. E.; O’Keeffe, M.; Yaghi, O. M. The Chemistry and Applications of Metal-Organic Frameworks. *Science*. **2013**, *341* (6149), 1230444. <https://doi.org/10.1126/science.1230444>.
- (33) Lu, W.; Wei, Z.; Gu, Z. Y.; Liu, T. F.; Park, J.; Park, J.; Tian, J.; Zhang, M.; Zhang, Q.; Gentle, T.; et al. Tuning the Structure and Function of Metal-Organic Frameworks via Linker Design. *Chem. Soc. Rev.* **2014**, *43* (16), 5561–5593. <https://doi.org/10.1039/c4cs00003j>.
- (34) Lohse, M. S.; Bein, T. Covalent Organic Frameworks: Structures, Synthesis, and Applications. *Adv. Funct. Mater.* **2018**, *28* (33), 1–71. <https://doi.org/10.1002/adfm.201705553>.
- (35) Wan, S.; Guo, J.; Kim, J.; Ihee, H.; Jiang, D. A Photoconductive Covalent Organic Framework: Self-Condensed Arene Cubes Composed of Eclipsed 2D Polypyrene Sheets for Photocurrent Generation. *Angew. Chemie - Int. Ed.* **2009**, *48* (30), 5439–5442. <https://doi.org/10.1002/anie.200900881>.

- (36) Chen, C. F. Novel Triptycene-Derived Hosts: Synthesis and Their Applications in Supramolecular Chemistry. *Chem. Commun.* **2011**, 47 (6), 1674–1688.
<https://doi.org/10.1039/c0cc04852f>.
- (37) Deng, C. L.; Xiong, X. D.; Chik, D. T. W.; Cai, Z.; Peng, X. S.; Wong, H. N. C. 6,7-Bismethoxy-2,11-Dihydroxytetraphenylene Derived Macrocycles: Synthesis, Structures, and Complexation with Fullerenes. *Chem. - An Asian J.* **2015**, 10 (11), 2342–2346.
<https://doi.org/10.1002/asia.201500689>.
- (38) Wang, M. X. Heterocalixaromatics, New Generation Macrocyclic Host Molecules in Supramolecular Chemistry. *Chem. Commun.* **2008**, (38), 4541–4551.
<https://doi.org/10.1039/b809287g>.
- (39) Irngartinger, H; Reibel, W. R. K. Structures of Dibenzo[*a,e*]cyclootetraene and tetrabenzo[*a,e,e,g*]cyclooctatetraene. *Acta. Cryst.* **1981**, 126 (1981), 1724–1728.
<https://doi.org/10.1107/S0567740881006985>.
- (40) Mak, T. C. W.; Wong, H. N. C. Inclusion Properties of Tetraphenylene and Synthesis of Its Derivatives. *Top. Curr. Chem.* **1987**, 140, 141–164.
- (41) Sarli, V. Transition-Metal-Catalyzed Asymmetric C-C Cross-Couplings in Stereoselective Synthesis. *Stereoselective Synth. Drugs Nat. Prod.* **2013**, 1–26.
<https://doi.org/10.1002/9781118596784.ssd013>.
- (42) Zhou, Z. hua; Yamamoto, T. Research on Carbon-Carbon Coupling Reactions of Haloaromatic Compounds Mediated by Zerovalent Nickel Complexes. Preparation of Cyclic Oligomers of Thiophene and Benzene and Stable Anthrylnickel(II) Complexes. *J. Organomet. Chem.* **1991**, 414 (1), 119–127. [https://doi.org/10.1016/0022-328X\(91\)83247-](https://doi.org/10.1016/0022-328X(91)83247-)

2.

- (43) Yamamoto, T.; Wakabayashi, S.; Osakada, K. Mechanism of C-C Coupling Reactions of Aromatic Halides, Promoted by Ni(COD)₂ in the Presence of 2,2'-bipyridine and PPh₃, to Give Biaryls. *J. Organomet. Chem.* **1992**, 428, 223–237.
- (44) Rüdiger, E. C.; Rominger, F.; Steuer, L.; Bunz, U. H. F. Synthesis of Substituted Trinaphthylenes. *J. Org. Chem.* **2016**, 81 (1), 193–196.
<https://doi.org/10.1021/acs.joc.5b02481>.
- (45) Berezhnaia, V.; Roy, M.; Vanthuyne, N.; Villa, M.; Naubron, J. V.; Rodriguez, J.; Coquerel, Y.; Gingras, M. Chiral Nanographene Propeller Embedding Six Enantiomerically Stable [5]Helicene Units. *J. Am. Chem. Soc.* **2017**, 139 (51), 18508–18511. <https://doi.org/10.1021/jacs.7b07622>.
- (46) Yin, J.; Qu, H.; Zhang, K.; Luo, J.; Zhang, X.; Chi, C.; Wu, J. Electron-Deficient Triphenylene and Trinaphthylene Carboximides. *Org. Lett.* **2009**, 11 (14), 3028–3031.
<https://doi.org/10.1021/ol901041n>.
- (47) Tilley, A. J.; Pensack, R. D.; Lee, T. S.; Djukic, B.; Scholes, G. D.; Seferos, D. S. Ultrafast Triplet Formation in Thionated Perylene Diimides. *J. Phys. Chem. C* **2014**, 118 (19), 9996–10004. <https://doi.org/10.1021/jp503708d>.
- (48) Chen, W.; Zhang, J.; Long, G.; Liu, Y.; Zhang, Q. From Non-Detectable to Decent: Replacement of Oxygen with Sulfur in Naphthalene Diimide Boosts Electron Transport in Organic Thin-Film Transistors (OTFT). *J. Mater. Chem. C* **2015**, 3 (31), 8219–8224.
<https://doi.org/10.1039/c5tc01519g>.

- (49) Asadirad, A. M.; Boutault, S.; Erno, Z.; Branda, N. R. Controlling a Polymer Adhesive Using Light and a Molecular Switch. *J. Am. Chem. Soc.* **2014**, *136* (8), 3024–3027. <https://doi.org/10.1021/ja500496n>.
- (50) Venkatramaiah, N.; Kumar, G. D.; Chandrasekaran, Y.; Ganduri, R.; Patil, S. Efficient Blue and Yellow Organic Light-Emitting Diodes Enabled by Aggregation-Induced Emission. *ACS Appl. Mater. Interfaces* **2018**, *10* (4), 3838–3847. <https://doi.org/10.1021/acsami.7b11025>.
- (51) Chen, Z.; Dong, S.; Zhong, C.; Zhang, Z.; Niu, L.; Li, Z.; Zhang, F. Photoswitching of the Third-Order Nonlinear Optical Properties of Azobenzene-Containing Phthalocyanines Based on Reversible Host-Guest Interactions. *J. Photochem. Photobiol. A Chem.* **2009**, *206* (2–3), 213–219. <https://doi.org/10.1016/j.jphotochem.2009.07.005>.
- (52) Marécot, P.; Paraiso, E.; Dumas, J. M.; Barbier, J. Deactivation of Nickel Catalysts by Sulphur Compounds. I. Benzene Hydrogenation. *Appl. Catal. A, Gen.* **1992**, *80* (1), 79–88. [https://doi.org/10.1016/0926-860X\(92\)85109-O](https://doi.org/10.1016/0926-860X(92)85109-O).
- (53) Schroeder, Z. W.; Ledrew, J.; Selmani, V. M.; Maly, K. E. Preparation of Substituted Triphenylenes via Nickel-Mediated Yamamoto Coupling. *RSC Adv.* **2021**, *11*, 39564–39569. <https://doi.org/10.1039/d1ra07931j>.
- (54) Zhai, L.; Shukla, R.; Wadumethrige, S. H.; Rathore, R. Probing the Arenium-Ion (ProtonTransfer) versus the Cation-Radical (Electron Transfer) Mechanism of Scholl Reaction Using DDQ as Oxidant. *J. Org. Chem.* **2010**, *75* (14), 4748–4760. <https://doi.org/10.1021/jo100611k>.
- (55) Osawa, T.; Kajitani, T.; Hashizume, D.; Ohsumi, H.; Sasaki, S.; Takata, M.; Koizumi, Y.;

- Saeki, A.; Seki, S.; Fukushima, T.; et al. Wide-Range 2D Lattice Correlation Unveiled for Columnarly Assembled Triphenylene Hexacarboxylic Esters. *Angew. Chemie - Int. Ed.* **2012**, *51* (32), 7990–7993. <https://doi.org/10.1002/anie.201203077>.
- (56) García-López, J. A.; Greaney, M. F. Use of 2-Bromophenylboronic Esters as Benzyne Precursors in the Pd-Catalyzed Synthesis of Triphenylenes. *Org. Lett.* **2014**, *16* (9), 2338–2341. <https://doi.org/10.1021/ol5006246>.
- (57) Frampton, C. S.; MacNicol, D. D.; Rowan, S. J. Synthesis and Structural Properties of the First Dodecakis(Aryloxy)Triphenylenes. *J. Mol. Struct.* **1997**, *405* (2–3), 169–178. [https://doi.org/10.1016/S0022-2860\(96\)09597-X](https://doi.org/10.1016/S0022-2860(96)09597-X).
- (58) Yang, Y.; Pei, Q.; Heeger, A. J. Efficient Blue Polymer Light-Emitting Diodes from a Series of Soluble Poly(Paraphenylene)S. *J. Appl. Phys.* **1996**, *79* (2), 934–939. <https://doi.org/10.1063/1.360875>.
- (59) Bloom, P. D.; Sheares, V. V. Synthesis of Poly(p-Phenylene) Macromonomers and Multiblock Copolymers. *J. Polym. Sci. Part A Polym. Chem.* **2001**, *39* (20), 3505–3512. <https://doi.org/10.1002/pola.1331>.
- (60) Hsieh, J. C.; Cheng, C. H. O-Dihaloarenes as Aryne Precursors for Nickel-Catalyzed [2 + 2 + 2] Cycloaddition with Alkynes and Nitriles. *Chem. Commun.* **2008**, (26), 2992–2994. <https://doi.org/10.1039/b801870g>.
- (61) Tran, V. T.; Li, Z. Q.; Apolinar, O.; Derosa, J.; Joannou, M. V.; Wisniewski, S. R.; Eastgate, M. D.; Engle, K. M. Ni(COD)(DQ): An Air-Stable 18-Electron Nickel(0)–Olefin Precatalyst. *Angew. Chemie - Int. Ed.* **2020**, *59* (19), 7409–7413. <https://doi.org/10.1002/anie.202000124>.

- (62) Montavon, T. J.; Türkmen, Y. E.; Shamsi, N. A.; Miller, C.; Sumaria, C. S.; Rawal, V. H.; Kozmin, S. A. Cycloadditions of Siloxy Alkynes with 1,2-Diazines: From Reaction Discovery to Identification of an Antiglycolytic Chemotype. *Angew. Chemie - Int. Ed.* **2013**, 52 (51), 13576–13579. <https://doi.org/10.1002/anie.201305711>.
- (63) Zhang, Y.; Zhang, Q.; Wong, C. T. T.; Li, X. Chemoselective Peptide Cyclization and Bicyclization Directly on Unprotected Peptides. *J. Am. Chem. Soc.* **2019**, 141 (31), 12274–12279. <https://doi.org/10.1021/jacs.9b03623>.
- (64) Hoshimoto, Y.; Ohashi, M.; Ogoshi, S. Catalytic Transformation of Aldehydes with Nickel Complexes through H₂ Coordination and Oxidative Cyclization. *Acc. Chem. Res.* **2015**, 48 (6), 1746–1755. <https://doi.org/10.1021/acs.accounts.5b00061>.
- (65) Zhang, F.; Wang, S. R.; Li, X. G.; Xiao, Y.; Pan, L. J. Studies on the Synthetic Process of 4, 5-Dicyano Dimethyl Phthalate. *Adv. Mater. Res.* **2014**, 1053, 252–256. <https://doi.org/10.4028/www.scientific.net/AMR.1053.252>.
- (66) Yuan, C.; Saito, S.; Camacho, C.; Irle, S.; Hisaki, I.; Yamaguchi, S. A π -Conjugated System with Flexibility and Rigidity That Shows Environment-Dependent RGB Luminescence. *J. Am. Chem. Soc.* **2013**, 135 (24), 8842–8845. <https://doi.org/10.1021/ja404198h>.
- (67) Bialecki, J. B.; Ruzicka, J.; Attygalle, A. B. Synthesis of [2,3,4,5,6-2H₅]Phenyl Glucosinolate. *J. Label. Compd. Radiopharm.* **2007**, 50 (8), 711–715. <https://doi.org/10.1002/jlcr.1407>.
- (68) Holsworth, D. D. Oxidation: Dess-Martin Periodinane Oxidation. *Name React. Funct. Gr. Transform.* **2010**, 218–236. <https://doi.org/10.1002/9780470176511.ch3>.

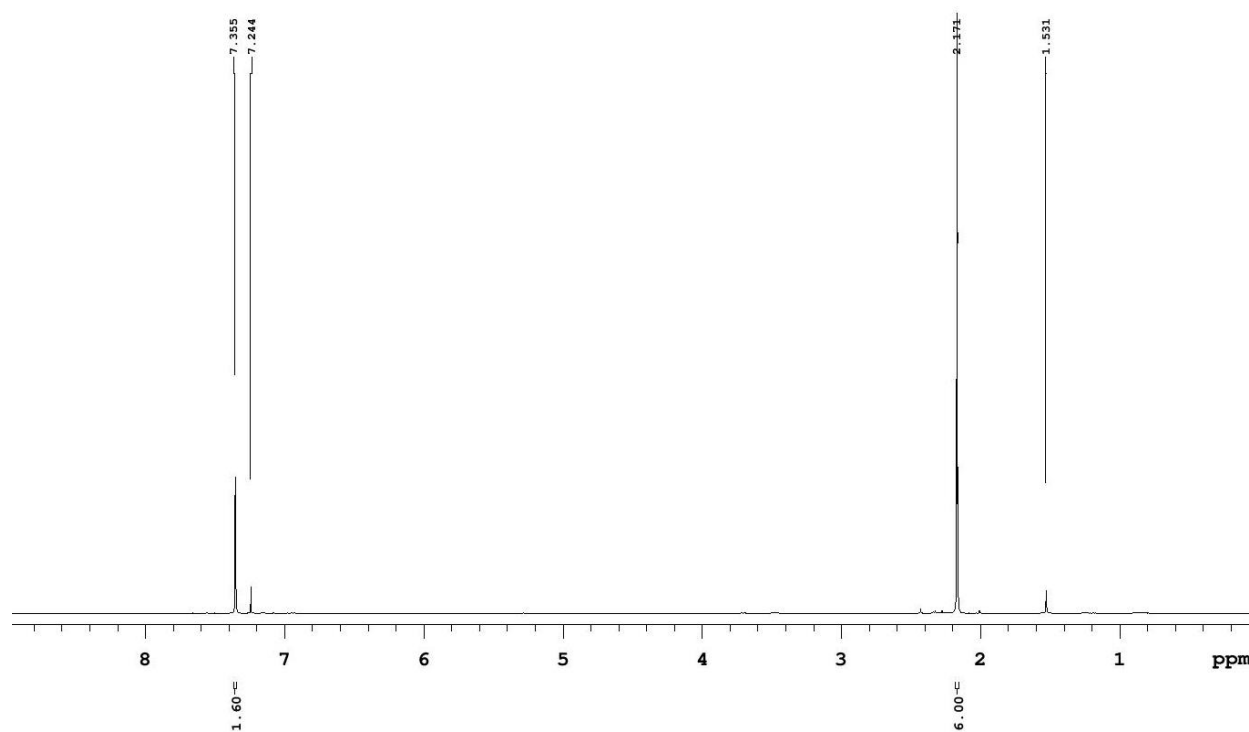
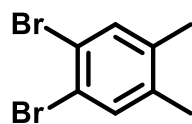
- (69) Sultane, P. R.; Bielawski, C. W. Burgess Reagent Facilitated Alcohol Oxidations in DMSO. *J. Org. Chem.* **2017**, *82* (2), 1046–1052. <https://doi.org/10.1021/acs.joc.6b02629>.
- (70) Zhang, Y.; Schilling, W.; Riemer, D.; Das, S. Metal-Free Photocatalysts for the Oxidation of Non-Activated Alcohols and the Oxygenation of Tertiary Amines Performed in Air or Oxygen. *Nat. Protoc.* **2020**, *15* (3), 822–839. <https://doi.org/10.1038/s41596-019-0268-x>.
- (71) Wang, Z.; Tao, F.; Xi, L. Y.; Meng, K. G.; Zhang, W.; Li, Y.; Jiang, Q. Two Novel Propylenedioxythiophene-Based Copolymers with Donor-Acceptor Structures for Organic Solar Cell Materials. *J. Mater. Sci.* **2011**, *46* (11), 4005–4012. <https://doi.org/10.1007/s10853-011-5328-8>.
- (72) Sánchez-Sánchez, C.; Dienel, T.; Nicolai, A.; Kharche, N.; Liang, L.; Daniels, C.; Meunier, V.; Liu, J.; Feng, X.; Müllen, K.; et al. On-Surface Synthesis and Characterization of Acene-Based Nanoribbons Incorporating Four-Membered Rings. *Chem. - A Eur. J.* **2019**, *25* (52), 12074–12082. <https://doi.org/10.1002/chem.201901410>.
- (73) Nagata, Y.; Kato, S.; Miyake, Y.; Shinokubo, H. Synthesis of Tetraaza[8]Circulenes from Tetrathia[8]Circulenes through an S_NAr-Based Process. *Org. Lett.* **2017**, *19* (10), 2718–2721. <https://doi.org/10.1021/acs.orglett.7b01074>.
- (74) Yu, Z.; Chen, X. M.; Liu, Z. Y.; Wang, M.; Huang, S.; Yang, H. A Phase-Dependent Photoluminescent Discotic Liquid Crystal Bearing a Graphdiyne Substructure. *Chem. Commun.* **2021**, *57* (7), 911–914. <https://doi.org/10.1039/d0cc05959e>.
- (75) Elangovan, A.; Wang, Y. H.; Ho, T. I. Sonogashira Coupling Reaction with Diminished Homocoupling. *Org. Lett.* **2003**, *5* (11), 1841–1844. <https://doi.org/10.1021/ol034320+>.

- (76) Foster, E. J.; Babuin, J.; Nguyen, N.; Williams, V. E. Synthesis of Unsymmetrical Dibenzoquinoxaline Discotic Mesogens. *Chem. Commun.* **2004**, 2 (18), 2052–2053. <https://doi.org/10.1039/b400998c>.
- (77) Kotha, S.; Meshram, M. Synthesis of Novel Fluoranthene-Based Conformationally Constrained α -Amino Acid Derivatives and Polycyclic Aromatics via the Diels-Alder Reaction. *Synth.* **2014**, 46 (11), 1525–1531. <https://doi.org/10.1055/s-0033-1341042>.
- (78) Ashton, P. R.; Girreser, U.; Giuffrida, D.; Stoddart, J. F.; Kohnke, F. H.; Mathias, J. P.; Raymo, F. M.; Slawin, A. M. Z.; Williams, D. J.; Kohnke, F. H.; et al. Molecular Belts. 2. Substrate-Directed Syntheses of Belt-Type and Cage-Type Structures. *J. Am. Chem. Soc.* **1993**, 115 (13), 5422–5429. <https://doi.org/10.1021/ja00066a010>.
- (79) Patra, A.; Wijsboom, Y. H.; Shimon, L. J. W.; Bendikov, M. Planar [6]Radialenes: Structure, Synthesis, and Aromaticity of Benzotriselenophene and Benzotrithiophene. *Angew. Chemie - Int. Ed.* **2007**, 46 (46), 8814–8818. <https://doi.org/10.1002/anie.200703123>.

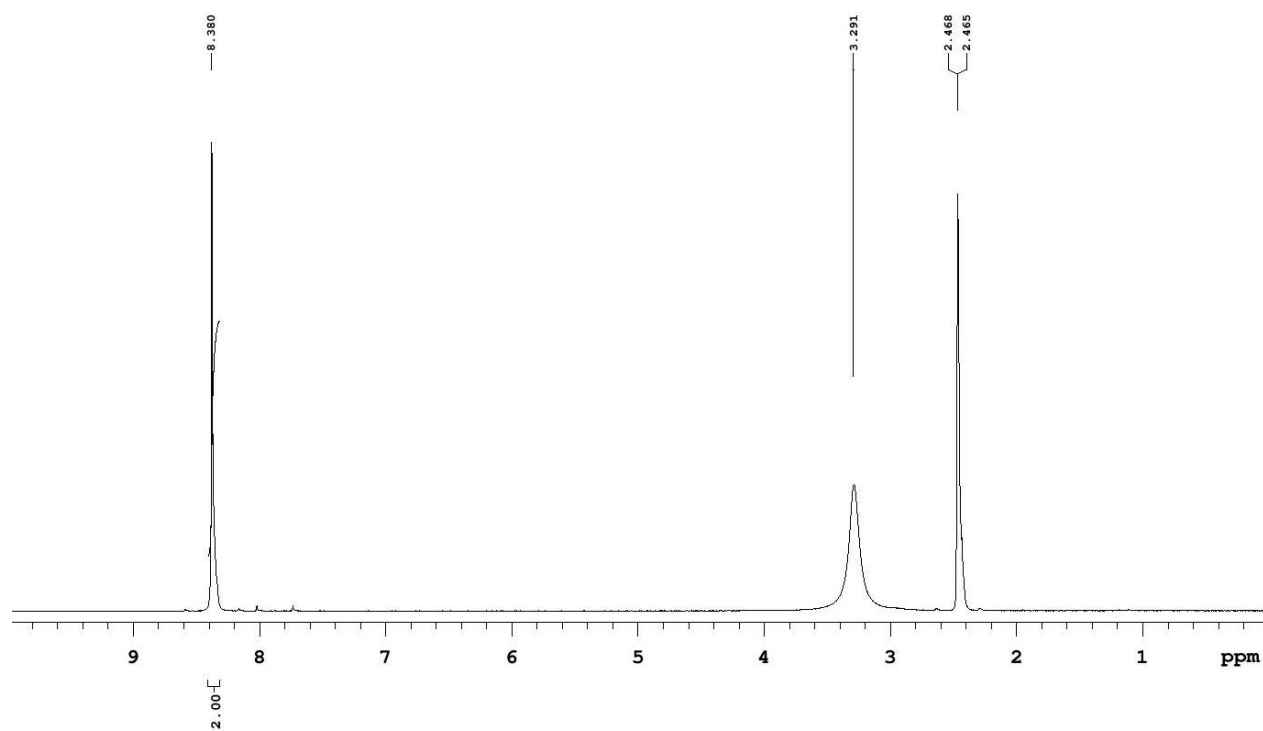
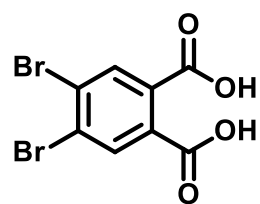
APPENDIX A: ^1H AND ^{13}C NUCLEAR MAGNETIC RESONANCE (NMR)

SPECTRA

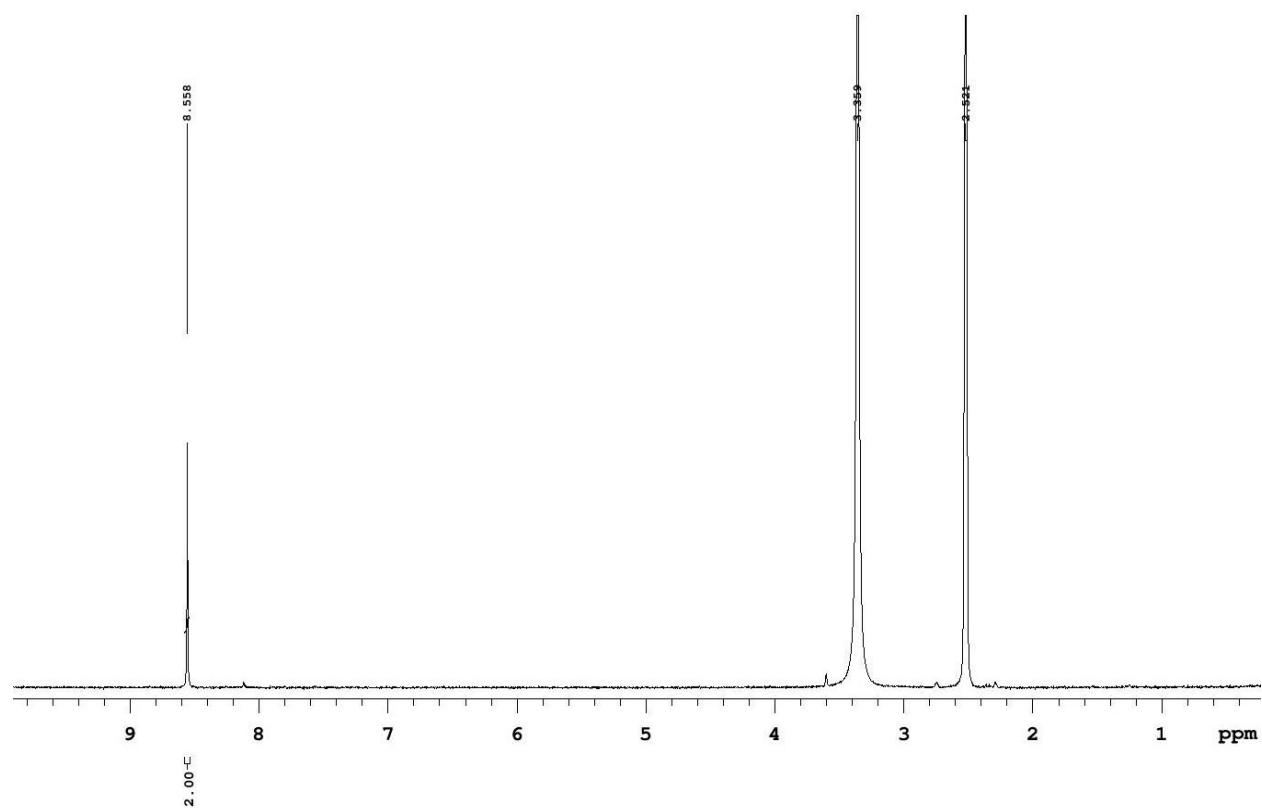
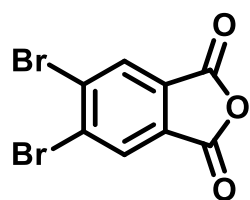
^1H NMR Spectrum of **52**: 1,2-dibromo-4,5-dimethylbenzene



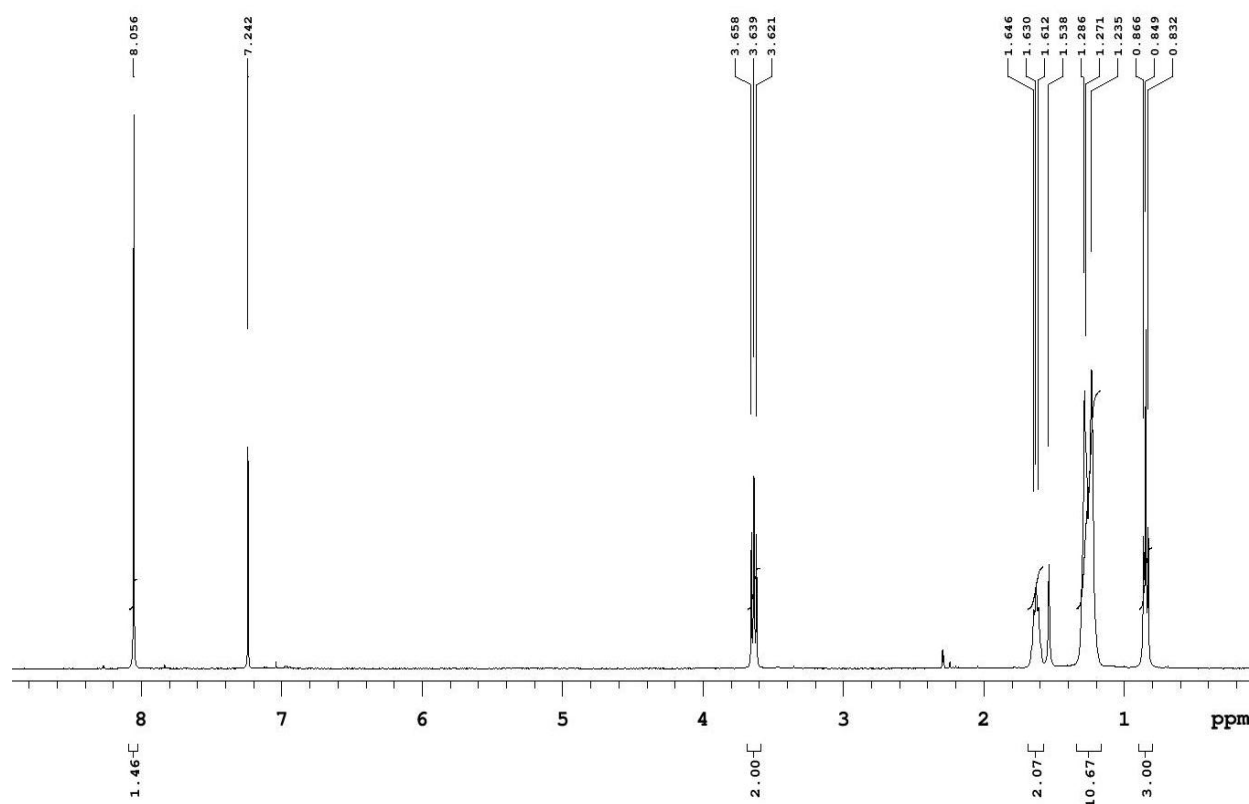
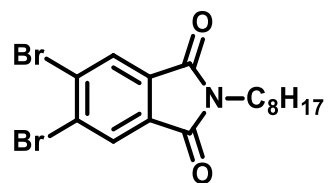
¹H NMR spectrum of 51: 4,5-dibromophthalic acid



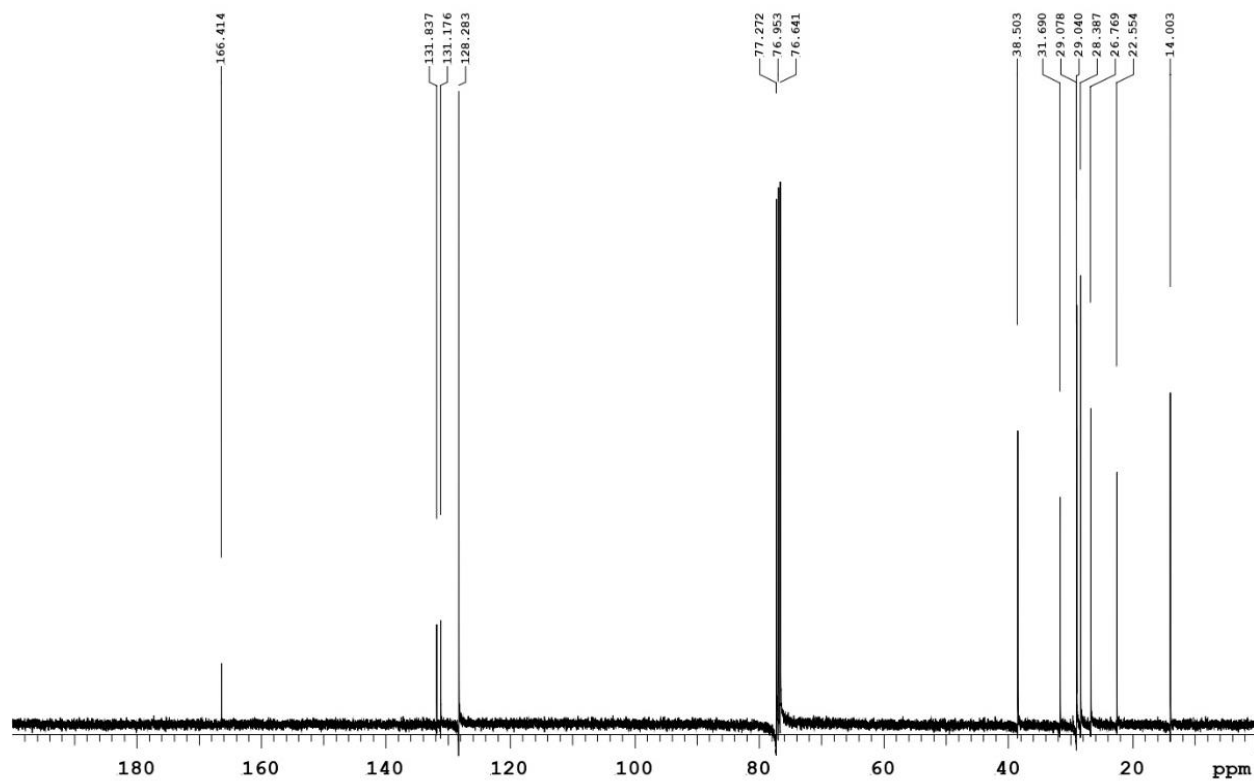
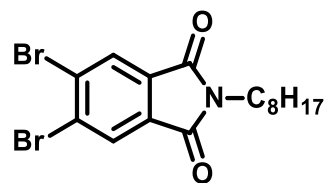
¹H NMR Spectrum of 50: 5,6-dibromoisobenzofuran-1,3-dione



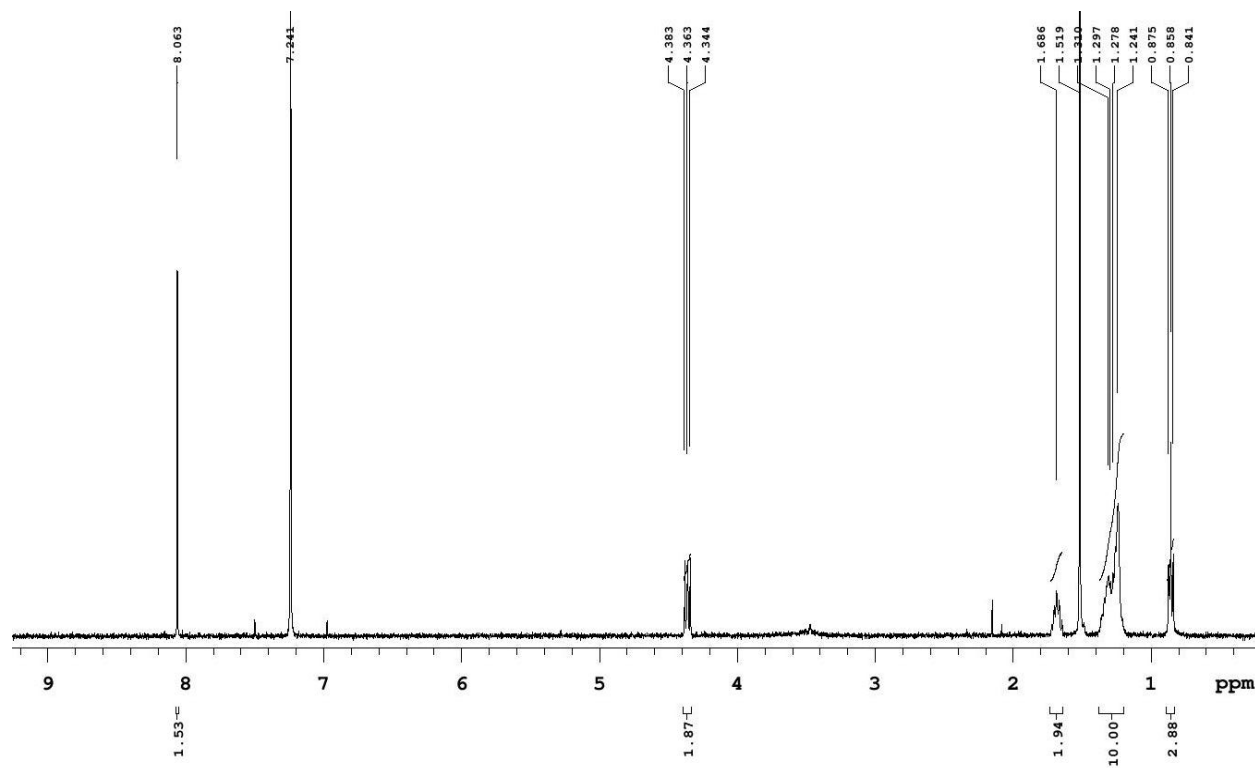
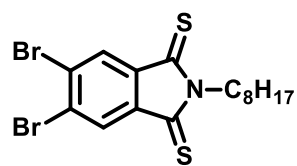
¹H NMR Spectrum of 41: 5,6-dibromo-2-octylisindoline-1,3-dione



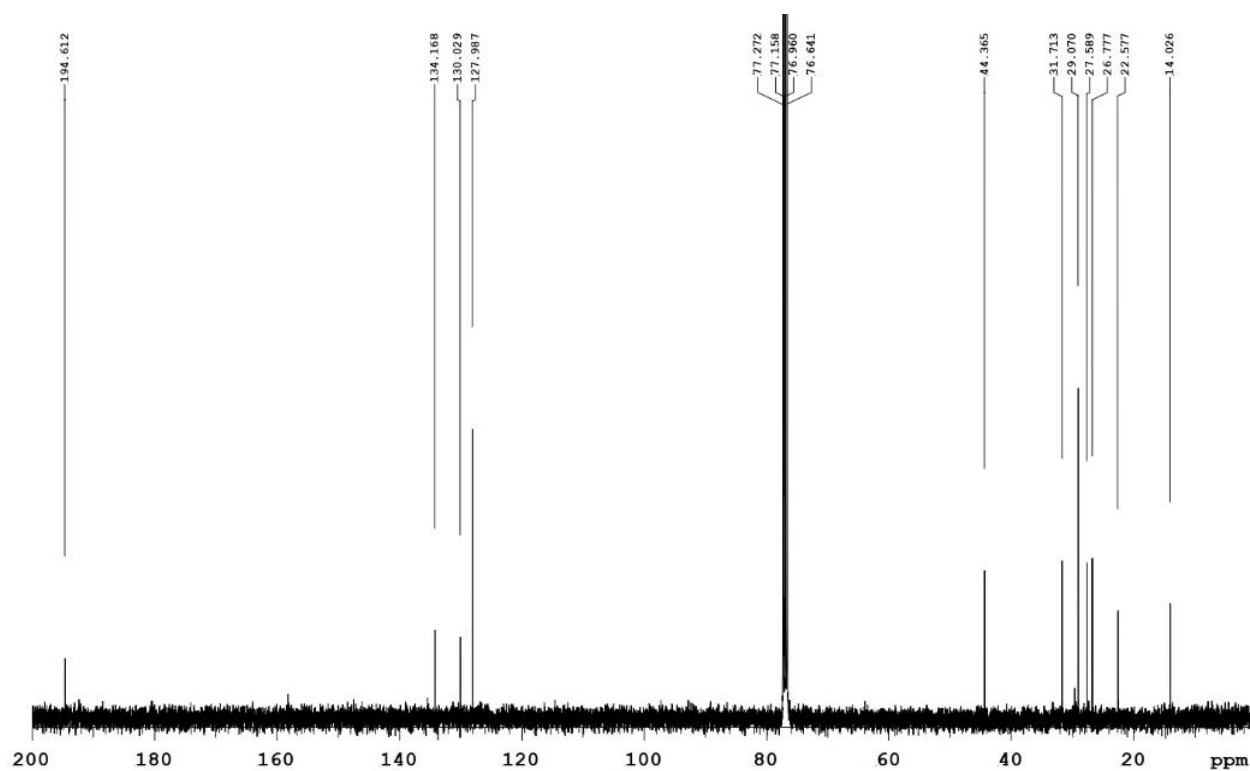
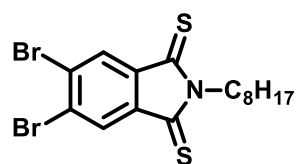
^{13}C NMR Spectrum of 41: 5,6-dibromo-2-octylisoindoline-1,3-dione



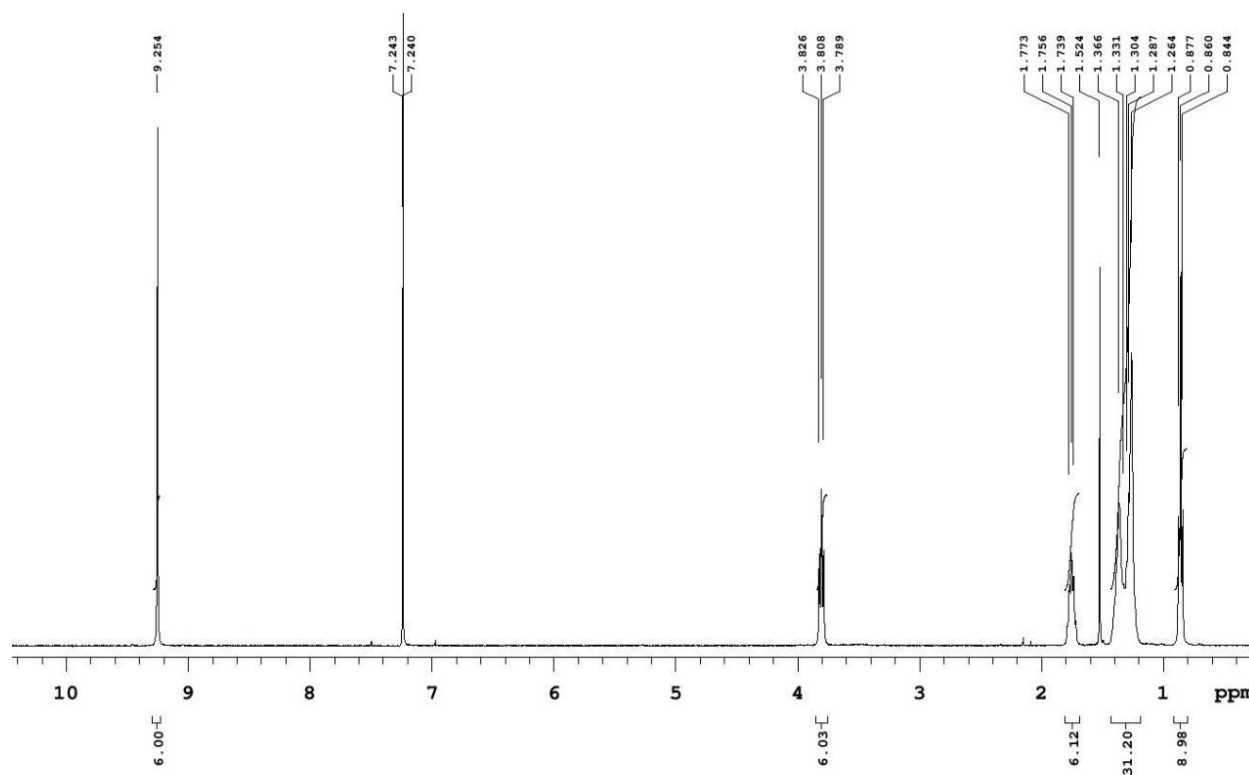
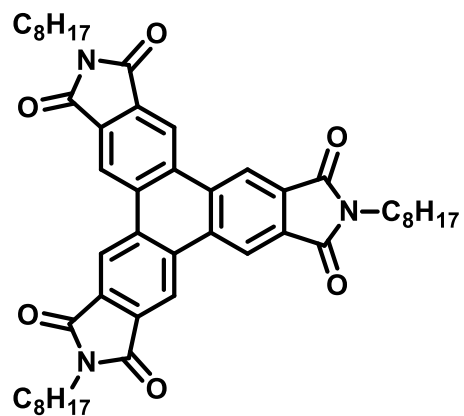
^1H NMR Spectrum of 55: 5,6-dibromo-2-octylisindoline-1,3-dithione



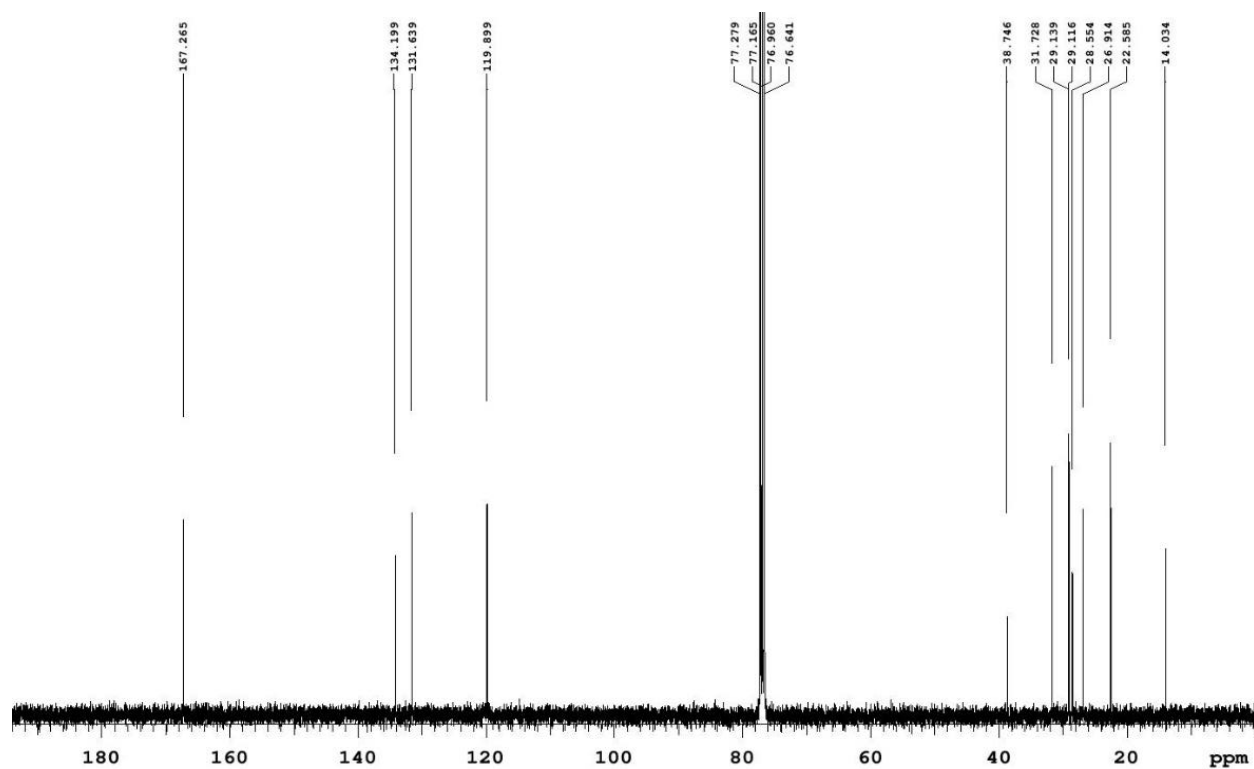
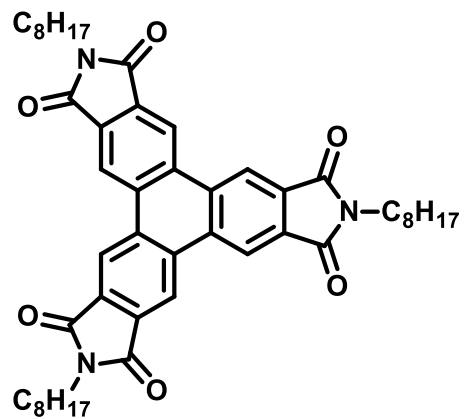
^{13}C NMR Spectrum of 55: 5,6-dibromo-2-octylisoindoline-1,3-dithione



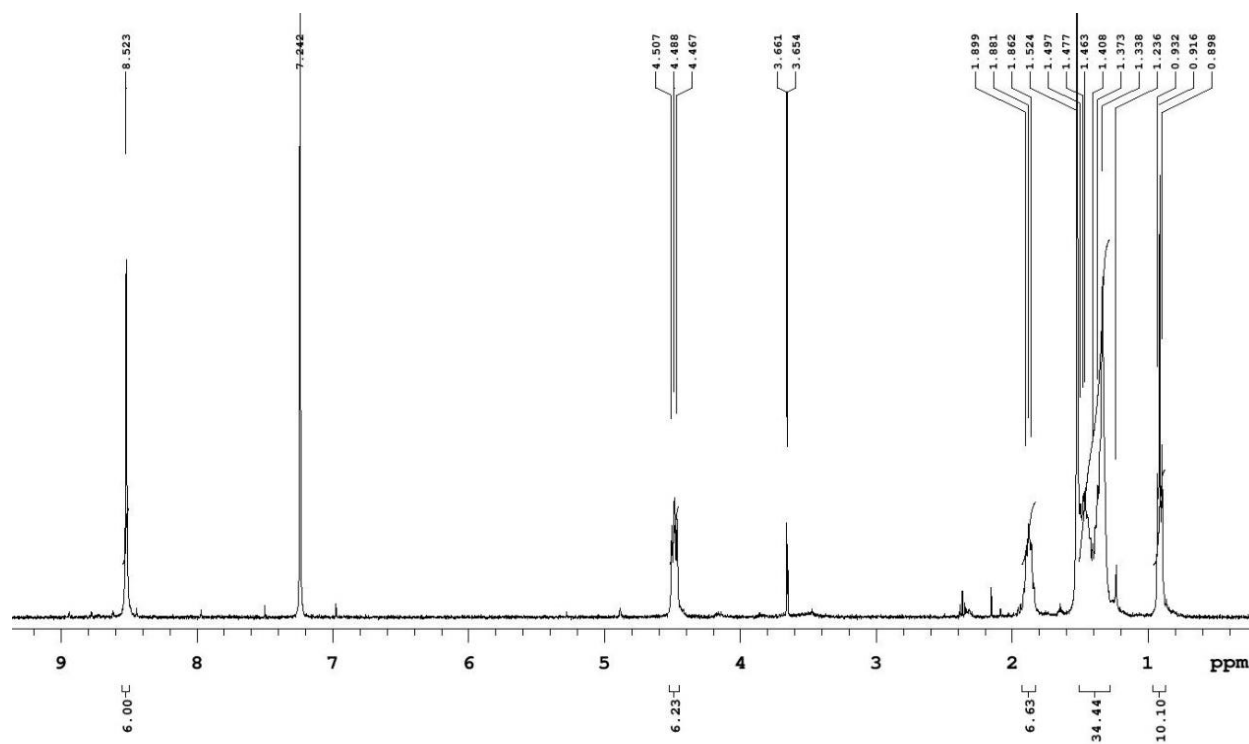
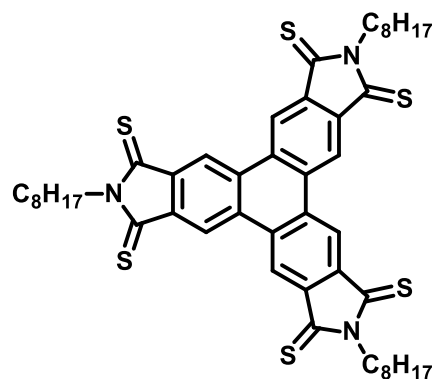
^1H NMR Spectrum of 1: 2,7,12-trioctyl-1*H*-benzo-[1,2-*f*:3,4-*f'*:5,6-*f''*]-triisindole-1,3,6,8,11,13-(2*H*,7*H*,12*H*)-hexaone



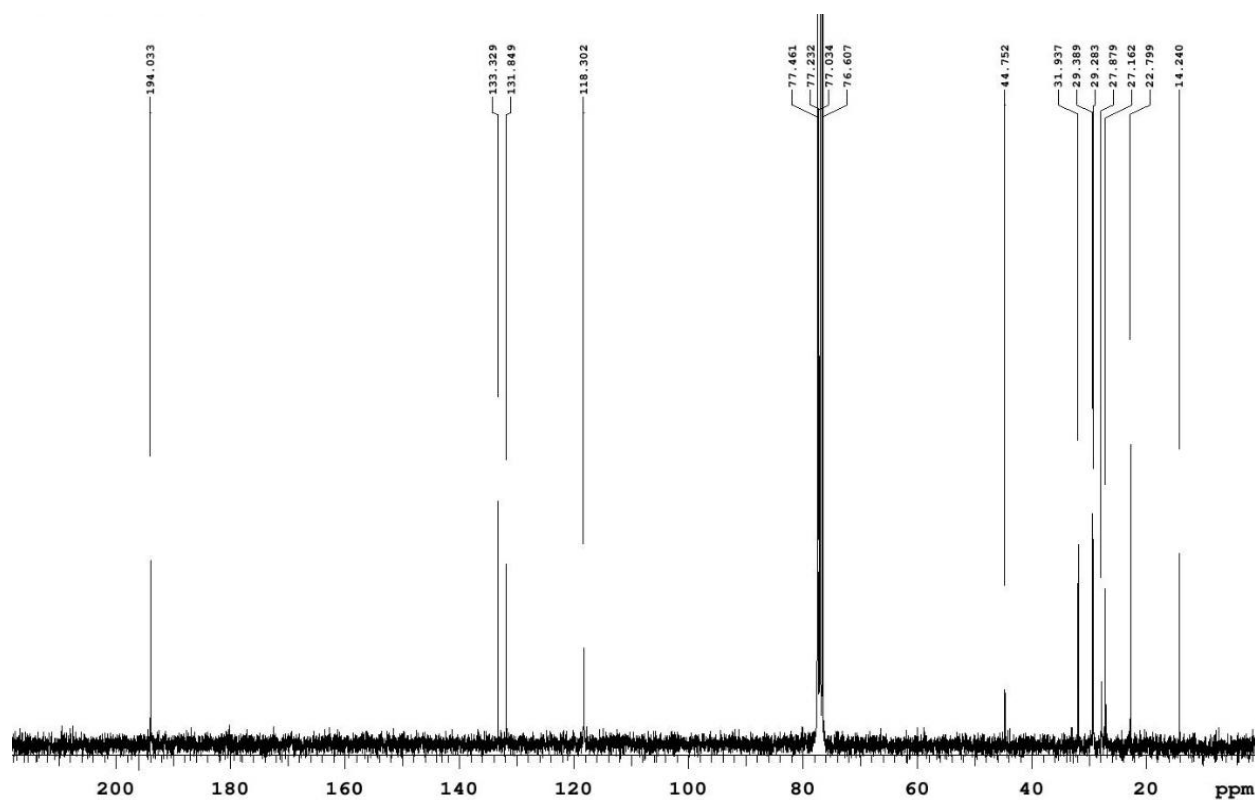
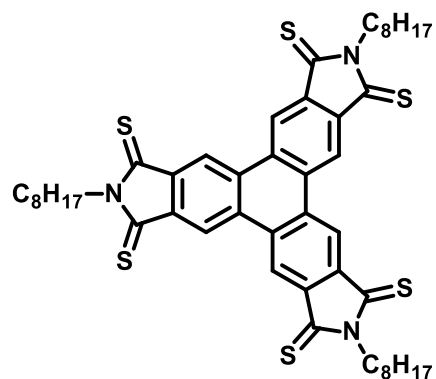
^{13}C NMR Spectrum of 1: 2,7,12-trioctyl-1*H*-benzo-[1,2-*f*:3,4-*f'*:5,6-*f''*]-triisindole-1,3,6,8,11,13-(2*H*,7*H*,12*H*)-hexaone



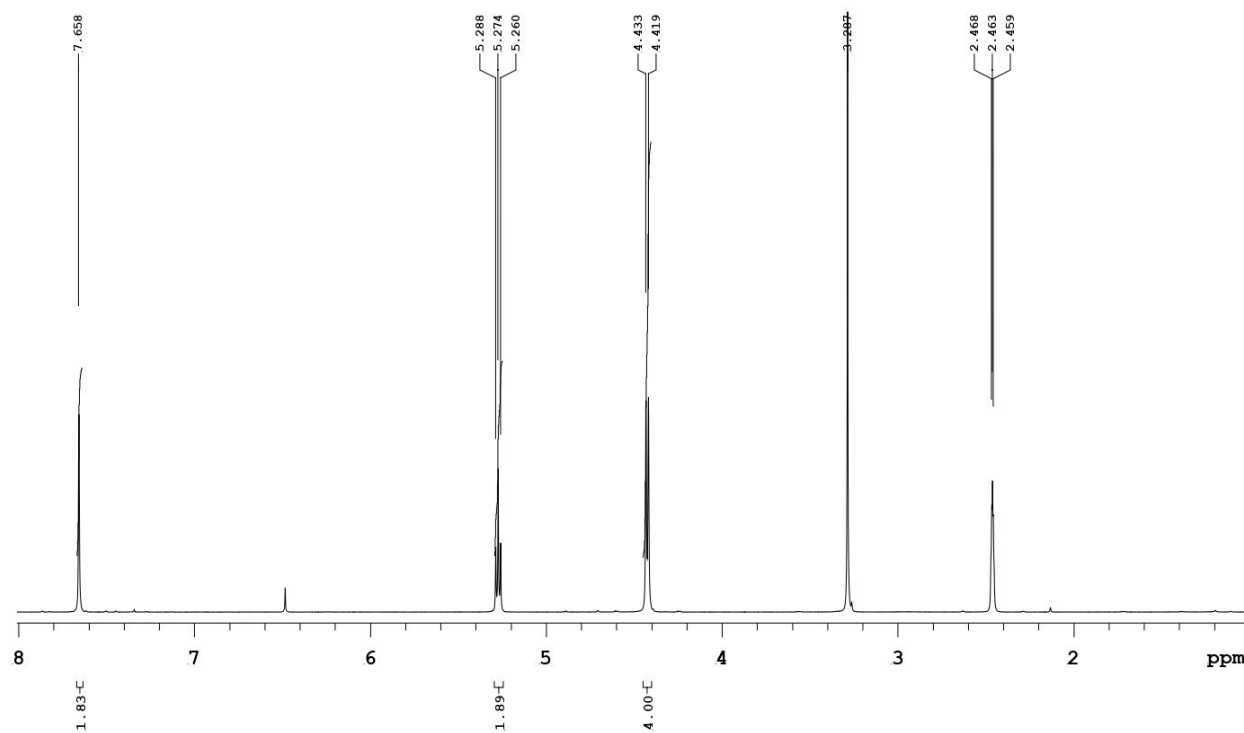
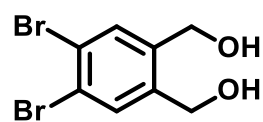
¹H NMR Spectrum of 2: 2,7,12-trioctyl-1*H*-benz-[1,2-*f*:3,4-*f'*:5,6-*f''*]-trisoindole-1,3,6,8,11,13(2*H*,7*H*,12*H*)-hexathione



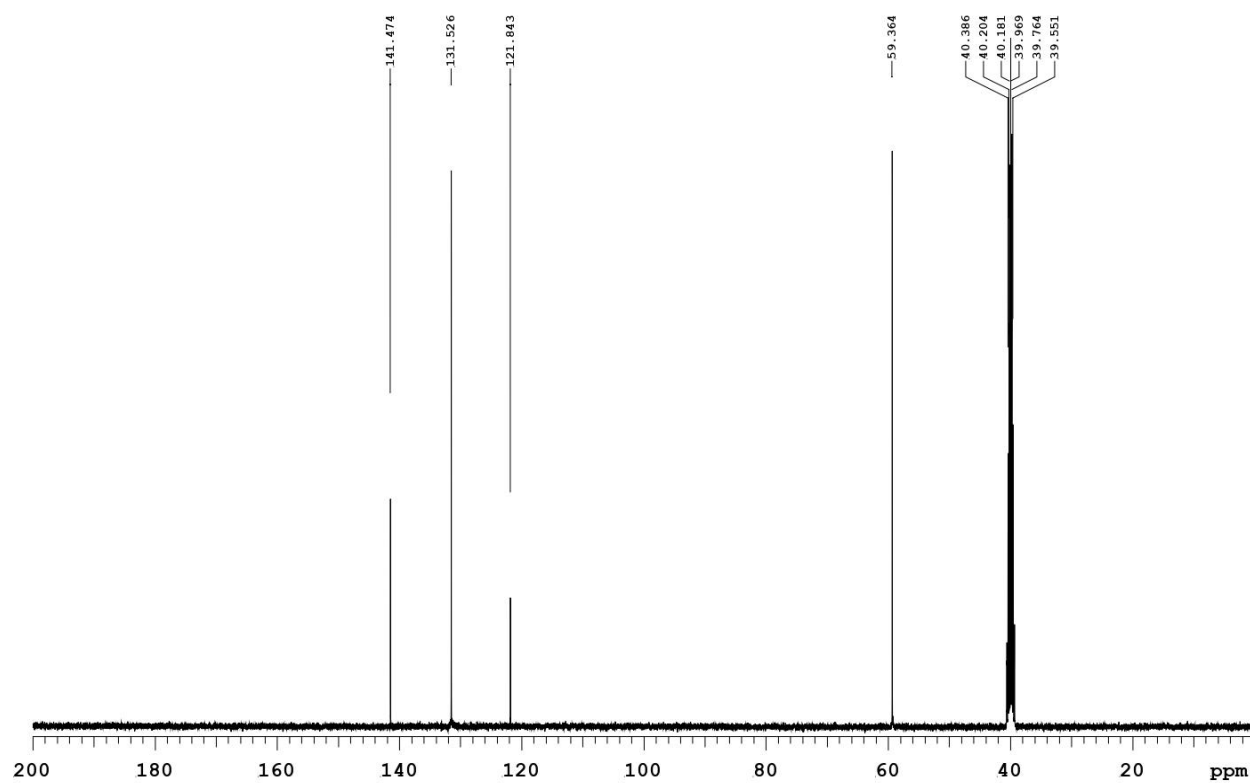
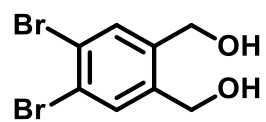
^{13}C NMR Spectrum of 2: 2,7,12-trioctyl-1*H*-benz-[1,2-*f*:3,4-*f'*:5,6-*f''*]-triisindole-1,3,6,8,11,13(2*H*,7*H*,12*H*)-hexathione



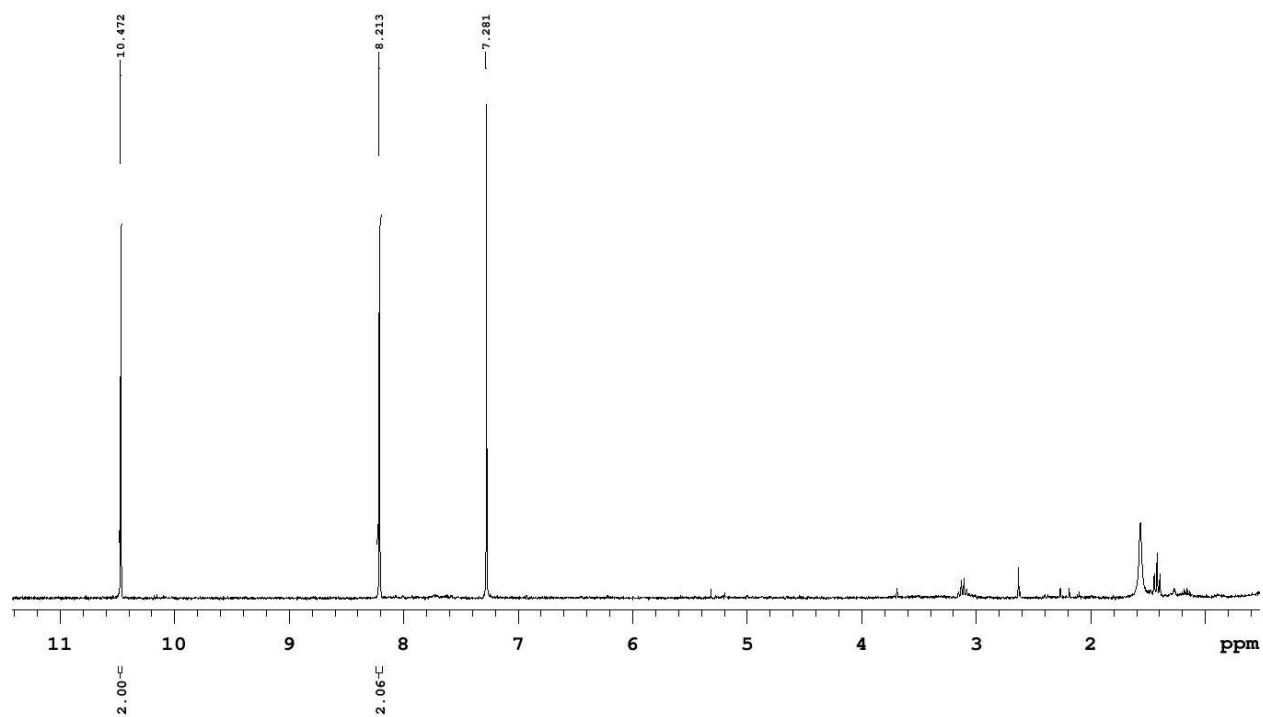
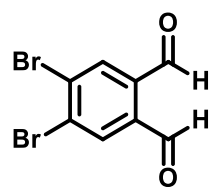
¹H NMR Spectrum of 78: (4,5-dibromo-1,2-phenylene)dimethanol



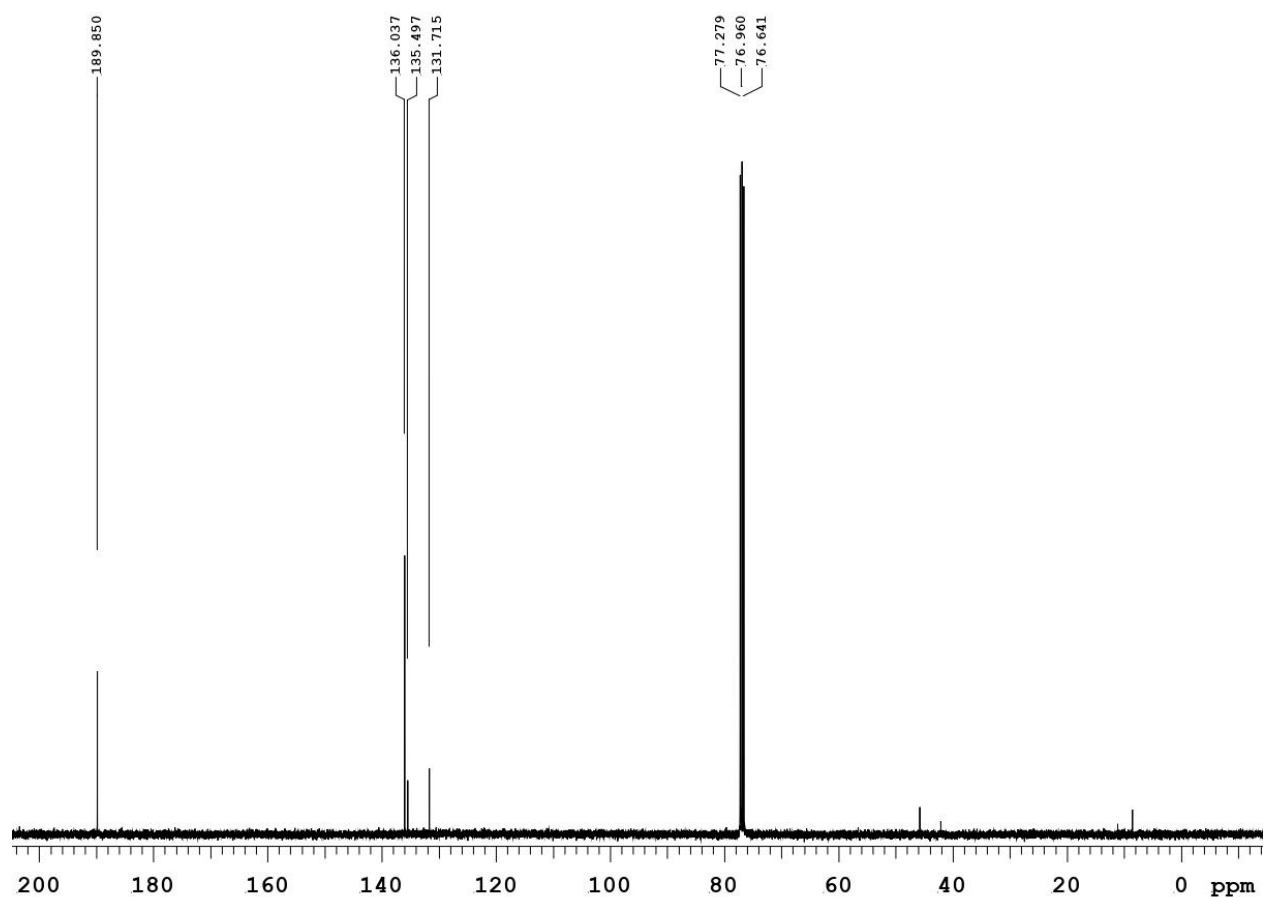
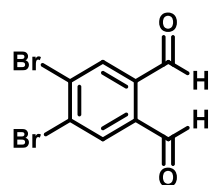
^{13}C NMR Spectrum of 78: (4,5-dibromo-1,2-phenylene)dimethanol



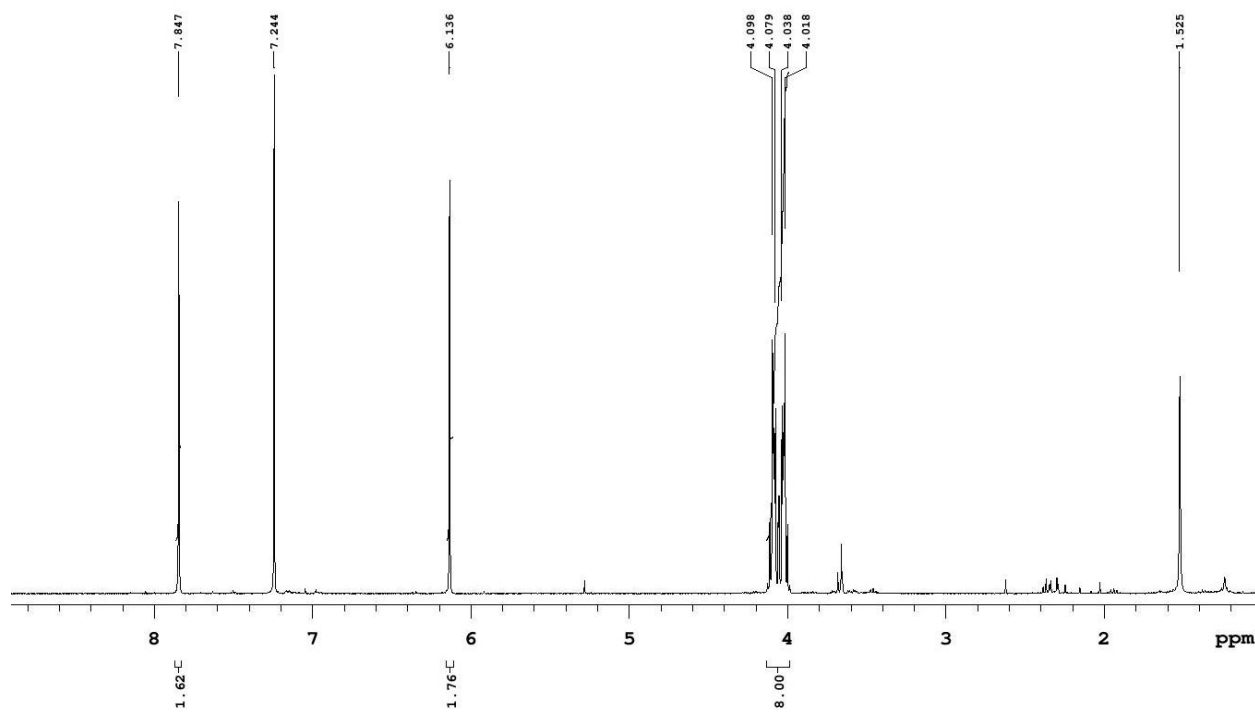
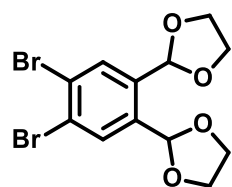
^1H NMR Spectrum of 42: 4,5-dibromophthalaldehyde



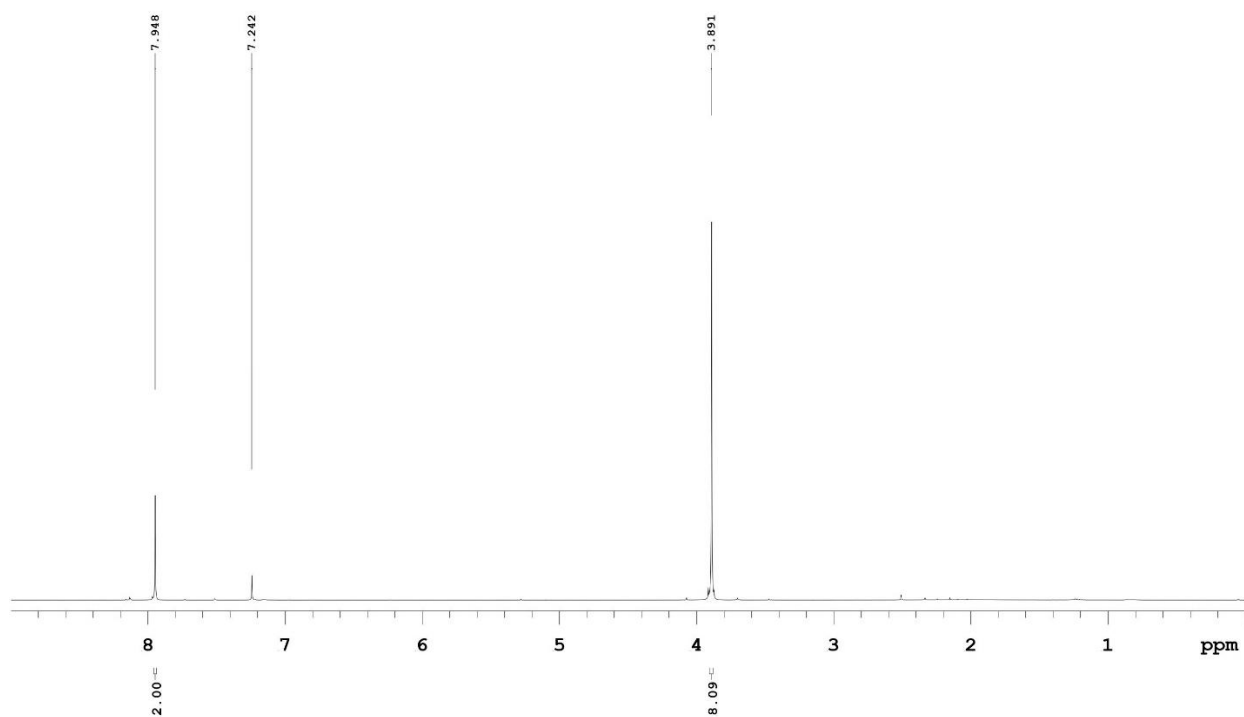
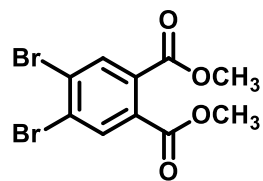
^{13}C NMR Spectrum of 42: 4,5-dibromophthalaldehyde



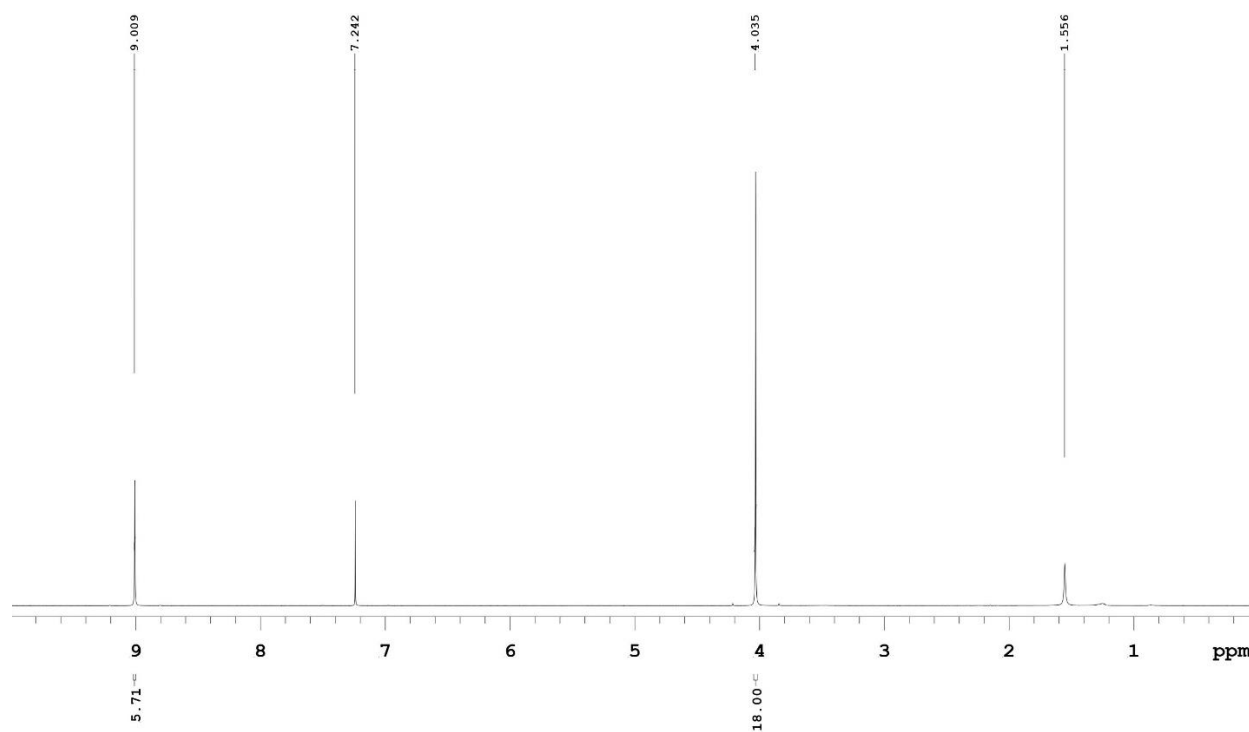
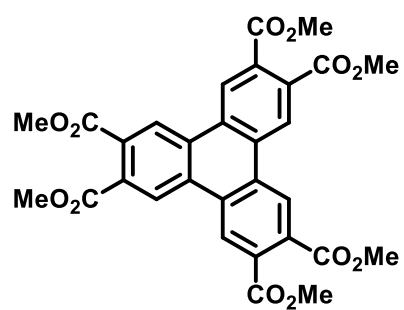
^1H NMR Spectrum of 77: 2,2'-(4,5-dibromo-1,2-phenylene)bis(1,3-dioxolane)



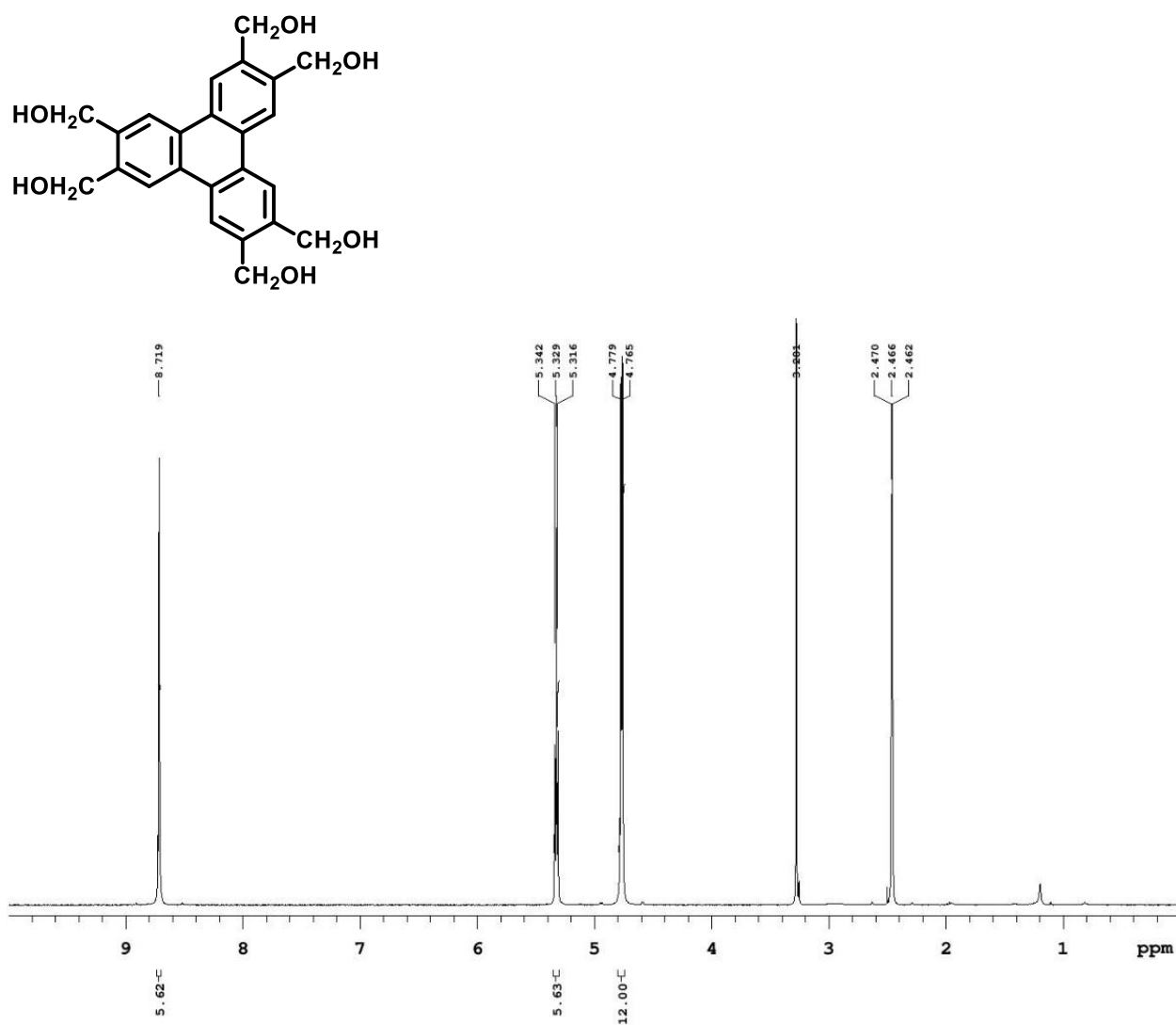
¹H NMR Spectrum of 57: Dimethyl-4,5-dibromophthalate



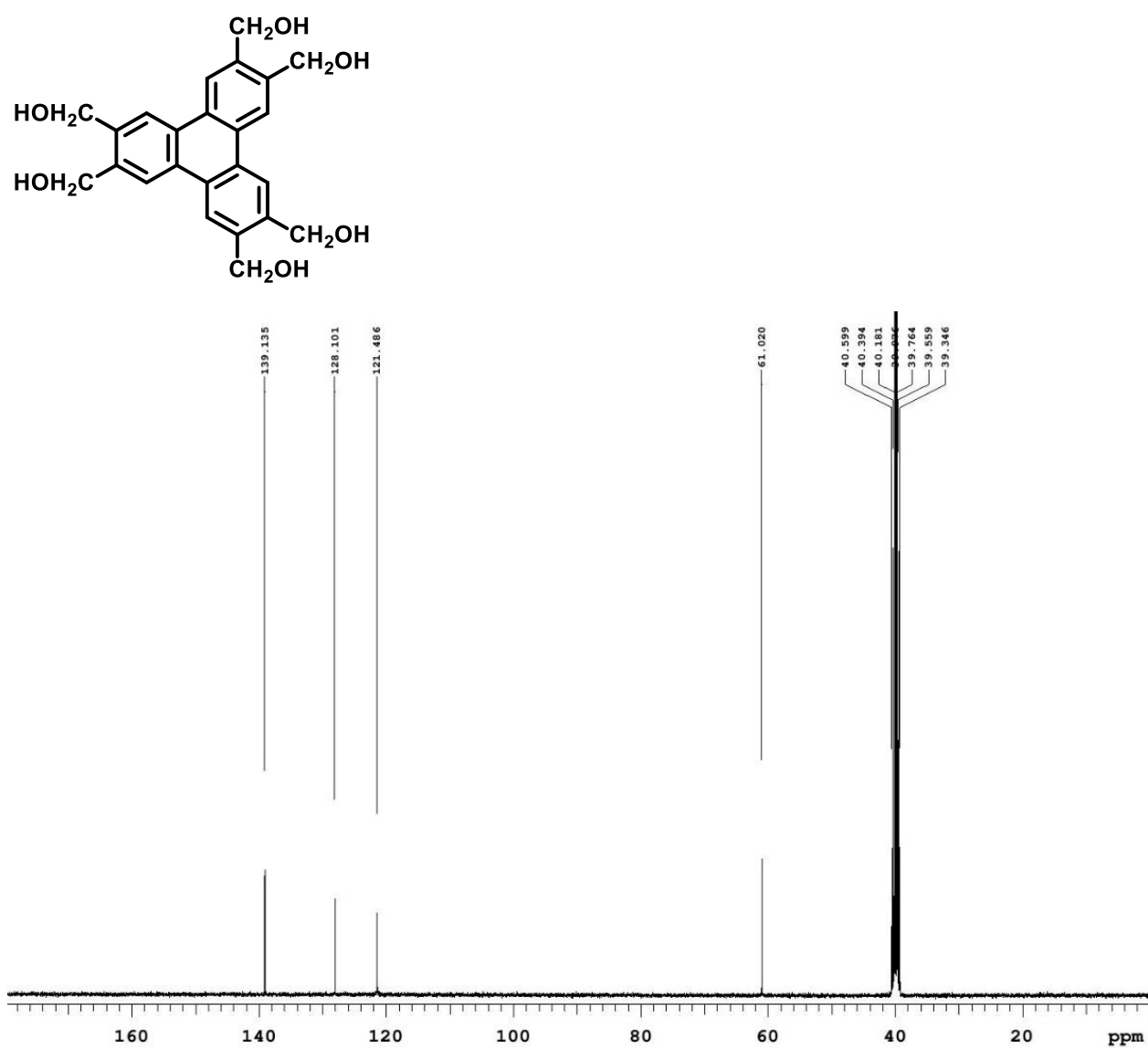
¹H NMR Spectrum of 37: Hexamethyl-triphenylene-2,3,6,7,10,11-hexacarboxylate



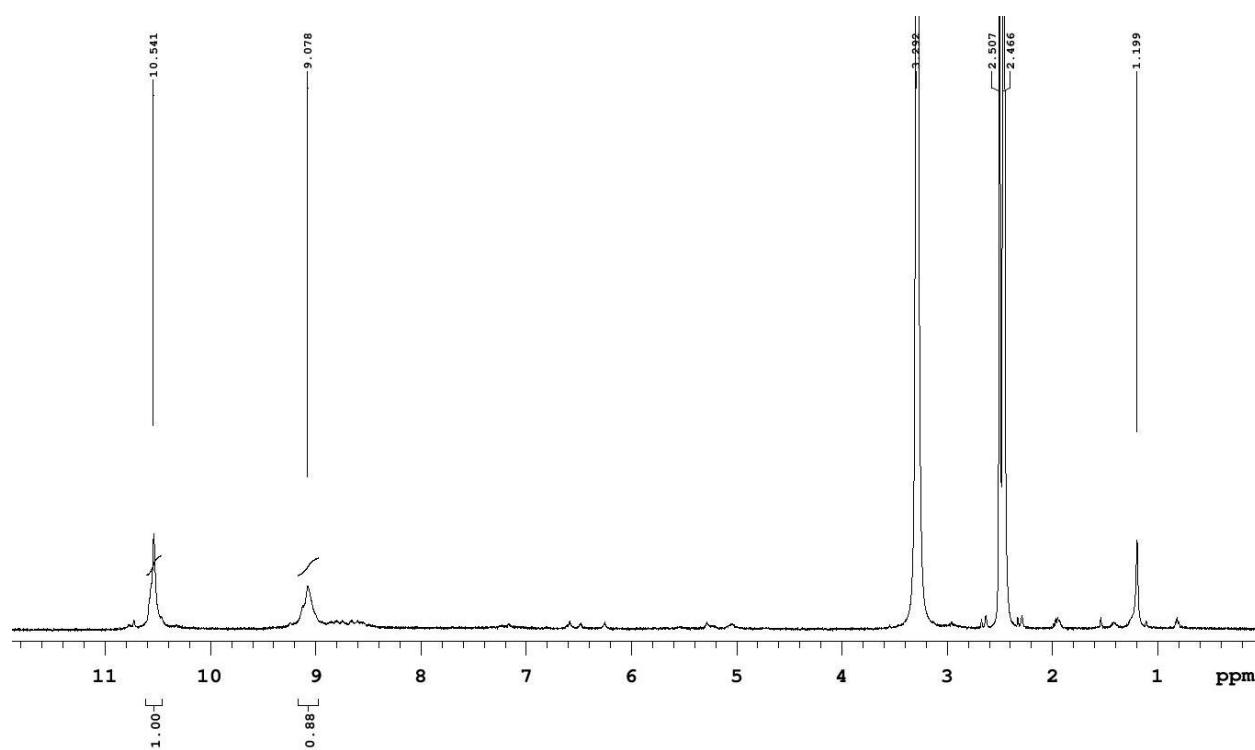
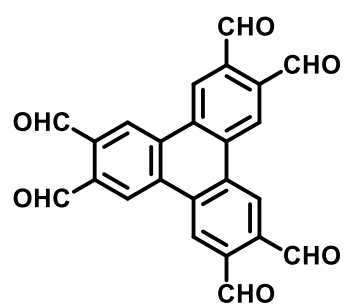
^1H NMR Spectrum of 80: Triphenylene-2,3,6,7,10,11-hexaylhexamethanol



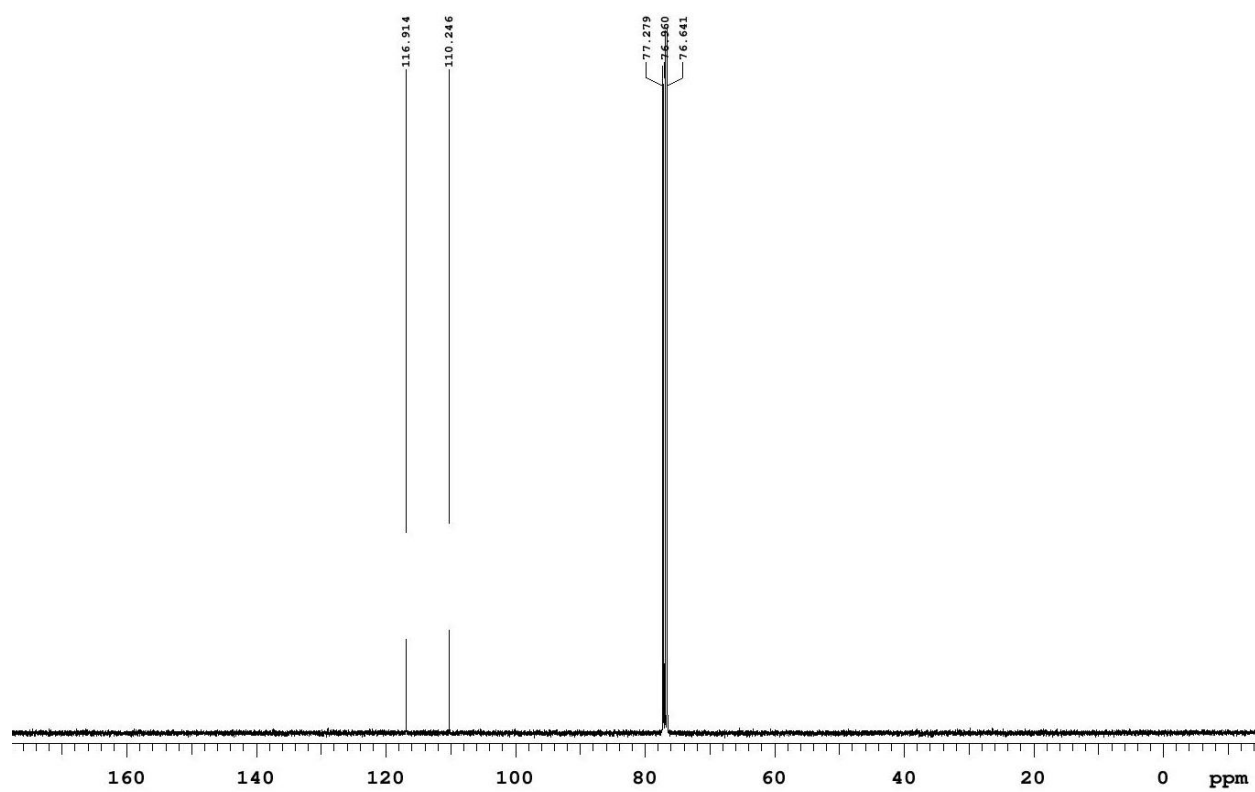
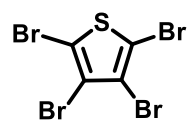
^{13}C NMR Spectrum of 80: Triphenylene-2,3,6,7,10,11-hexaylhexamethanol



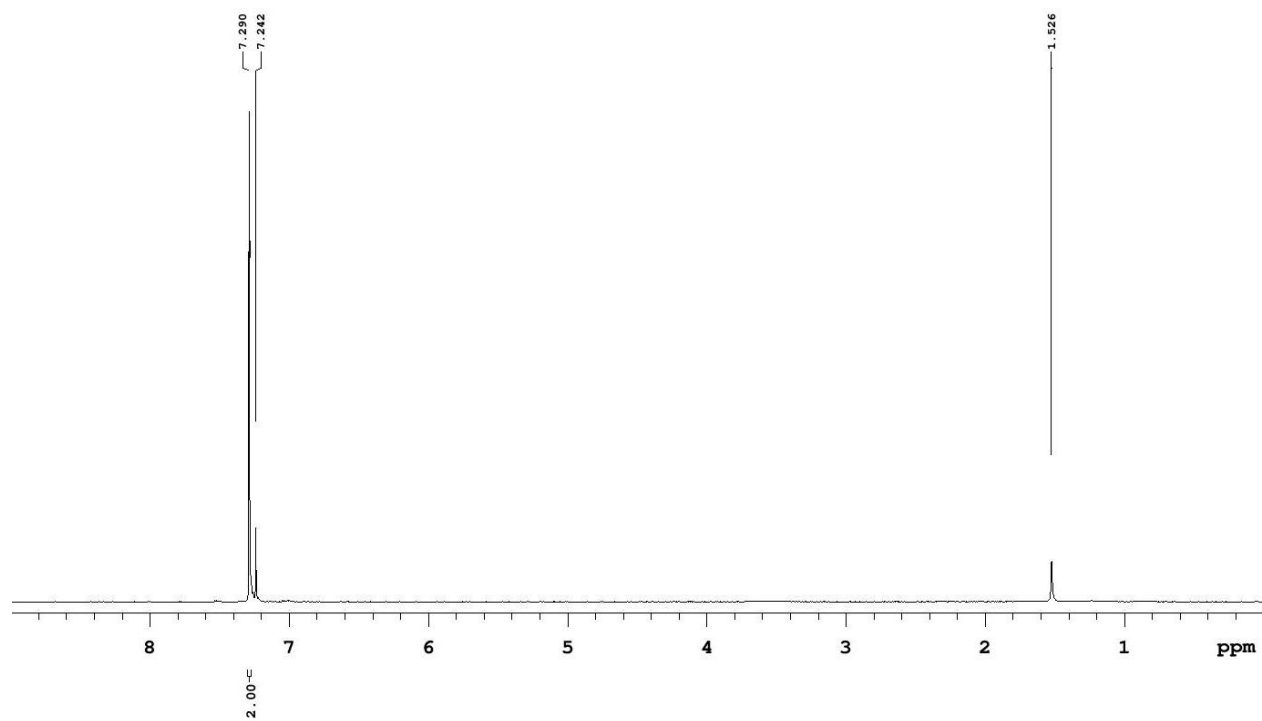
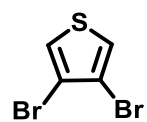
¹H NMR Spectrum of crude 3: Triphenylene-2,3,6,7,10,11-hexacarbaldehyde



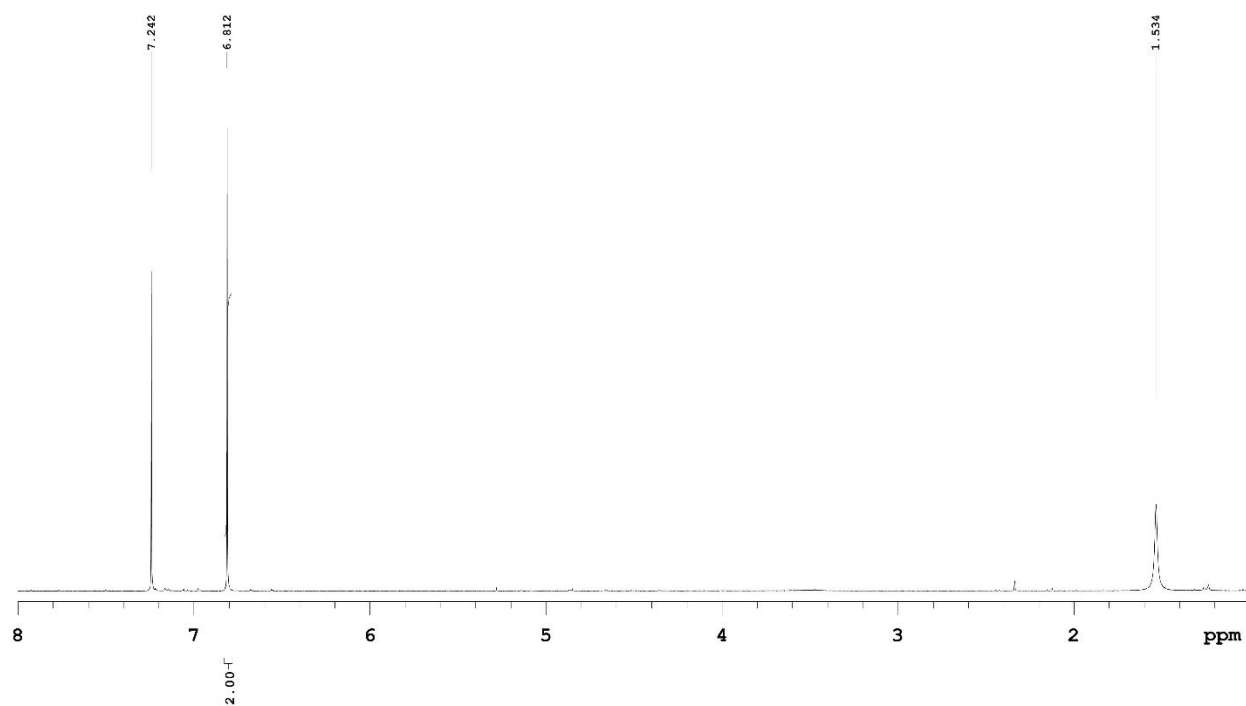
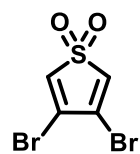
^{13}C NMR of 85: 2,3,4,5-tetrabromothiophene



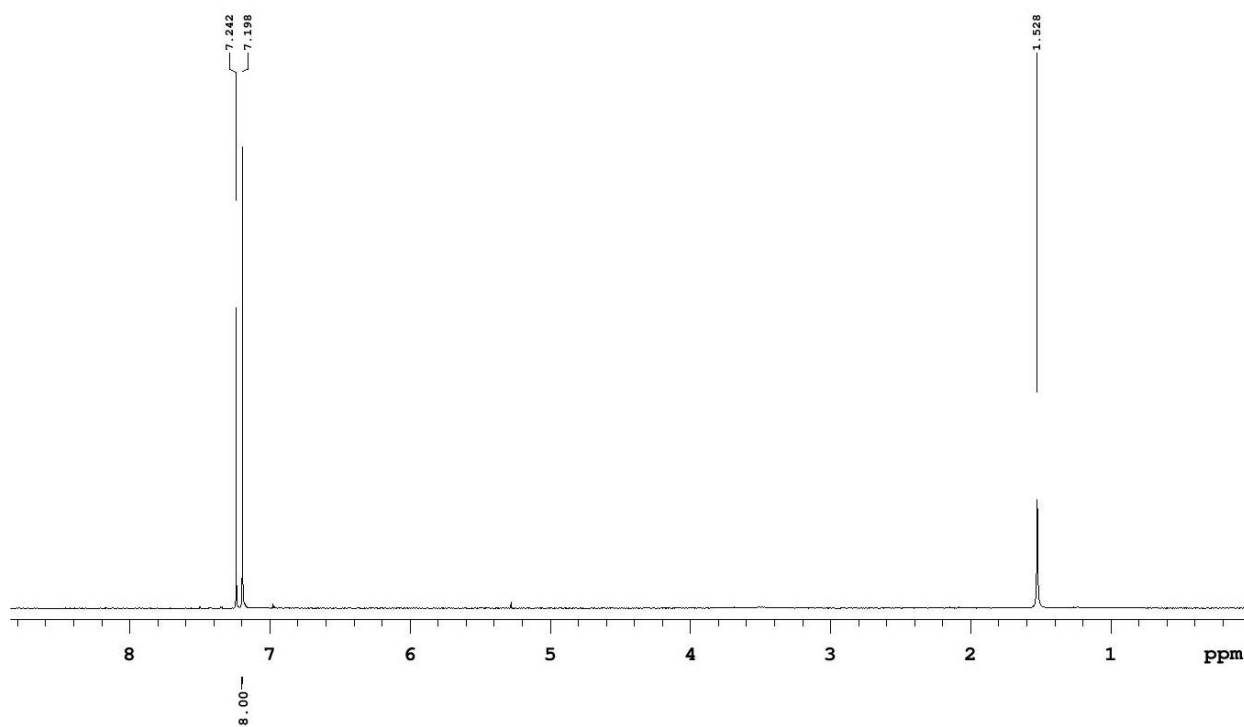
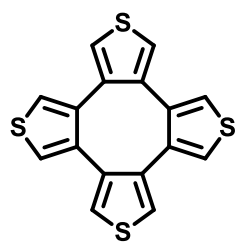
¹H NMR of 43: 3,4-dibromothiophene



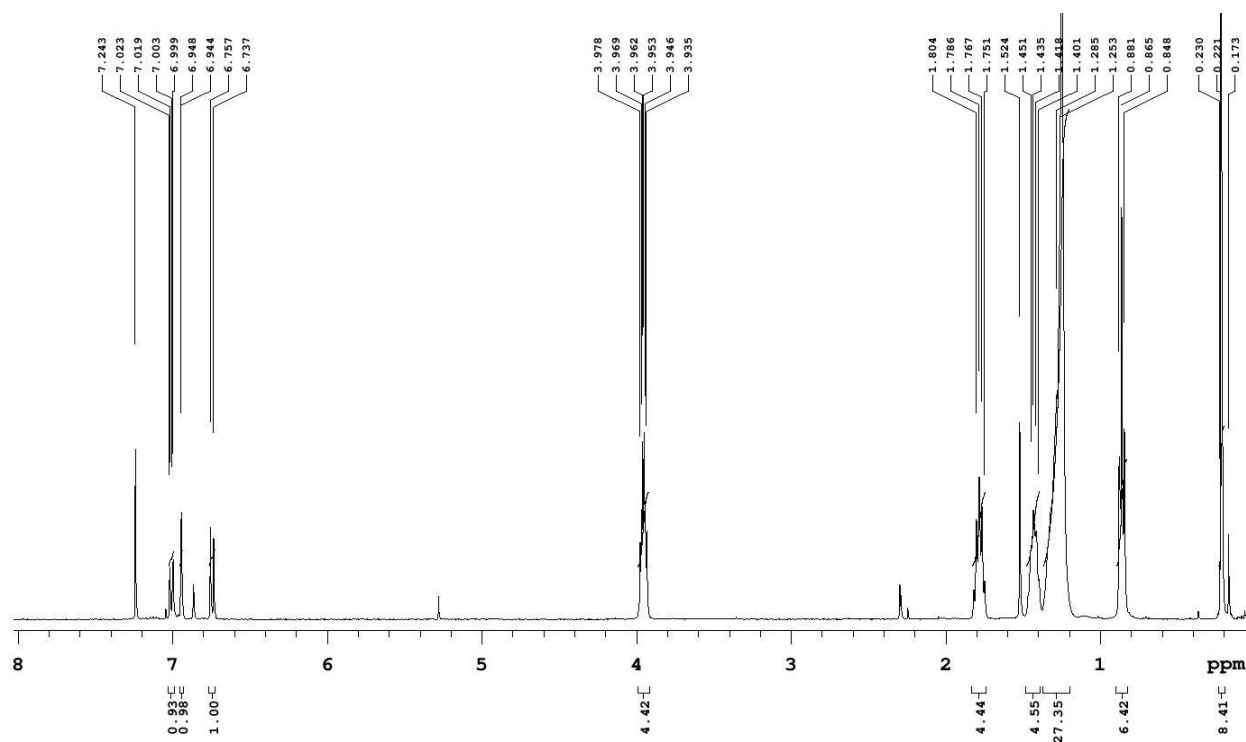
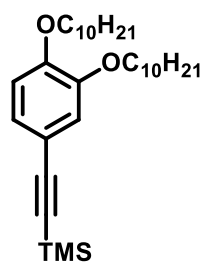
¹H NMR Spectrum of 86: 3,4-dibromothiophene 1,1-dioxide



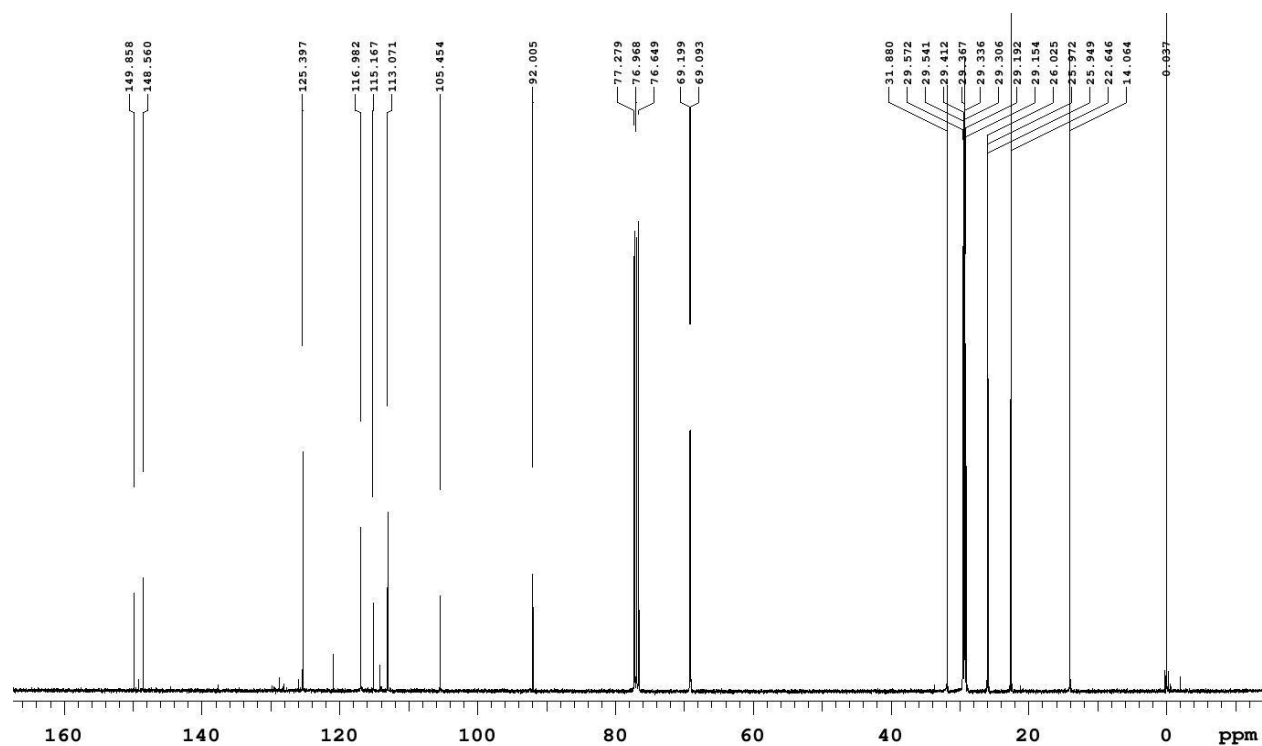
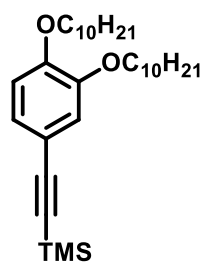
^1H NMR Spectrum of 32: Cycloocta[1,2-*c'*:5,6-*c''*:7,8-*c'''*]tetrathiophene



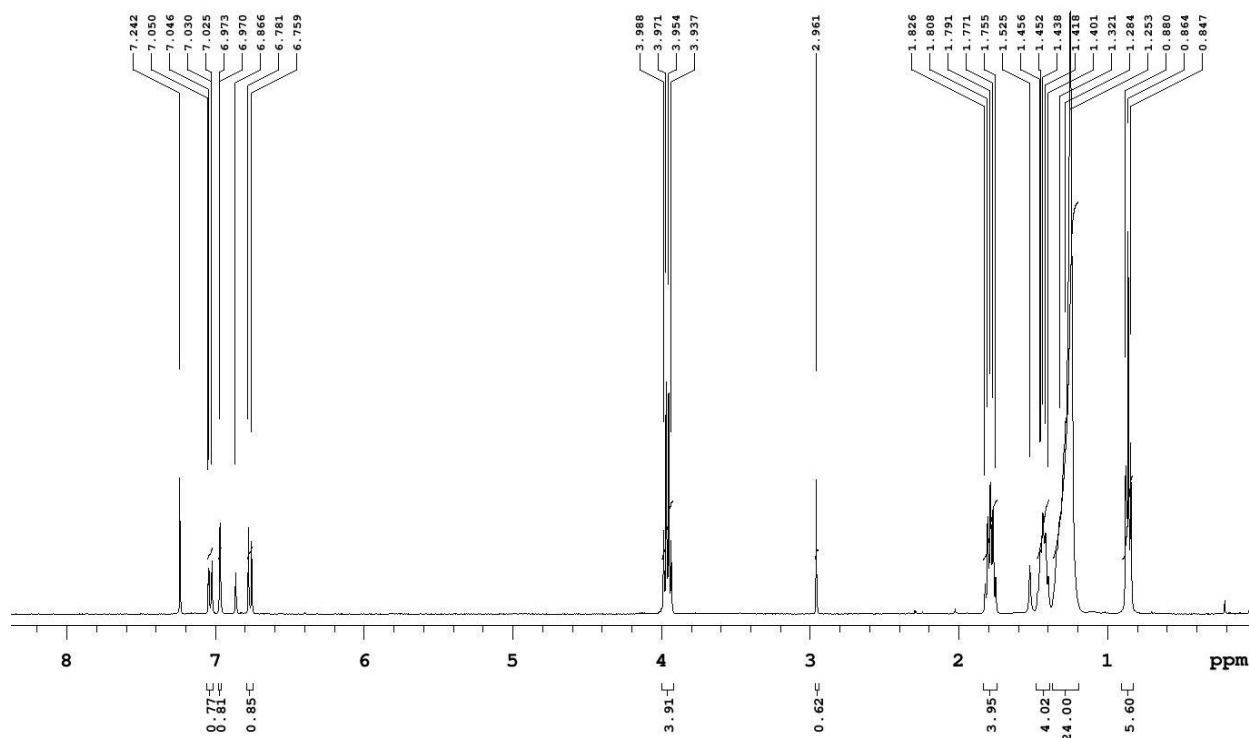
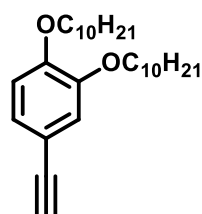
¹H NMR Spectrum of 88: ((3,4-bis(decyloxy)phenyl)ethynyl)trimethylsilane



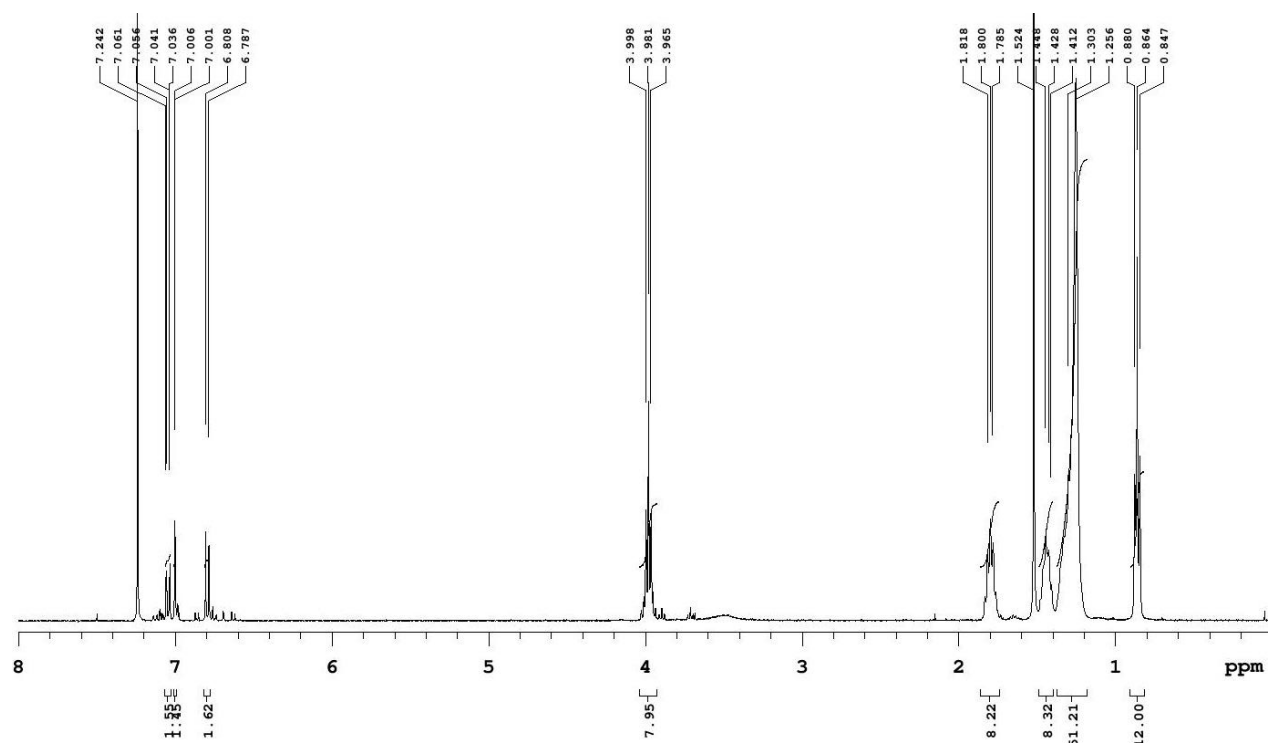
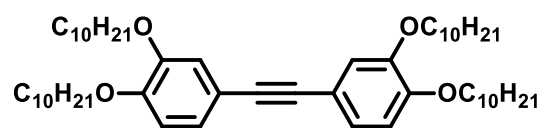
^{13}C NMR Spectrum of 88: ((3,4-bis(decyloxy)phenyl)ethynyl)trimethylsilane



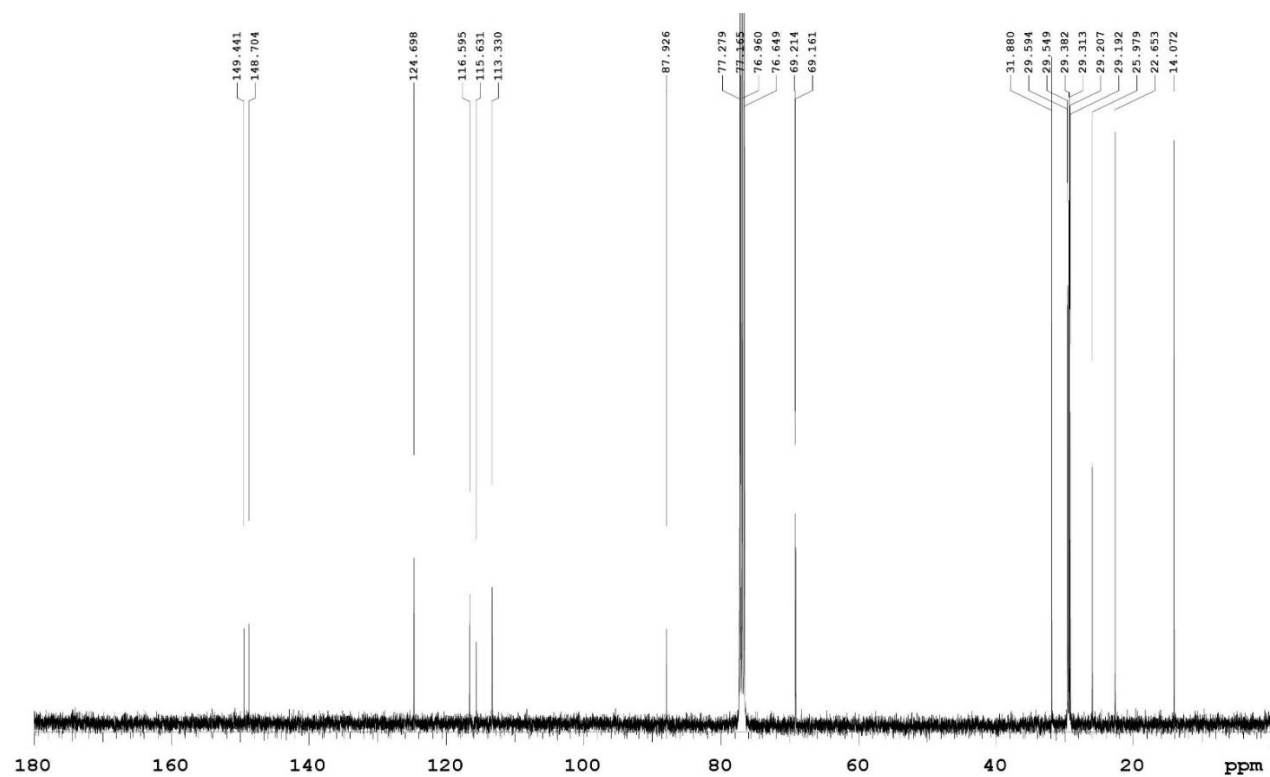
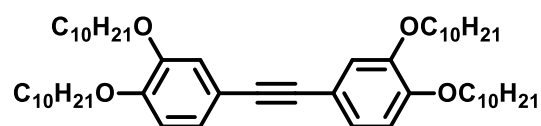
^1H NMR Spectrum of 89: 1,2-bis(decyloxy)-4-ethynylbenzene



^1H NMR Spectrum of 82: 1,2-bis(3,4-bis(decyloxy)phenyl)ethyne



^{13}C NMR Spectrum of 82: 1,2-bis(3,4-bis(decyloxy)phenyl)ethyne



¹H NMR Spectrum of 91: Acenaphthylene

